University of Technology Sydney

Faculty of Engineering and Information Technology

ELECTROCARDIOGRAM AND HYBRID SUPPORT VECTOR ALGORITHMS FOR DETECTION OF HYPOGLYCAEMIA IN PATIENTS WITH TYPE 1 DIABETES

By

NURYANI NURYANI

Supervisor: Prof. Hung Nguyen
Co-Supervisor: Dr. Steve Ling

A thesis submitted in partial fulfillment of the requirement for the Degree of Doctor of Philosophy

CERTIFICATE OF AUTHORSHIP/ORIGINALITY

I certify that the work in this thesis has not previously been submitted for a degree nor has it been submitted as part of requirements for a degree except as fully acknowledged within the text.

I also certify that the thesis has been written by me. Any help that I have received in my research work and the preparation of the thesis itself has been acknowledged. In addition, I certify that all information sources and literature used are indicated in the thesis.

Nuryani Nuryani

Acknowledgement

Nuryani Nuryani

Table of Contents

List of Figures

List of Tables

List of Abbreviations

DCCT : Diabetes Control and Complications Trial

ECG : Electrocardiographic

FIS : Fuzzy Inference system

FMR : Fuzzy Inference System Multiple Regression

Gm : Geometric mean

IDDM : Insulin-dependent diabetes mellitus

MR : Multiple regression

PSO : Particle swarm optimization

PSOWM : Particle swarm optimization with wavelet mutation

RBF : Radial basis function

ROC : Receiver operating characteristic

rSVML : SVM (with linear kernel function) in which their parameters are determined randomly.

rSVMP : SVM (with polynomial kernel function) in which their parameters are determined randomly.

rSVMR : SVM (with RBF kernel function) in which their parameters are determined randomly.

rSVMS : SVM (with sigmoid kernel function) in which their parameters are determined randomly.

Sensitivities : Sensitivity

SFSVM : Swarm based fuzzy inference system support vector machine

SMR1 : Swarm based multiple regression (order 1)

SMR2 : Swarm based multiple regression (order 2)

SMR3 : Swarm based multiple regression (order 3)

Specificity : Specificity

SSVML : Swarm based support vector machine with linear kernel function

SSVMP : Swarm based support vector machine with polynomial kernel

function

SSVMR	: Swarm based support vector machine with RBF kernel function
SSVMRF	: Swarm based support vector machine with RBF kernel function with the input of ECG parameter corrected using Fridericia formula
SSVMS	: Swarm based support vector machine with sigmoid kernel function
SSVMw	: Swarm based support vector machine without weight optimization
SVM	: Support vector machine
SVML	: Support vector machine with linear kernel function
SVMP	: Support vector machine with polynomial kernel function
SVMR	: Support vector machine with RBF kernel function
SVMS	: Support vector machine with sigmoid kernel function

List of Symbols

Q	:	the start of QRS complex
R	:	the peak of QRS complex
S	:	the end of QRS complex
To	:	the starting point of T-wave
Tp	:	the peak of T-wave
Te	:	the end of T-wave
$TpTe_c$	:	interval from the peak of T-wave Tp to the end of T-wave Te
$ToTe_c$	:	the interval from the beginning of T-wave To to the end of T-wave Te
RTp_c	:	the interval from R point to the peak of T-wave Tp
QTe_c	:	the interval from Q point to the end of T-wave Te
QTp_c	:	the interval from Q point to the peak of T-wave Tp
STo_c	:	the interval from S point to the beginning of T-wave To and
D	:	polynomial degree of polynomial kernel function
γ	:	The width of RBF kernel function
α	:	Lagrangain multiplier
$k()$	:	Kernel function
ξ	:	A slack variable introduced for soft margin SVM
C	:	The SVM parameter "*cost*"
$\tilde{z}$	:	Personal best position in particle swarm optimization
$\hat{z}$	:	Global best parameter in particle swarm optimization
φ	:	Inertia weight in particle swarm optimization
$\varphi_{max}, \varphi_{min}$	:	Upper and lower bound of inertia weight
c_1, c_2	:	Acceleration constants in particle swarm optimization
β	:	Coefficient of independent variables of multiple regression
m	:	Mean of Gaussian membership function
σ	:	Standard deviation of Gaussian membership function
η	:	The output of fuzzy inference system
h	:	The fuzzy singleton in the if-then part of the inference engine (FIS)

ρ : Rule number of rules in the if-then part of the inference engine (FIS)

q : Constriction factor in particle swarm optimization with wavelet mutation (PSOWM)

ρ_{max}, ρ_{min} : The upper and lower boundary, respectively, of the element of particle.

$\vartheta_{tr}, \vartheta_v$: Sensitivity of training and validation, respectively

$\mathcal{S}_{tr}, \mathcal{S}_v$: Specificity of training and validation

δ : Morlet wavelet function

$\wp_{max}, \wp_{min}$: The upper and lower boundary of the element of particle in PSOWM

β_{wm} : The shape parameter of the monotonic increasing function in PSOWM

ABSTRACT

Hypoglycaemia is the most acute and common complication of type 1 diabetes. Physiological changes occur when blood glucose concentration falls to a certain level. A number of studies have demonstrated that hypoglycaemia causes electrocardiographic (ECG) alteration.

The serious harmful effects of hypoglycaemia on the body motivate research groups to find an optimal strategy to detect it. Detection of hypoglycaemia can be performed by puncturing the skin to measure the blood glucose level. However, this method is unsuitable as frequent puncturing may produce anxiety in patients and periodic puncturing is difficult to conduct, not to mention inconvenient, while the patient is sleeping. Therefore, a continuous and non-invasive technique can be considered for hypoglycaemia detection. Several techniques have been reported, such as reverse iontophoresis and absorption spectroscopy.

Another approach to hypoglycaemia detection is based on the physiological effects of hypoglycaemia on the various parts of the body such as the brain, heart and skin. Physiological effects of hypoglycemia to the brain are studied by investigating electroencephalography (EEG) features. Hypoglycemic effects to the heart include alteration of electrocardiographic (ECG) parameters such as heart rate, QT intervals and T-wave amplitude alteration.

Several algorithms were developed to process ECG parameters for hypoglycemia detection. The algorithms include neural network and fuzzy system based intelligent algorithms. Furthermore, hybrid systems were also developed, such as fuzzy neural network and genetic-algorithm-based multiple regression with fuzzy inference systems.

So far, hypoglycaemia detection systems which are based on the physiological effects still require extensive validation before they can be adopted for worldwide clinical practices.

The research in this thesis introduces several ECG parameters especially which relate to the repolarization phase and could contribute to hypoglycaemia detection. Furthermore, this research aims to introduce novel computational intelligent techniques for hypoglycaemia detection. The detection is based on electrocardiographic (ECG) parameters. A support vector machine (SVM) is the first algorithm introduced for hypoglycaemia detection in this research. The second algorithm is a hybrid of SVM with particle swarm optimization (PSO), which is called an SSVM algorithm. This algorithm is intended to improve the performance of the first algorithm. PSO is an evolutionary technique based on the movement of swarms. It is employed to optimize SVM parameters in order that the SVM perform well for hypoglycaemia detection. The third algorithm is for the improvement of the second algorithm where a fuzzy inference system (FIS) is included. This algorithm involves SVM, FIS and a PSO, which is called SFSVM. The FIS is used to process some ECG parameters to find a better performance of hypoglycaemia detection. FIS is an effective intelligent system which employs fuzzy logic and fuzzy set theory. Its frameworks are based on the concepts of fuzzy set theory, fuzzy if-then rules, and fuzzy reasoning. In addition, the proposed algorithms are compared with the other algorithms. All the algorithms are investigated with clinical electrocardiographic data. The data is collected from a hypoglycaemia study of type 1 diabetic patients.

This study shows that the selected ECG parameters in hypoglycaemia differ significantly from those in nonhypoglycaemia ($p<0.01$). This difference might consider that the ECG parameters are part of repolarization, in which repolarization prolongs hypoglycaemia. It implies that the ECG parameters are important parameters which possibly contribute to hypoglycaemia detection. Therefore, the ECG parameters are used for inputs of hypoglycaemia detection in this study.

The result also shows that the hypoglycaemia detection strategy which uses SSVM performs better than that which uses SVM (80.04% vs. 73.63%, in terms of geometric mean). Furthermore, the SFSVM performs better than the SSVM (87.22% vs. 80.45% in terms of sensitivity and 79.41% vs. 79.64% in terms of specificity). In summary, SFSVM performs better than the other two algorithms (SVM and SSVM), with acceptable sensitivity, specificity and geometric mean of 87.22%, 79.41% and 83.22%, respectively.

CHAPTER 1.
INTRODUCTION

Hypoglycaemia is the most acute and common complication of type 1 diabetes (The Diabetes Control and Complications Trial Research Group, 1997). Its serious harmful effects on the body motivate the efforts to find an optimal strategy to detect it early (Klonoff, 2001). Thus, hypoglycaemia detection is an important issue in health technologies. As an introduction, this chapter begins with the background of this doctoral research. The next two sections present the problem statement and the objectives of the research. Contributions and the structure of the thesis are described in the following two sections. At the end, this chapter lists the publications presented during the doctoral course.

1.1 BACKGROUND

Hypoglycaemia is a disease where the glucose level in the body is abnormally low (<3.0 mmol/l). It is a consequence of the limitation in glycaemic control on diabetes. Thus, it is a fear for all people living with diabetes. In diabetic management, a diabetic patient needs to control the body's blood glucose level to be stable in the normal range (about 4.0 mmol/l). Unfortunately, hypoglycaemia can still often happen in diabetic management, which causes hypoglycaemic complications (The Diabetes Control and Complications Trial Research Group, 1997).

A study showed that prevalence of hypoglycaemia in patients with type 1 diabetes was 82% and was lower in patients with type 2 diabetes, which was 45% (Donnelly et al., 2005). Estimation of the prevalence of people with diabetes worldwide is 2.8% in 2000 (171 million people) and higher in 2030 which is 4.4% (366 million people) (Belegundu and Chandrupatla, 2011a). The increase of diabetes could increase hypoglycaemic cases.

Severe hypoglycaemia is a serious problem resulting in significant morbidity, even death. In correlation with cardiovascular complications, it could cause atrial fibrillation (Sommerfield et al., 2003, Braak and Stades, 2009), ventricular ectopics, ventricular fibrillation and sustained ventricular tachycardia. Hypoglycaemia also affects the brain in which regional blood flow within the brain is altered acutely. The serious neurological consequence of severe hypoglycaemia is coma.

Extreme hypoglycaemia is suggested as a factor of death in diabetic patients. Hypoglycaemia of a type 1 diabetic patient, which happens during sleep, is associated with the cause of the "dead in bed" syndrome (Tattersall and Gill, 1991). Moreover, the Diabetes Control and Complications Trial (DCCT) estimates that around 55% of severe hypoglycaemia episodes occur during sleep (The DCCT Research Group, 1991).

To prevent or minimize hypoglycaemic morbidities and mortalities, actions are necessary to obtain a normal blood glucose level soon after a hypoglycaemic event happens. This could be achieved by consuming sugar, such as candy or by taking glucose tablets to raise the blood glucose level. For more severe hypoglycaemia, and where there is a problem taking sugar orally, an injection of glucagon or intravenous glucose may be needed. To take action, patients obviously have to know when hypoglycaemia is happening, and therefore, an early warning is important for this (Osareh and Shadgar, 2008). In other words, an alarm for

hypoglycaemia is important for a blood glucose control for diabetic patients (Klonoff, 2001).

Detection of hypoglycaemia can be performed by puncturing the skin to see the blood glucose level. Microblood sampling is conducted by puncturing one or more finger tips (Graaff et al., 1999). Efforts have been made to improve the convenience of this method, such as by reducing blood sample volume and by choosing a less painful area of the body. However, the puncturing method is still unsuitable while it is conducted frequently and periodically, especially during manual activities or sleeping. Therefore, noninvasive –or minimally invasive– and continuous methods can provide the solution. Studies have been conducted with the aim that hypoglycaemia detection systems can be used continuously without pain. Amaral and Wolf (2008) provided a review of the approaches for noninvasive glucose monitoring. The approaches include reverse iontophoresis, absorption spectroscopy, photoacoustic spectroscopy, polarimetry, fluorescence, Raman spectroscopy, metabolic heat conformation, bioimpedance, electromagnetic, ultrasound and spectroscopy. The review also presented the available devices of noninvasive blood glucose monitoring in the market with their technologies.

Another approach of hypoglycaemia detection is based on the physiological effects of hypoglycaemia on the body. Based on this approach, several studies have investigated hypoglycaemia detections by means of hypoglycaemic effects on the heart (Alexakis et al., 2003, Nguyen et al., 2008, Ling and Nguyen, 2011), brain (Nguyen and Jones, 2010, Laione and Marques, 2005, Claus B. Juhl, 2010) and skin (Johansen et al., 1986). This hypoglycaemia detection approach utilized intelligent algorithms to process hypoglycaemic physiological effects. In other words, this hypoglycaemia detection approach concerned about two things. The first concern identifies physiological aspects which significantly respond to hypoglycemia. The second one explores intelligent algorithms which can process these physiological

effects and yield a powerful hypoglycemic detection system.

During the past decade, several studies investigated electrocardiographic (ECG) parameters which contributed to hypoglycaemia detection. Ghevondian et al. (1997) and Hastings et al. (1998) developed a hypoglycaemia detection system which used the inputs of heart rate and skin impedance. The inputs were then completed with QT interval, which is the interval from the Q point to the end of the T-wave of an electrocardiogram (Nguyen et al., 2006, Nguyen et al., 2007). The difference between two consecutive heart rates and the difference between two consecutive QT intervals were introduced for hypoglycaemia detection in 2011 (Ling and Nguyen, 2011). Another research group studied hypoglycaemia detection using different ECG parameters: RT interval, T wave amplitude, T wave skewness and T wave kurtosis (Alexakis et al., 2003). Three years later, they investigated hypoglycaemia detection using two ECG parameters, which are T wave amplitude and RT interval (Alexakis et al., 2006).

The above studies of hypoglycaemia detection developed algorithm techniques to process ECG parameters. Ghevondian et al. (1997) and Hastings et al. (1998) implemented fuzzy neural network and self-organizing fuzzy estimator, respectively, for hypoglycaemia detection. Alexakis et al. (2003) and Alexakis et al. (2006) developed artificial neural network and knowledge-based system, respectively, for their hypoglycaemia detection system. Nguyen et al. (2006) and Nguyen et al. (2007) employed a neural network. Genetic-algorithm-based multiple regression was introduced for hypoglycaemia detection by (Ling and Nguyen, 2011).

1.2 THE PROBLEM STATEMENT

Klonoff (2005) presented a review of several continuous glucose monitoring devices. Some of the devices have been approved by the U.S. Food and Drug Administration (FDA) or CE marking (Europe). Alarm for indicating hypoglycaemia was included in the devices. In the review, the Guardian Continuous Monitoring (Medtronic MiniMed) provided a hypoglycaemia alarm of glucose level ≤ 70 mg/dl with 67% sensitivity[1], 90% specificity[2] and 47% false alert[3]. The review also presented the performance of a hypoglycaemia alarm of the continuous glucose monitoring system (CGMS) Gold with different threshold values; using the glucose level threshold ≤ 60 mg/dl the sensitivity and specificity were 49% and 42%, respectively. The GlucoWatch G2 Biographer (GW2B) was also reviewed with 23% sensitivity and 49% specificity in the glucose setting ≤ 60 mg/dl. In summary, the performances of the hypoglycaemic alarms still need improvement.

The hypoglycaemia detection devices based on physiological effects which correspond to the fall of low blood glucose levels have been reported. The Sleep Sentry™ provides an alarm for hypoglycaemia considering to a fall in skin temperature and electrical conductance. In the study of 24 type-1 diabetic patients the Sentry generated 150 alarms without evidence of hypoglycaemia (Hansen and Duck, 1983). Eight of eighteen insulin-dependent diabetic subjects failed to activate the hypoglycaemia alarm of the Sentry despite a mean plasma glucose of 50.5 ± 8.2 mg/l (Clarke et al., 1988). Another device, HypoMon®, which is from AiMedics Pty Ltd, detects hypoglycaemia based on skin impedance, heart rate and *QTc* interval (Nguyen et al., 2006, Nguyen et al., 2009) and is still in the investigation stage. So far, to the best of my knowledge, hypoglycaemia detection systems which are based on the physiological effects still require further validation and clinical

---

[1] Sensitivity refers to ability of a test to correctly identify those patients with the disease.
[2] Specificity refers to ability of a test to correctly identify those patients without the disease.
[3] A false alert is a detection alert which is issued when a defined disease does not exist.

studies of the devices, before they can be adopted for worldwide clinical practices. In addition, research regarding this issue is still being investigated (Remvig et al., 2012, Nguyen et al., 2012).

As described above several ECG parameters have been tested for hypoglycaemia detections. There are the other ECG parameters which could contribute to hypoglycaemia detection, such as the width of electrocardiographic T–wave (Koivikko ML et al., 2008) and the QT interval corrected using Fridericia (Lee et al., 2005). However, these ECG parameters are not yet investigated for a hypoglycaemia detection system. Thus, questions arise in relation to the performances of hypoglycaemia detection systems which employ the ECG parameters.

A further question arises in relation to algorithms which, as yet, have not been investigated for hypoglycaemia; a study is necessary to investigate the algorithms for hypoglycaemia detection. Support vector machine (SVM) is an algorithm which, as yet, has not been applied to hypoglycaemia detection. SVM is a classification technique which is successfully employed in many applications (Barakat et al., 2010), including a cardiac signal classification (Georgoulas and Stylios, 2006). It also showed good generalization as a classifier, even with a small size sample in the training (Duin, 2000). Therefore, because of these advantages, SVM is selected as a classification technique for this research. Furthered investigation is to be conducted in relation to a hybrid system which employs SVM. Questions arise in relation to the contribution of the hybrid system to the improvement in performance of the hypoglycaemia detector.

1.3 OBJECTIVES

Considering the problem statement above, the main purpose of this research is to introduce novel computational intelligent techniques for hypoglycaemia detection. The detection is based on electrocardiographic (ECG) parameters. Hence,

two main objectives are explored.

The first objective identifies ECG parameters which significantly respond to hypoglycemia. The ECG parameters include the parameters which relate to the repolarization phase. The identification is used to find potential ECG parameters which contribute to the performance of hypoglycaemia detection.

The second objective is to introduce several intelligent algorithms for hypoglycaemia detection. The support vector machine (SVM) classifier is the first algorithm introduced for hypoglycaemia detection in this research. The second algorithm is a hybrid of SVM with particle swarm optimization (PSO), which is intended to improve the performance of the first algorithm. PSO is an evolutionary technique based on the movement of swarms and is inspired by the social behavior of bird flocking and fish schooling (del Valle et al., 2008). The swarm optimization is employed to optimize SVM parameters in order that the SVM perform well for hypoglycaemia detection. The third algorithm is the improvement of the second algorithm where a fuzzy inference system (FIS) is included. This algorithm involves SVM, FIS and a swarm optimization. The FIS is used to process some ECG parameters differently to find a better performance of hypoglycaemia detection. FIS is an effective intelligent system which employs fuzzy logic and fuzzy set theory (Ly et al., 2009). Its frameworks are based on the concepts of fuzzy set theory, fuzzy if-then rules, and fuzzy reasoning. The advantages of FIS include its ability to handle linguistic concepts and a universal approximator, performing a nonlinear relationship between inputs and outputs. In general, the proposed algorithms are implemented using MATLAB. This objective yields models for hypoglycemia detection which are realized in the form of software. In addition, the proposed algorithms are compared with the other algorithms, including genetic-algorithm-based multiple regression with fuzzy inference system (Ling and Nguyen,

2011), artificial neural network (Alexakis et al., 2003) and linear discriminant analysis (Alexakis et al., 2006).

All the algorithms are investigated with clinical electrocardiographic data. The data is collected from a hypoglycaemia study of type 1 diabetic patients.

1.4 CONTRIBUTION OF THE DOCTORAL RESEARCH

This doctoral research has provided contributions to hypoglycaemia detection models. Novel algorithms and ECG parameters have been introduced for hypoglycaemia detection. Considering the results provided by this doctoral research, several papers have been presented, either in journal paper or conference papers mentioned in Section 1.6. It is published by the Biomedical Engineering Society™ (www.bmes.org). The full–reviewed conference papers are presented in conferences organized by IEEE Engineering in Medicine & Biology Society (www.embs.org) and IEEE Computational Intelligence Society (www.ieee-cis.org).

The contributions of this doctoral research can be described in the following:

(i) The doctoral research has introduced a hypoglycaemia detection model which employs SVM. The model is presented in Nuryani et al. (2010b). The models with different SVM parameters and different kernel functions are tested and their performances are presented in Chapter III.

(ii) The doctoral research also has introduced a hypoglycaemia detection model which employs a hybrid of swarm optimization and SVM (SSVM). This model is presented in Nuryani et al. (2012a) and Nuryani et al. (2011). This model includes a swarm optimization to optimize SVM parameters to find an optimal hypoglycaemia detection. The model has been tested with different inputs and its performance has been compared with the other models, as described in Chapter IV.

(iii) A novel hybrid swarm optimization, fuzzy inference system (FIS) and SVM

(SFSVM) model has been investigated for hypoglycaemia detection. The model is presented in Nuryani et al. (2012b). This hybrid system includes FIS to process some inputs and its outputs are fed to SVM. Swarm optimization in this hybrid system is used to optimize FIS and SVM parameters. Chapter V of this dissertation describes the model.

(iv) Ventricular repolarization parameters: the interval from Q-point to the end of T-wave (QTp_c), T-wave interval or the interval from the beginning of T-wave to the end of T-wave ($ToTe_c$), the interval from R-peak to the paek of T-wave (RTp_c) and the interval from the peak of T-wave to the end of T-wave ($TpTe_c$) are introduced for hypoglycaemia detection (Nuryani et al., 2012a, Nuryani et al., 2010a). The parameters are investigated in experiments using different algorithms, as presented in Chapter III – Chapter V.

1.5 STRUCTURE OF THE DISSERTATION

The dissertation consists of 6 chapters, appendix and reference. The contents are organized sequentially from the first chapter until the last chapter. The contents commence with the introduction of hypoglycaemia and finish with the conclusion of the dissertation.

Chapter II presents a review of literature relevant to hypoglycaemia detection. It includes hypoglycaemia, physiological effects of hypoglycaemia, relation of hypoglycaemia to cardiac dysrhythmia. The existing techniques of hypoglycaemia detection are also presented in this chapter. The techniques include hypoglycaemia detections which use ECG parameters from its initial research until recent developments. This chapter is finalized by a brief outline of the proposed hypoglycaemia detection strategy.

Chapter III describes the hypoglycaemia detection model which uses SVM with the input of an electrocardiogram. Initially, the description is of the general construction and is then followed by more details of the parts of the construction.

The parts include ECG acquisition, feature extraction and SVM. Several experiments of hypoglycaemia detections with different SVM parameters are presented. The presentation of this chapter is completed with a discussion and conclusion.

Chapter IV presents a hypoglycaemia detection model employing a hybrid of particle swarm optimization (PSO) and SVM (called SSVM). SSVM, essentially, is to improve the performance of the SVM by finding the optimal SVM parameters. Thus, by using the optimal parameter, the SSVM could perform well. Several variations on SSVM are developed to find the best one. The variations include SSVM with different kernel functions and SSVM with different inputs. In addition, the performance of SSVM is also compared with the other methods. This chapter is completed with a discussion and conclusion.

Chapter V presents a hypoglycaemic detection strategy by including a fuzzy inference system (FIS) to SSVM, which emerge as SFSVM. SFSVM provides different process for ECG parameters which provide a new input for the SVM part of the SFSVM. Variation of the inputs and different membership functions are investigated in the experiments. The related discussion and conclusion are presented in the end of this chapter.

Chapter VI provides discussion and conclusion. The discussion includes the comparison of the three hypoglycaemia detection models (SVM, SSVM and SFSVM). The discussion also presents the future research for hypoglycaemia detection and the limitation of this research. Conclusion is presented in the end of this chapter.

1.6 PUBLICATIONS PRESENTED DURING THE DOCTORAL RESEARCH

The following journal and conference papers have been published during the doctoral research:

Journal paper:

Nuryani, N., Ling, S. & Nguyen, H. 2012a, 'Electrocardiographic Signals and Swarm-Based Support Vector Machine for Hypoglycaemia Detection', *Annals of Biomedical Engineering*, vol. 40, no. 4, pp. 934-945. (ERA[4] rank: A*; Impact Factor: 2.374)

Conference papers:

Nuryani, N., Ling, S. S. H. & Nguyen, H. T., 2012b, 'Hybrid Particle Swarm - based Fuzzy Support Vector Machine for Hypoglycaemia Detection, in *Proceedings of the IEEE World Congress on Computational Intelligence*, pp. 450 - 455 (ERA rank: A).

Nuryani, N., S. Ling, and H. T. Nguyen, 2011, 'Ventricular repolarization variability for hypoglycaemia detection', in *Proceedings of the 32nd Annual International Conference of the IEEE Engineering in Medicine and Biology Society*, pp. 7961-7964 (ERA rank: A)

Nuryani, N., S. H. Ling, and H. T. Nguyen, 2010a, 'Hypoglycaemia detection for type 1 diabetic patients based on ECG parameters using fuzzy support vector Machine,' in *Proceedings of the IEEE World Congress on Computational Intelligence*, pp. 2253 - 2259. (ERA rank: A)

Nuryani, N., S. Ling, and H. T. Nguyen, 2010b, 'Electrocardiographic T-wave peak-to-end Interval for hypoglycaemia detection,' in *Proceedings of the 32nd Annual International Conference of the IEEE Engineering in Medicine and Biology Society*, pp. 618-621. (ERA rank: A)

S. H. Ling, N., Nuryani and H. T. Nguyen, 2010, 'Evolved fuzzy reasoning model for hypoglycaemic detection', in *Proceedings of the 32nd Annual International Conference of the IEEE Engineering in Medicine and Biology Society*, pp. 4662 - 4665. (ERA rank: A)

---

[4] ERA: The Excellence in Research for Australia (www.arc.gov.au/era/)

CHAPTER 2.
LITERATURE REVIEW

The review of literature about hypoglycaemia and the existing hypoglycaemia detections provides the justification of the proposed model. The description of hypoglycaemia and its effects on the heart is provided to give us an understanding of how electrocardiograms could be used for hypoglycaemia detection. Presentation of the existing hypoglycaemia detections could provide the idea for a novel strategy which provides an alternative in hypoglycaemia detection technologies. The proposed strategy for hypoglycaemia detection is presented in the last part of this chapter.

2.1 HYPOGLYCAEMIA

Blood glucose is essential for the body to function properly as a whole. Typically, the glucose level in the body is maintained in the normal range by a homeostasis system. If the blood glucose level in the body is lower than the normal level (called hypoglycaemia) a mechanism in the body works to return the blood glucose level to a normal range. However, this mechanism is not working properly in patients with type-1 diabetes.

Hypoglycaemia is a common complication in patients with type 1 diabetes. Type-1 diabetes is a disease with an attribute of absolute insulin deficiency resulting in hyperglycaemia (Braak and Stades, 2009). The deficiency of absolute insulin is caused by autoimmune-mediated destruction of the pancreatic β-cells. The

pancreatic β-cell is a cell which normally produces insulin. Type-1 diabetes mellitus (T1DM) is also called insulin-dependent diabetes mellitus (IDDM). A T1DM patient is dependent on insulin which is necessary to maintain the blood glucose level.

The definitions of hypoglycaemia were presented in several studies. The blood glucose level of 3.9 mmol/l (70 mg/dl) is proposed by the American Diabetes Association as a threshold to represent hypoglycaemia (American Diabetes Association Workgroup on Hypoglycemia, 2005). A different definition was provided by the Diabetes Control and Complications Trial (DCCT). DCCT defines hypoglycaemia by considering the ability of the affected individual to treat hypoglycaemia. Using the definition, there were mild and severe levels of hypoglycaemia. Mild hypoglycaemia was indicated by the ability to self-treat, while severe hypoglycaemia was indicated by the requirement of external assistance to induce recovery of the affected individual (The Diabetes Control and Complications Trial Research Group, 1997).

Hypoglycaemia could be caused by a mismatch between the blood glucose level and insulin. The mismatch occurs because there is either too much injected insulin compared to the meal or not enough meal compared to insulin. Injected insulin decreases the blood glucose level, contrary to the meal which increases the blood glucose level. Extra physical activity also leads to hypoglycaemia through accelerated absorption of insulin and depletion of muscle glycogen stores. Another cause of hypoglycaemia is alcohol which enhances the risk of prolonged hypoglycaemia by inhibiting hepatic gluconeogenesis. Strachan (2007) listed six causes of hypoglycaemia in type-1 diabetes: (i) inappropriate insulin injection, (ii) inadequate exogenous carbohydrate, (iii) increased carbohydrate utilization, (iv) decreased endogenous glucose production, (v) increased insulin sensitivity and (vi) decreased insulin clearance.

In glycaemic control, people with type-1 diabetes reduce their high level of blood glucose to find a normal glycaemia. This reduction has been of benefit in preventing or delaying microvascular complications and macrovascular events, whereby T1DM patients have the possibility of increasing life expectancy and improving the quality of life. However, error of dosage or timing of insulin administration is common in glycaemic control and can happen in several ways. For example, the ambient temperature and injection depth could affect the profile of an insulin time-action. DCCT suggested that the incidence of severe hypoglycaemia in the intensively treated group was threefold of that in a conventionally treated group (The Diabetes Control and Complications Trial Research Group, 1997).

Physiological changes occurred when blood glucose concentration fell to a
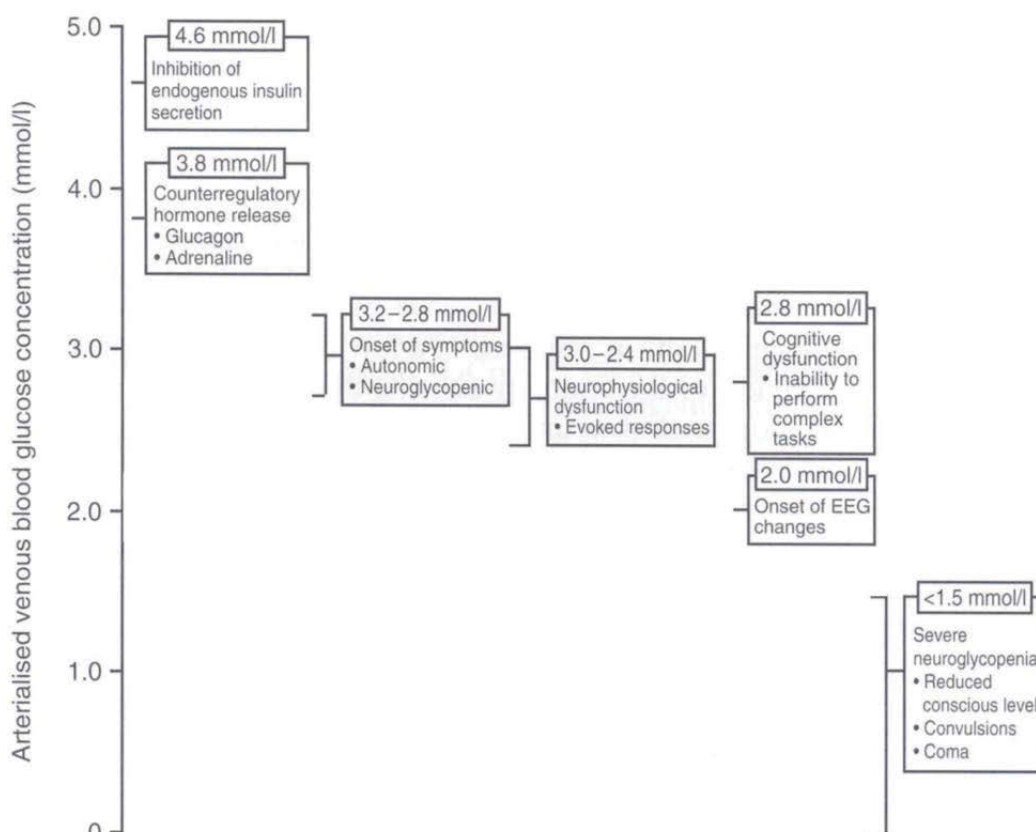
Figure 2.1: Counterregulatory mechanisms including hormones secretion and onset of physiological, symptomatic and cognitive changes in response to different blood glucose level thresholds (Frier and Fisher, 2007).

certain level (Frier and Fisher, 2007). These changes are a counterregulatory to hypoglycaemia, and become the mechanism for raising blood glucose levels to normal levels (Figure 2.1). When a falling of blood glucose level is detected, a mechanism to modulate insulin secretion is activated. This is followed by the secretion of glucagon and epinephrine hormones, activated by the brain. This secretion stimulates the peripheral autonomic nervous system, particularly the sympathoadrenal system. In the liver, glucagon stimulates glycogenolysis and gluconeogenesis.

2.2 EFFECT OF HYPOGLYCAEMIA ON THE ELECTRICAL ACTIVITY OF THE HEART

In recent years, a number of studies have demonstrated that hypoglycaemia causes ECG alteration. The ECG alteration was indicated by the alteration of several selected ECG parameters. Table 2.1 lists seven ECG parameters altered by hypoglycaemia, reported by several studies. The alteration of ECG parameters by hypoglycaemia could happen in patients with type-1 diabetes (Heger et al., 1996); type-2 diabetes (Marques et al., 1997) or healthy subjects (Robinson et al., 2002).

Moreover, both hyperinsulinemic hypoglycaemia and spontaneous hypoglycaemia could result in ECG alteration. In hyperinsulinemic hypoglycaemia

Table 2.1: Studies of alterations in ECG during hypoglycaemia. *a, b, c, d, e, f, g, h, i, j* **represent the studies as listed in the bottom of the table.** ″x″ **is to show that the associated ECG parameter is significant to indicate hypoglycaemia in the associated study.**

ECG parameter	*a*	*b*	*c*	*d*	*e*	*f*	*g*	*h*	*i*	*j*
HR	x						x			
QTcb		x	x	x	x		x	x	x	
QTcf						x		x		x
T-wave amplitude							x	x		
T-wave area							x	x		
R-wave amplitude								x		
R-wave area								x		

a : Heger et al. (1996)   with 24 T1DM and 7 health participants
b : Marques et al. (1997)   with 8 T1DM and 7 T2DM participants
c : Robinson et al. (2002) with 17 healthy participants
d : Robinson et al. (2003) with 10 healthy participants
e : Murphy et al. (2004)   with 44 T1DM participants
f : Lee et al. (2005)   with 8 T1DM participants
g: Koivikko et al. (2008) with 16 T1DM and 8 healthy participants
h : Laitinen et al. (2008)   with 18 healthy participants
i : Christensen et al. (2010) with 21 T1DM participants
j : Lipponen et al. (2011) with subject of 13 T1DM and 9 healthy participants
    HR: heart rate
    QTcb: The corrected QT interval with Bazett formula
    QTcf: The corrected QT interval with Fridericia formula
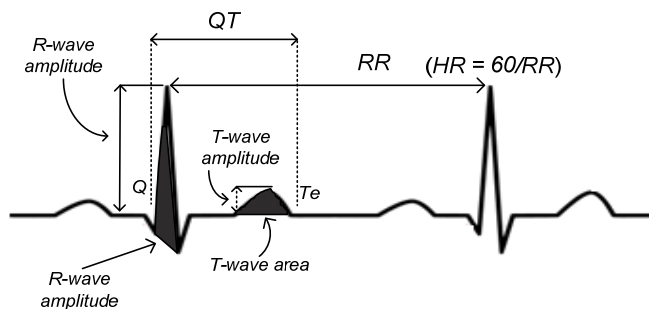
Figure 2.2: QT interval in an electrocardiogram

the plasma insulin concentration was acutely raised and maintained at a level by a continuous infusion of insulin. Meanwhile, the plasma glucose concentration was held constant at the hypoglycaemic level by a variable glucose infusion. For example, in the study of (Lee et al., 2005) insulin (Human Actrapid; Novo Nordisk Pharmaceuticals, Crawley , UK) was infused to maintain the blood glucose level of the subjects in the level of 2.5 mmol/l. Spontaneous hypoglycaemia was the hypoglycaemia which happens without excessive insulin. For example, in the study of Robinson et al. (2004), blood glucose levels were taken at hourly intervals from the subjects of the study while they are sleeping and following their normal routine, without an excessive infusion of insulin. It was suggested that the ECG change provoked by spontaneous hypoglycaemia was smaller than that by hyperinsulinemic hypoglycaemia (Robinson et al., 2004, Marques et al., 1997).

As presented in Table 2.1, the corrected *QT* interval (*QTc*) indicates significant differences in hypoglycaemia as against euglycaemia. *QT* interval represents the duration of ventricular depolarization and subsequent repolarization
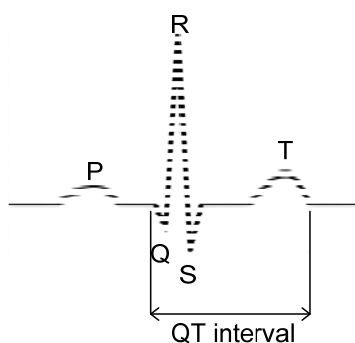
Figure 2.3: QT interval in an electrocardiogram

to occur. In the heart's electrical cycle, the interval is from the start of the Q wave to the end of the T wave (Figure 2.3). The *QT* interval includes the *QRS* interval, representing depolarization of ventricles, and the T wave, representing repolarization of the ventricles. Essentially, the *QT* interval relates to action potentials of the heart muscles, necessary for the electrical conduction system of the heart. The relation is illustrated in Figure 2.4. The electrical activity detected in surface ECG is the normal coordinated electrical functioning of the whole heart, which is attributed to action potential in individual cardiac cells.

Marques et al. (1997) investigated a *QTc* change by hypoglycaemia in 8 type-1 and 7 type-2 diabetic subjects. To make sure that the *QTc* change was not caused by heart disease, none of the type-1 diabetic patients had evidence of microvascular complications. The subjects did not have autonomic neuropathy. All subjects had a normal ECG and did not have symptoms of cardiovascular diseases. In the study, the blood glucose level was clamped for two hours for hypoglycaemia
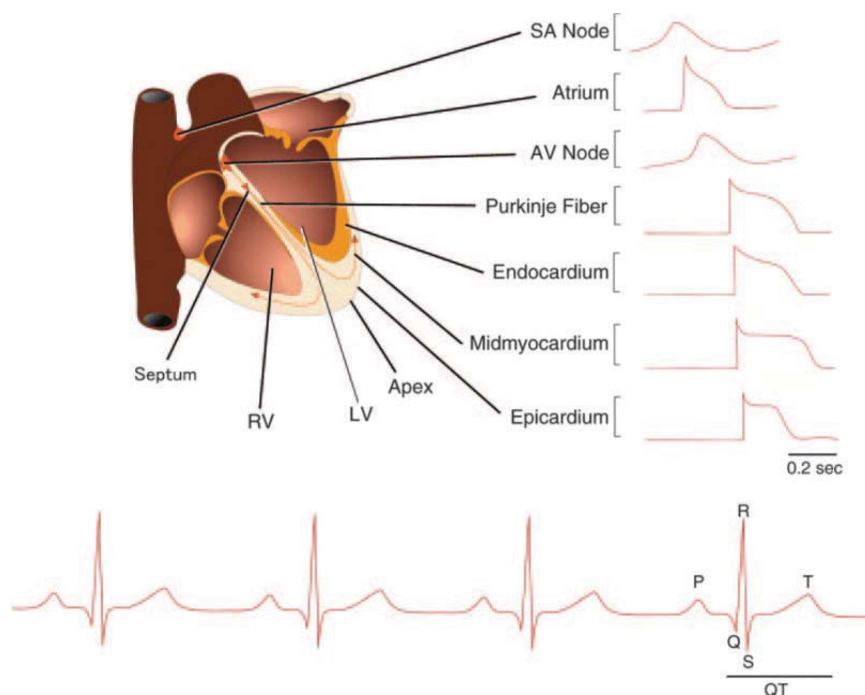
Figure 2.4: Schematic of a human heart accomplished with typical action potential waveforms in different regions and an electrocardiogram (Nerbonne and Kass, 2005).

at around 3.0 mmol/l and euglycaemia at 5.0 mmol/l. The result showed that *QTc* in hypoglycaemia was longer than in the baseline. At 60-minute hypoglycaemic clamp *QTc* of type-1 diabetes was 583(425-620) ms, against 421(362-436 ms) in euglycaemia.

Robinson et al. (2003) studied the mechanism of *QTc* interval prolongation affected by hypoglycaemia. A subject group of the study underwent two euglycaemic and two hypoglycaemic clamps. One euglycaemic and one hypoglycaemic clamp were with β-blockade, and another two clamps were without β-blockade. β-blockade is a sympatholytic drug that binds the action of the sympathetic nervous system of the heart. In pharmacology it is prescribed to a patient with cardiac arrhythmia. In the study, β-blockade was given by pre-treating a patient for seven days with atenolol 100 mg daily before one euglycaemic clamp and one hypoglycaemic clamp. The result of the study was that *QTc* increased significantly in the hypoglycaemia without β-blockade but insignificantly in hypoglycaemia with β-blockade. The result indicates that β-blockade could prevent the *QTc* prolongation. As the characteristic of β-blockade, the prevention was by counteracting the sympathoadrenal activation. In other words, sympathoadrenal activation was responsible for the *QTc* prolongation during hypoglycaemia.

Two studies (Christensen et al., 2010, Koivikko et al., 2008) presented the impact of two correction formulas which were Bazett and Fridericia formulas for *QT* interval prolongation during hypoglycaemia. In the two studies, during hypoglycaemia, the *QT* interval corrected by Bazett formula (QTcb) increased statistically significantly, but the *QT* interval corrected by Fridericia formula (QTcf) was not associated with a statistical change. However, in another study, the *QT* interval corrected by Fridericia formula statistically significantly increased during hypoglycaemia (Lipponen et al., 2011). Using the Bazett formula, *QT* is corrected by dividing it by the square root of the electrocardiographic RR interval; $QT_{cb} =$

QT/(RR)$^{1/2}$ (Moss, 1993). Using the Fridericia formula, QT is corrected by dividing it by the cube root of the electrocardiographic RR interval; QT$_{cf}$ = QT/(RR)$^{1/3}$ (Fridericia, 2003).

Effects of hypoglycaemia on T-wave amplitude and T-wave of electrocardiogram (Figure 2.5) were investigated by Koivikko et al. (2008). The two ECG parameters represent the shape of the T-wave. The subjects of the study were 16 IDDM aged 32±8 years and 8 healthy participants aged 34±10 years. The diabetic duration of the subjects was 13 years (range 2 – 29 years). All subjects had normal ECGs and none of them had heart disease. The result showed that the area and the maximum amplitude of T-wave were significantly lower in hypoglycaemia than those of euglycaemia. The hypoglycaemia and euglycaemia were clamped in 2.0–2.5 mmol/l and 4.5–5.5 mmo/l, respectively.

2.3   EXISTING STRATEGIES OF HYPOGLYCAEMIA DETECTION

Early warning of a hypoglycaemia event can play a significant role in preventing hypoglycaemia. Garg et al. (2006) studied the effectiveness of glucose monitoring in 91 subjects with Type 1 diabetes. They found that subjects who wore the glucose monitor spent 21% less time in hypoglycaemia, compared with the
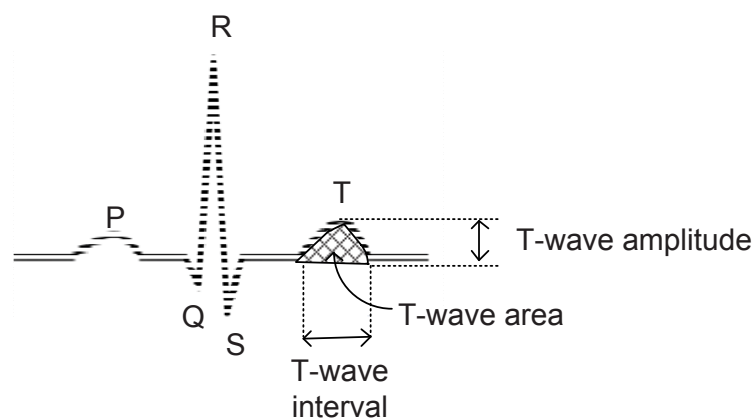
Figure 2.5: Illustration of T-wave interval, T-wave amplitude
and T-wave area in an electrocardiogram

control subjects.

Hypoglycaemia can be detected by a glucose monitor with an alarm system. The alarm system was active when a detected blood glucose level passes a defined threshold of hypoglycaemia. An important stage of glucose monitoring technologies was to be found in the Ames Reflectance Meter (Oliver et al., 2008). The Ames Reflectance Meter was the first glucose meter which can automatically assess the color change of enzyme-based reagent strips. The color wasinfluenced by the glucose concentration. The assessed color can result in a number which indicates a blood glucose concentration. Before the advent of the Ames Reflectance Meter, blood glucose level was measured by reading the color change according to a chart (by eye).

Following the Ames Reflectance Meter, various methods for hypoglycaemia detection were developed. Klonoff (2005) presented five continuous glucose monitors (CGMs) approved by FDA or CE mark, as in Table 2.2. FDA (Food and Drug Administration) is an agency of the United States Department of Health and Human Services, and CE mark (abbreviation of French: *Conformité Européenne*) is a mandatory mark for products sold on the European market. Four of the five CGMs are with the alarm which is active when the measured blood glucose level passes a defined threshold.

Regarding the frequency of measurement, generally there are two types of blood glucose measurement techniques: point sample and continuous. The point sample or intermittent measurement of blood glucose uses a finger-prick glucose meter or urine test. Glucose-level intermittent-measurement is not properly suitable for hypoglycaemia detection because of its limited frequency of measurement. In this case the continuous method is more suitable. It varies in invasiveness, from non-invasive, to minimally invasive or invasive. In the continuous method, there are two options which are transdermal and optical methods. Further variants of the

Table 2.2: Specification of continuous glucose monitoring [adopted from Klonoff (2005)]

Product	Continuous Glucose Monitoring System Gold	GlucoWath G2 Biographer	Guardian Telemetered Glucose Monitoring System	GlucoDay	Pendra
FDA approved	Yes	Yes	Yes	No	No
CE marked	Yes	Yes	Yes	Yes	Yes
Year first approved or marked	1999	2001	2004	2001	2004
Sensor type	Minimally invasive	Minimally invasive	Minimally invasive	Minimally invasive	Non-invasive
Sensor mechanism	Enzyme-tipped catheter	Reverse iontophoresis	Enzyme-tipped catheter	Microdialysis	Impedance spectroscopy
Sensor location	Subcutaneous abdomen	External on arm or forearm	Subcutaneous arm	Subcutaneous abdomen	External on wrist
Sensor warmup	2	2	2	0	1
Calibrations per lifetime of sensor	12	1	12	1	20
Sensor lifespan (h)	72	13	72	48	3 months
Frequency of testing (min)	5	10	5	3	1
Time of blood glucose data display	Retrospective	Real time	Retrospective	Real time retrospective	Real time
Alarm	No	Yes	Yes	Yes	Yes

glucose measurement techniques are described in Figure 2-5, adopted from Oliver et al. (2008).

Another method of hypoglycaemia detection was through measuring the physiological responses of hypoglycaemia on the body. Hypoglycaemia detections which used this method mostly used a noninvasive technique. Some of them have been available on the market, and their performances are being studied. Others are
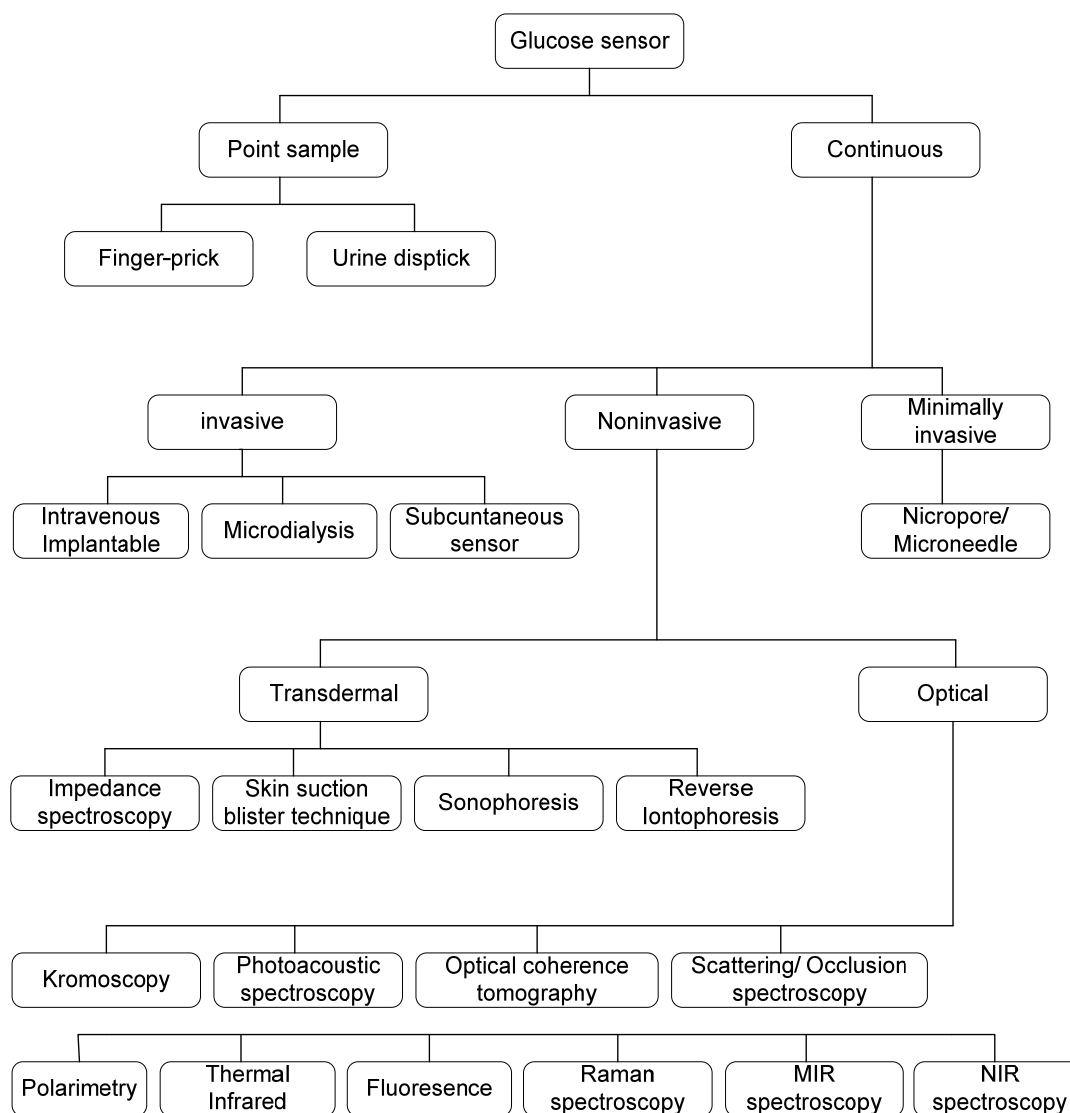
Figure 2.6: Methods of glucose sensor [adopted from (Oliver et al., 2008)].

still in the clinical study stage or in research development before going to market.

The following is the description of noninvasive techniques for hypoglycaemia detection. It presents one method of transdermal which is iontophoresis and one method of optic which is near-infrared spectroscopy. The other presented techniques are those which employed the following physiological effects: skin temperature, skin conductance, electroencephalography and electrocardiography.

2.3.1   Iontophoresis technique

Essentially, an iontophoresis measured glucose concentration by measuring the glucose extracted across the skin. The extraction was conducted by introducing a low electric current to the skin (Leboulanger et al., 2004). The introduction of the electric current was to enhance the extracted glucose at much greater rates through a passive permeability mechanism. The schematic diagram of reverse iontophoresis is described in Figure 2.7. The concept of a glucose meter based on reverse iontophoresis was introduced in 1993 by G. Rao, *et al* (G Rao et al., 1993) using in vitro, and followed by an in vivo study in 1995 (Rao et al., 1995).

GlucoWatch® was the market product for the glucose level meter which works using the principle of reverse iontophoresis. GlucoWatch was worn on the wrist like a wrist watch (Figure 2.8). It, however, had some limitations, which include: two hours for warming-up; sensitivity to an excessive sweating of the skin; reduction of performance by temperature change. It also needed a standard finger-stick meter for a predefined set of measurements, which means that it wasinherently an invasive device. Another limitation is that it provides only three readings per hour, consequently, it is unsuitable as a continuous hypoglycaemic alarm.
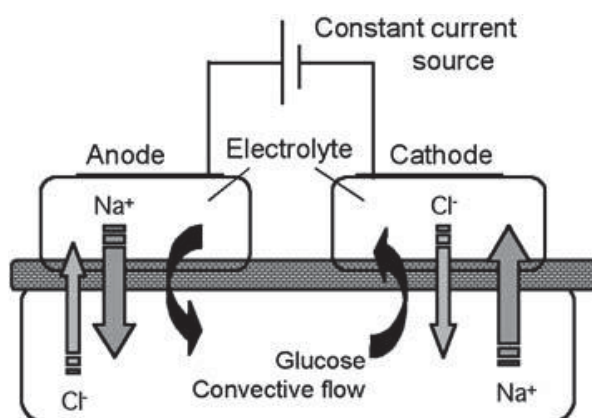
Figure 2.7: Schematic diagram of reverse iontophoresis for glucose extraction through the skin(Sieg et al., 2005).

**Figure 2.8: GlucoWatch G2 Biographer; Cygnus, Inc., Redwood
City, CA (Takahashi et al., 2008)**

2.3.2   Near-infrared spectroscopy (NIR) technique

The Glucose meter, using NIR, works on the basis of optical method using interrogation of light absorbed by an objected tissue, such as the skin. The basic principle of the optical method was that the light absorbed by the objected substance is in parallel with the concentration of the substance. The light was mostly in the near infrared region. Because the object of detection is glucose, the method is designed whereby the absorbed light was in parallel with the concentration of glucose in the substance. One of the optical methods uses dermis as the objected substance (Maruo et al., 2003) as in Figure 2.10.

Limitations of the optical method using near infrared light for blood glucose level measurements was in the technical difficulties to be realized as a commercial instrument. These limitations included calibration bias, time lag and sampling problems. Another issue is the existence of other substances in the skin affecting the measured signal.
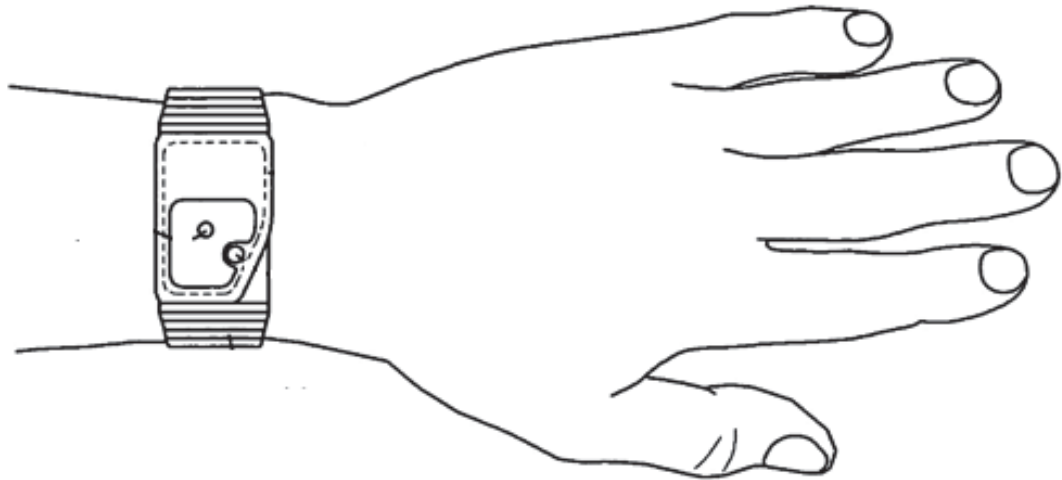
Figure 2.9: A wristwatch-like Diabetes Sentry (Miller and Evans, 2006)

2.3.3   Hypoglycaemia detection using skin temperature and skin conductance

The Sleep Sentry™ (or with its new name of Diabetes Sentry), Figure 2.9, performed an alarm for hypoglycaemia with a base of a fall in skin temperature and change in skin resistance (or skin conductance). According to Hansen and Duck (1983), Sleep Sentry was a wristwatch-like device, utilized with a stainless steel-plated thermistor to monitor the skin temperature. An alarm was activated when the thermistor detects a fall of 2.30C from baseline. The skin resistance was associated with sweat production. A fall from 300 kΩ to 190 kΩ in the skin resistance activates the alarm.
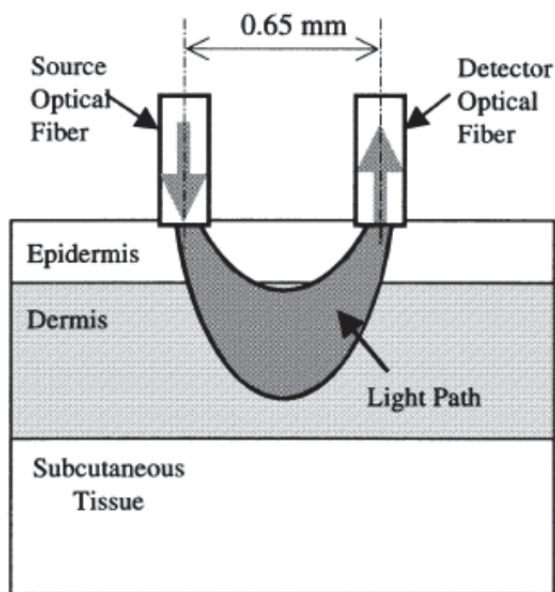
Figure 2.10: Schematic diagram to measure glucose concentration using near infrared wave (Maruo et al., 2003).

Clarke et al. (1988) reported the performance of Sleep Sentry according to a study involving eighteen IDDM subjects in a hospital room. The subjects wore the Sleep Sentry on their wrists, for 20 minutes before the insulin infusion. The result showed that the Sleep Sentry alarm was activated by only 10 (55.6%) of the eighteen subjects despite the plasma glucose of all the subjects not being significantly different. The lowest plasma glucose of the 10 subjects was 52.8±13.8 mg/dl, whereas that of the other 8 subjects was 50.5±8.2 mg/dl. The study also reported that falling plasma glucose to as low as 30 mg/dl did not decrease by 2^0C. Hansen and Duck (1983) studied the Sentry with 24 type-1 diabetic patients. In the study the Sentry generated 150 alarms without evidence of hypoglycaemia. In another investigation on 22 adults with insulin treated diabetes, Sleep Sentry showed performances 67% and 69% in terms of sensitivity and specificity, respectively (Johansen et al., 1986). Ghevondian et al. (1997) presented a correlation between blood glucose levels and skin resistance (or skin impedance) in patients with type-1 diabetes, and healthy subjects, as depicted in Figure 2.11. The graph shows that the skin impedance is lower in hypoglycaemia. The change in skin
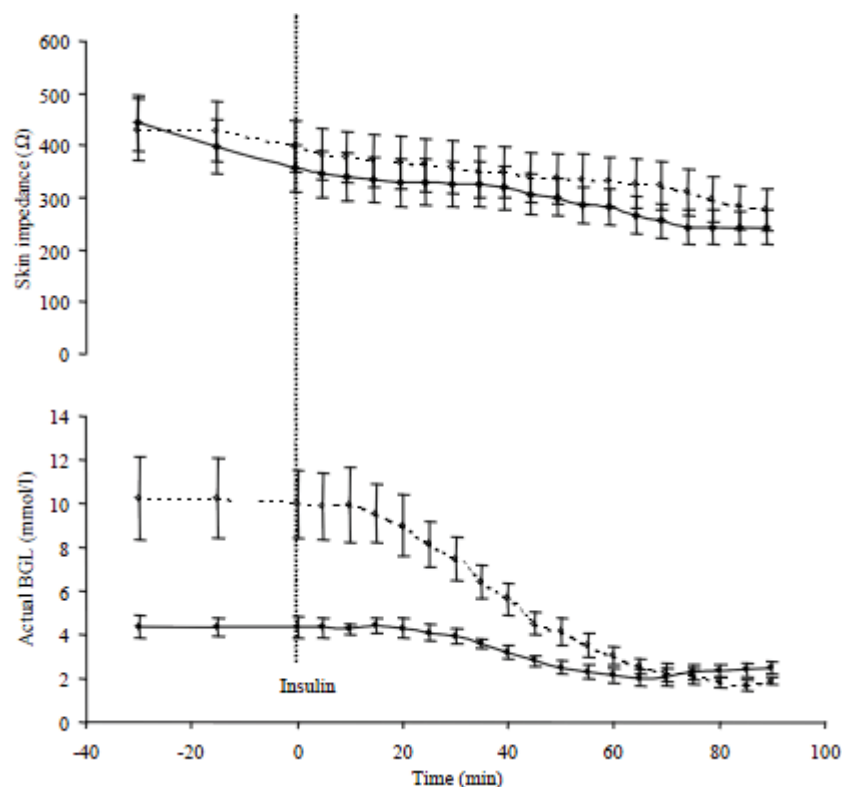
Figure 2.11: Relation of skin impedance and blood glucose level in healthy subjects (group A) and patients with type 1 diabetes (group B) (Ghevondian et al., 1997).

impedance wasinfluenced by sweating. Sweating is an autonomic response of hypoglycaemia (Hepburn et al., 1991).

2.3.4   Hypoglycaemia detection using electroencephalogram

A blood glucose level of the body in the normal range is necessary to the functioning of the brain. Hypoglycaemia, which is an abnormally low blood glucose level, can cause a disturbance in the brain function. A falling blood glucose level to below normal can cause impaired cognitive function. Memory systems are affected significantly by acute hypoglycaemia, particularly working memory and delayed memory (Sommerfield et al., 2003). Electroencephalography (EEG) is a system which measures the electrical function of the brain. An abnormal pattern of EEG can be used to interpret a dysfunction in the brain (Tatum, 2007).

EEG changes caused by insulin-induced hypoglycaemia were investigated
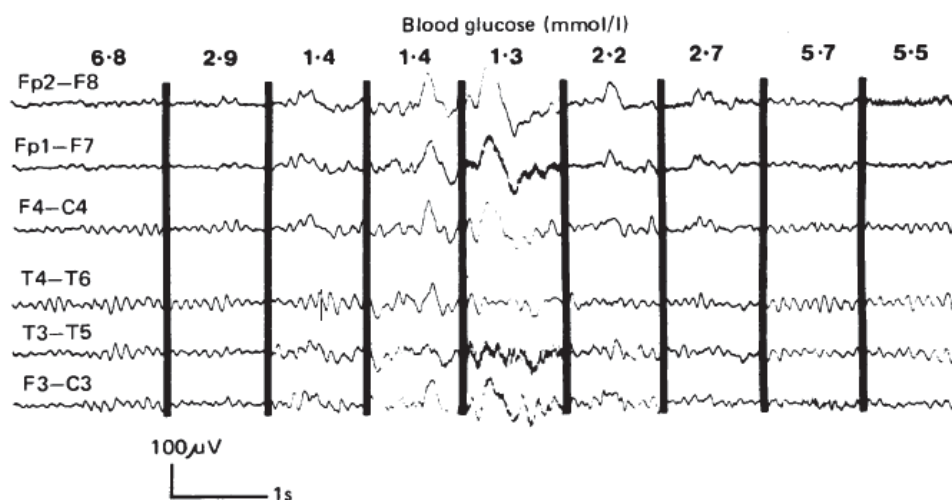
Figure 2.12: EEG of a patient with different blood glucose levels in the study of Pramming et al. (1988).

by Pramming et al. (1988). The investigation involved 13 patients with type-1 diabetes. At a blood glucose level of 2.0 mmol/l electroencephalographic alpha activity decreased abruptly, and simultaneously the theta activity increased. The EEG at different blood glucose levels are presented in Figure 2.12. Laione and Marques (2005) developed a hypoglycaemia detection using EEG. They evaluated the EEG-based hypoglycaemia detection by involving 8 type–1 diabetic patients. In this study, the difference of hypoglycaemic and nonhypoglycaemic EEG is presented, as shown in Figure 2.13. Using artificial neural network (ANN) training

on EEG recorded from the subjects, the classification results of this study are 49%, 76% and 32.5% in terms of accuracy, sensitivity and specificity.

In 2010, H.T. Nguyen and T.W. Jones studied the use of EEG signals for hypoglycaemia detection (Nguyen and Jones, 2010). This study used 2-second epochs EEG, with spectral analysis of four frequency bands: delta (0.5-3.0 Hz), theta (3.5-7.5 Hz), alpha (8-13 Hz) and beta (13.5-45 Hz). The developed hypoglycaemia detection obtained a performance with 78% and 55% in terms of sensitivity and specificity, respectively.

2.3.5 Hypoglycaemia detection employing electrocardiogram

There are at least two main objects explored in hypoglycaemia detection research which employ the electrical activity of the heart. The two objects are (i) ECG parameters which are used for the input of the hypoglycaemia detection system and (ii) the strategy to process the ECG parameters. The appropriate inputs and strategy need to be investigated to find a hypoglycaemic detection with high performance.

Inputs of the electrocardiogram (ECG) based-hypoglycaemia detection
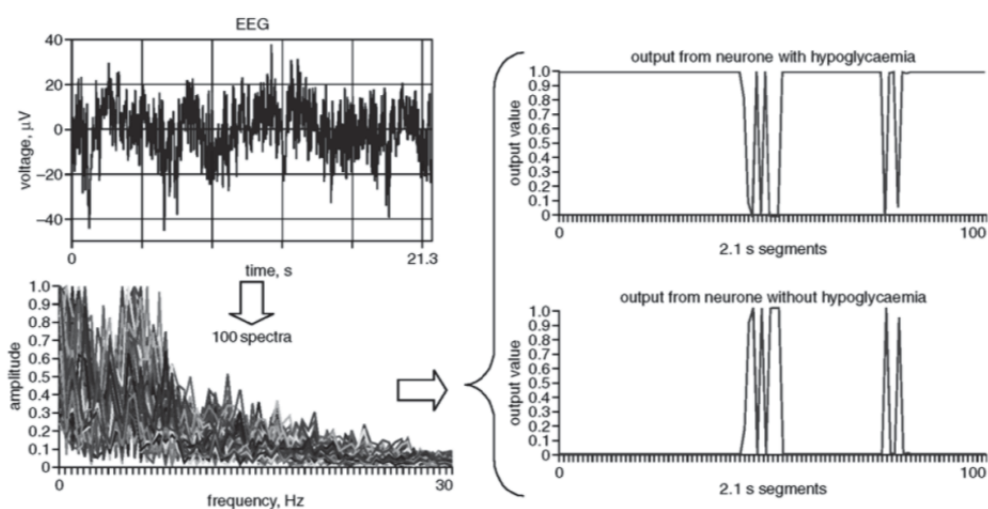
Figure 2.13: Output of neurone in hypoglycaemic and nonhypoglycaemic state(Laione and Marques, 2005)

Hypoglycaemia detections with a base of ECG parameter changes in relation to hypoglycaemia were studied by several research groups. Table 2.3 lists ECG parameters, and the associated intelligent techniques, employed for hypoglycaemic detection. Initially, the idea of using heart rate for hypoglycaemia detection was presented in 1997. Three years later, QT interval was issued to be used for hypoglycaemia detection. After that, various studies developed hypoglycaemia detections using other ECG parameters. At the same time during the decade, methods using intelligent techniques were developed to classify ECG parameters for hypoglycaemia detection systems.

Table 2.3: ECG parameter and algorithm used for hypoglycaemia detection

ECG Parameters	Method
Heart rate (Ghevondian and Nguyen, 1997) (Hastings et al., 1998)	Fuzzy system
Heart rate (Ghevondian et al., 1997)	Fuzzy neural network
QT interval (Harris et al., 2000)	
RT interval, T wave amplitude, T wave skewness and T wave kurtosis (Alexakis et al. 2003)	Artificial neural networks
Heart rate, QT interval (Nguyen et al., 2006)	Neural-Network
T wave amplitude and RT interval (Alexakis et al. 2006)	Knowledge-Based Electrocardiogram
Heart rate, QT interval (Nguyen et al., 2007)	Bayesian neural network algorithm
Heart rate, QT interval (Ling and Nguyen, 2011)	Genetic-alghorithm-based multiple regression
Heart rate, QT interval (Chan et al., 2011b)	Neural network based rule discovery system

The idea of heart rate to be used for input of hypoglycaemia detection was presented in 1997 (Ghevondian and Nguyen, 1997). A more comprehensive study using heart rate for hypoglycaemia detection was conducted in 2001 (Ghevondian et al., 1997). This hypoglycaemia detection system used two inputs which were heart rate and skin impedance. In this study, using heart rate as the input for hypoglycaemia detection, the relation between heart rate and BGL in hypoglycaemia study is considered. The relation is shown in Figure 2.14, which was obtained from a hypoglycaemia study on 6 healthy and 6 type 1 diabetic subjects aged 26±3 years. The study used hyperinsulinemic hypoglycaemia, in
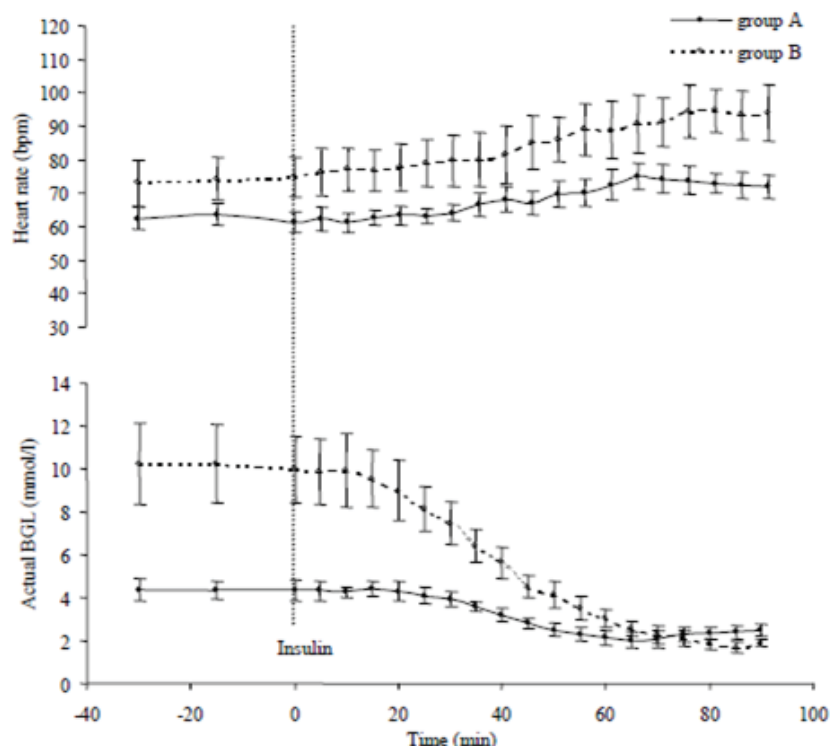
Figure 2.14: Relation of heart rate and BGL in healthy subjects (group A) and patients with type 1 diabetes (group B) (Ghevondian et al., 1997).

which hypoglycaemia in the body happened on account of infused insulin (instead of naturally occurring hypoglycaemia). The graph in Figure 2.14 shows that heart rate increases in relation to the decreasing BGL.

The study found that the mean heart rate of healthy and diabetic subjects increased by 11 and 21 beats per minute (bpm), respectively. The increasing heart rate in response to hypoglycaemia was confirmed by a previous study (Hilsted et al., 1984). The study involved seven healthy men aged 22±0.6 years. In the study, heart rate increased significantly in the nadir of BGL after 30 minutes insulin infusion (Figure 2.15).
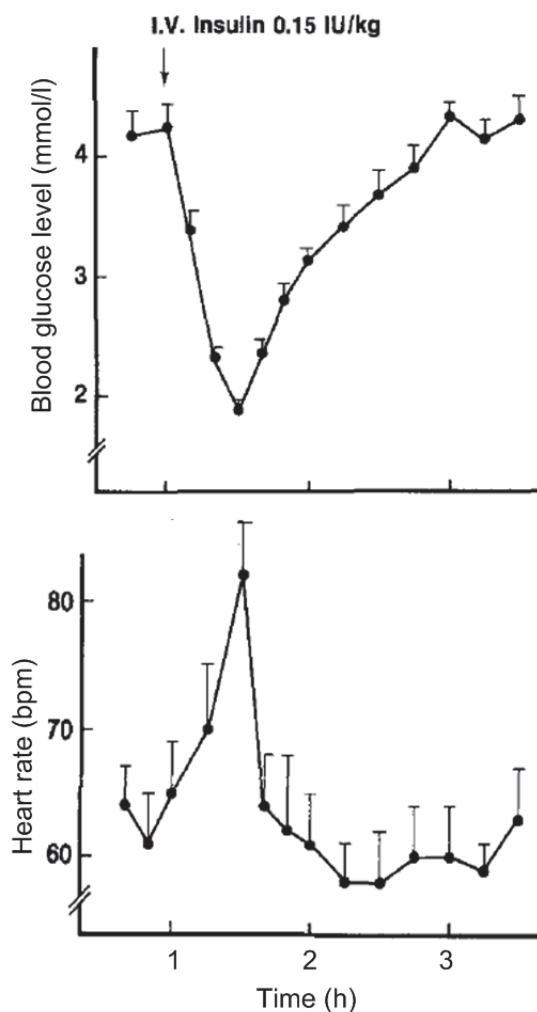
Figure 2.15: Heart rate in relation to insulin induced hypoglycaemia of healthy subjects (Hilsted et al., 1984).

Harris et al. (2000) studied QT interval in relation to hypoglycaemia In the study, QT interval alteration in relation to naturally occurring hypoglycaemia (BGL<3.5 mmol/l) of 14 type–1 diabetic patients was investigated. The patients were attached to an ECG monitor and were asked to find blood glucose at 23:00, 03:00 and 07:00 hours during the day of the study. As indicated in Figure 2.16, the study reported that QT interval was altered during hypoglycaemia. QT interval was also studied by another research group for input of hypoglycaemia detection (Nguyen et al., 2006) and (Nguyen et al., 2007). In the study, QT interval increased
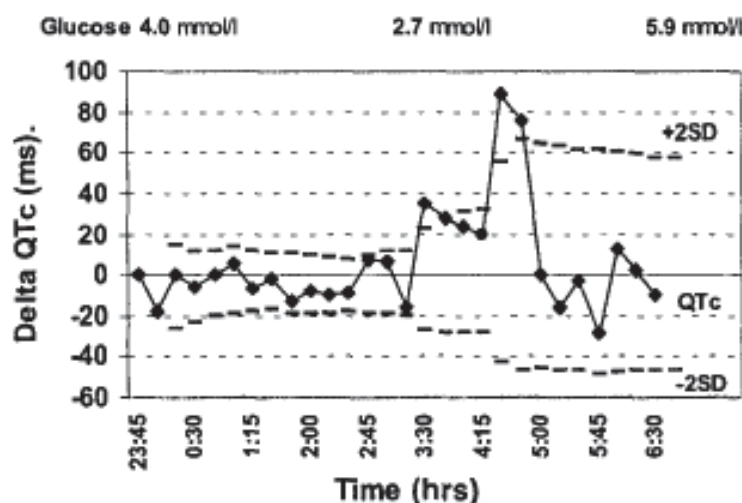
Figure 2.16: Alteration of QTc relating to BGL in a diabetic patient participating in the study (Harris et al., 2000)

during hypoglycaemia   (1.09±0.09 vs 1.02±0.07).

ECG parameters which relate to electrocardiographic T–waves were examined for hypoglycaemia detection (Alexakis et al. 2003), (Alexakis et al. 2006). The ECG parameters involve T wave amplitude, T wave skewness and T wave kurtosis. Skewness measures the degree to which a distribution is asymmetrical. The skewness value of a normal distribution is 0. Shown in Figure 2.17, the left graph has a positive skewness and the right graph has a negative skewness. Kurtosis measures the degree of peakedness of a distribution. For example, distributions in Figure 2.18 have different kurtosis; kurtosis of the left

Positive skewness   Negative skewness
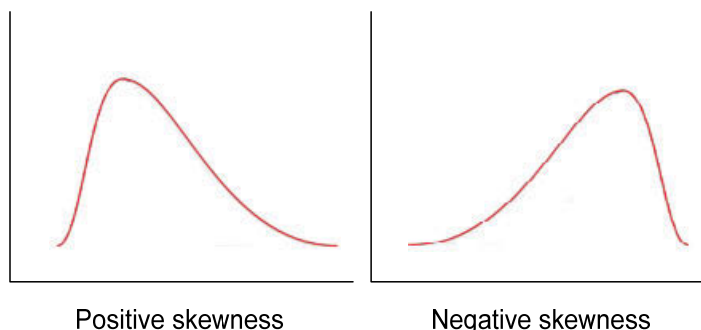
Figure 2.17: A positive and negative skewness
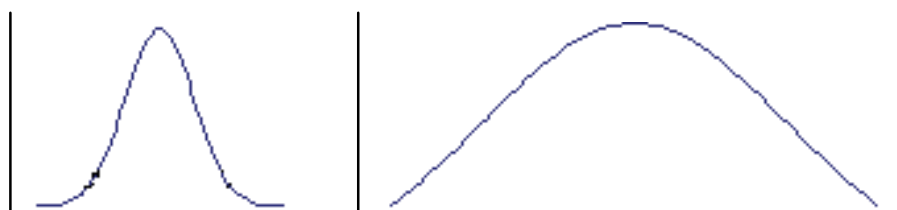
Figure 2.18: Distributions with different kurtosis; kurtosis of the left distribution is larger than kurtosis of the right one.

distribution is larger than kurtosis of the right one. In other words, kurtosis is a dimensionless measure that compares the T-wave with a Gaussian distribution curve. A positive kurtosis indicates that the T-wave is more pointed and has higher amplitude than predicted from a Gaussian distribution. A negative kurtosis indicates that the T-wave is flatter than a Gaussian distribution curve, with longer tails in each end of the wave. Kurtosis and skewness could be used for reference values of electrocardiographic repolarization (Garg et al., 2006).

Intelligent techniques for ECG based-hypoglycaemia detection

The above studies developed algorithm techniques to process ECG parameters to find a hypoglycaemia detection. A fuzzy system (Figure 2.19) was introduced for ECG-based hypoglycaemia detection in 1997 (Ghevondian and Nguyen, 1997). The fuzzy system had three inputs, which were heart rate, snoring and sweating (or skin impedance). The output of the fuzzy system is a hypoglycaemic state. A fuzzification with three membership functions was used. The membership functions were normal, high and very high. Three hypoglycaemic levels were created, which were normal, light hypoglycaemia and heavy hypoglycaemia. The MAX-MIN fuzzy reasoning method was used for the fuzzy inference system, and Mamdani's minimum operation was used in the defuzzification. The illustration of the experimental result is presented in Figure 2.20. A modification of the fuzzy system was developed by creating a self–

Figure 2.19: Fuzzy system for hypoglycaemia detection with input of ECG parameter and the output of hypoglycaemic state. (Ghevondian and Nguyen, 1997)

organizing fuzzy estimator (Hastings et al., 1998). In the self-organizing fuzzy, membership function was created to match each patient.

A fuzzy neural network estimator, FNNE (Figure 2.21), was developed using a parallel combination of fuzzy inference mechanism (FIM) and multilayered neural network (NN) (Ghevondian et al., 1997). The FNNE was examined using
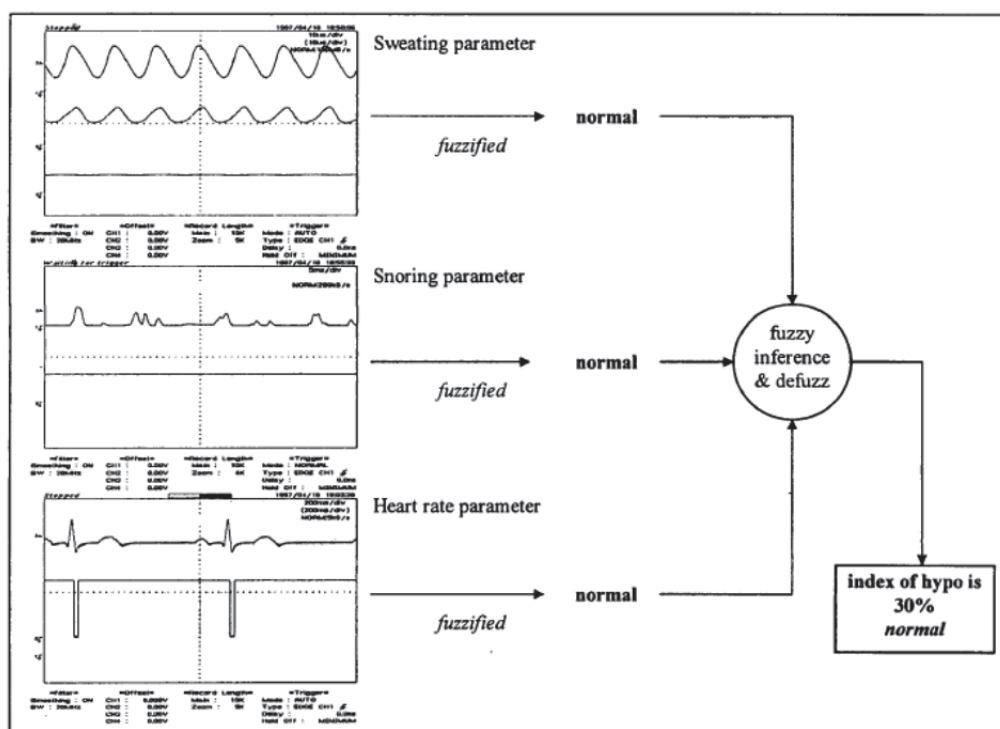
Figure 2.20: Example of experimental result of hypoglycaemia detection using input of ECG parameter and the output of hypoglycaemic state. (Ghevondian and Nguyen, 1997)

two inputs, which were heart rate and skin impedance, and the output was estimated BGL. The artificial neural network (ANN) algorithm was also studied for hypoglycaemia detection using three ECG parameters, which are heart rate, *QT* interval and skin impedance. Another hypoglycaemic detection used ANN with inputs of electrocardiographic RT interval, T wave amplitude, T wave skewness and T wave kurtosis. A furthered ANN technique which is Bayesian neural network (BNN) algorithm was developed for hypoglycaemia detection by (Nguyen et al., 2007). Training in BNN adjusts weight decay parameters automatically to optimal values to find the best generalization. Compared to conversional ANN, the computationally intensive search in BNN for the weight decay parameters is no longer needed.

Alexakis et al. (2006) developed an algorithm with the name of knowledge-based system (KBS). A KBS is based on a set of rules generated from the observation of ECG changes altered by hypoglycaemia, within guidelines provided by clinical experts. An example of rule among the eight rules was:

IF (T-amplitude is flattened) and (previous T-amplitude) is flattened and (RT interval is prolonged) and (previous RT interval is prolonged) THEN (diabetic state is hypoglycaemic).

2.4   THE PROPOSED STRATEGY OF HYPOGLYCAEMIA DETECTION

Several ECG parameters have been investigated for the development of hypoglycaemia detection. Heart rate, *QT* interval, T-wave amplitude and so on have shown a contribution in hypoglycaemia detection, as presented in section 2.3.5. However, the investigation might still need further work as not all ECG parameters have been examined for hypoglycaemia detection. Thus, this research proposes new ECG parameters for hypoglycaemia detection. Integrating the new one with those which have been tested might provide a good performance in hypoglycaemia detection. The ECG parameters proposed in this research might already be available

in other research, but these parameters are new in hypoglycaemia detection. This idea is also supported by a study which stated that the *QT* interval is not the one and only repolarization parameter for a long *QT* syndrome predictor (Benhorin et al., 1990); there are other ECG parameters which could indicate a long *QT* syndrome and are independent of the *QT* interval.

Furthermore, another important point in the ECG based–hypoglycaemia detection is the processing of ECG parameters. The processing should yield the hypoglycaemia detection which provides the correct output considering the ECG parameter in the input. A computational intelligence plays an important role in the processing. Fuzzy system, fuzzy neural network and other computational intelligences have been investigated for ECG-based hypoglycaemia detection, as presented in section 2.3.5.2. However, the innovation of computational intelligence in hypoglycaemia detection might still need further study as the research in the field of computational intelligence keeps developing. This research introduced a
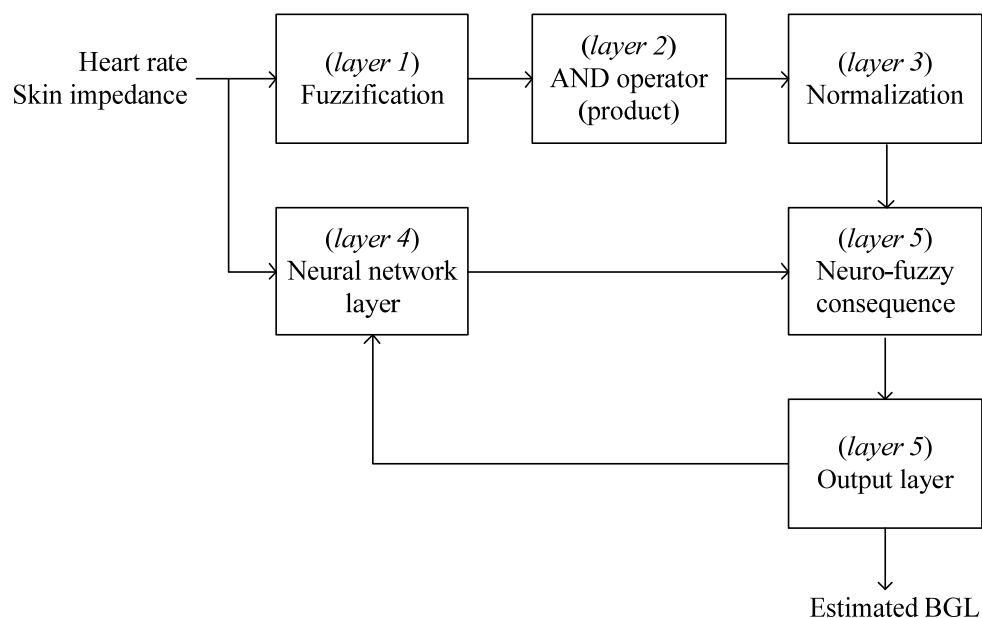
Figure 2.21: Architecture of fuzzy neural network for hypoglycaemia detection with input of heart rate and skin impedance (Ghevondian et al. 1997b

computational intelligence based on support vector machine (SVM) for the ECG-based hypoglycaemia detection.

SVM has proved to be mostly good for classification performance in varied applications, for both real and artificial standard benchmarking data (Meyer et al., 2003). SVM also performed well in medical fields. Osowski et al. (2004) presented heartbeat recognition using SVM on the basis of ECG waveform. Nollo et al. (2008) developed an automatic system for the analysis and classification of atrial fibrillation form intracardiac electrograms. Application of SVM for automatic recognition of obstructive sleep apnea syndrome based on ECG was studied by Khandoker et al. (2009).

SVM has been compared with other algorithms for some applications. For pathologies detection in brain magnetic resonance images (MRI), SVM outperforms an adaptive neuro-fuzzy inference system (ANFIS) (Lahmiri and Boukadoum, 2011). ANFIS is a hybrid algorithm which combines the computational power of neural network and fuzzy inference systems. It is an algorithm based on a fuzzy inference model in which its membership function and the associated parameter are controlled by neural network training method. For the application of the intrusion detection in computer networks, SVM outperforms a neural network (Osareh and Shadgar, 2008).

The concept of SVM is firstly introduced in 1992 in the Fifth Annual ACM Conference on Computational Learning Theory (COLT 1992), Pittsburgh, PA, USA; Boser et al. (1992) presented this concept. Three years later Vapnik (1995) wrote the well-known textbook on statistical learning theory with a special emphasis on support vector machine. SVM was developed from a theoretical background then to implementation and experiments. In the beginning of the SVM theoretical development, SVM was unnoticed. However, serious attention was given to SVM in many different fields after its excellent performances indicated in
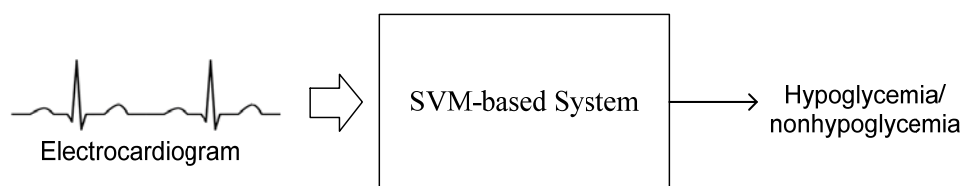
Figure 2.22: The general structure of the proposed hypoglycaemia detection employing SVM

practical benchmarks.

Boser et al. (1992) described a training algorithm for classification by maximizing the margin (or distance) between the training data points and the decision boundary. The decision boundary is the boundary which optimally separates two class data. The training technique which is conducted by maximizing the margin has the advantage of easily identifying outliers or meaningless patterns. On the contrary, another classifier technique which performs training by minimizing the mean square error quietly ignores atypical patterns (Boser et al., 1992).

In general the proposed hypoglycaemia detection is presented in Figure 2.22. The input of the detection is electrocardiogram. The output is a binary hypoglycaemic state, which is hypoglycaemia or nonhypoglycaemia. The detection is based on SVM. Hybrid techniques on SVM are developed to find a high performance of the detection.

CHAPTER 3.
ELECTROCARDIOGRAPHIC BASED HYPOGLYCAEMIA DETECTION STRATEGY EMPLOYING SUPPORT VECTOR MACHINE

SVM is a classification tool which has good generalization. Its powerful capability in classification has been indicated in many applications. Duin (2000) presented the advantage of SVM for its generalization capability. SVM utilizes procedure for reducing the training data points which participates in defining discriminant function. Thus, the participating data points, which are called support vectors, are minimized. Data points which do not participate in defining a classifier are ignored. This can reduce noise and, consequently, can improve the generalization capability.

SVM has proved mostly good performance for classification in varied applications, both for real and artificial standard benchmarking data (Meyer et al., 2003), including applications in medical fields with the basis of ECG. Osowski et al. (2004) presented heartbeat recognition using SVM on the basis of ECG waveform. Nollo et al. (2008) developed an automatic system for the analysis and classification of atrial fibrillation form intracardiac electrograms. The superiority of SVM in the automatic classification of ECG is presented in (Melgani and Bazi, 2008). Application of SVM for automatic recognition of obstructive sleep apnea syndrome based on ECG was studied by Khandoker et al. (2009).

This chapter presents a novel hypoglycaemia detection model which

employs SVM. Its input is ECG parameters. The model provides output of binary glycaemic levels (hypoglycaemia or nonhypoglycaemia) according to the ECG signal fed to its input. The construction of the model is presented. Its details which include ECG acquisition, delineation of ECG fiducial points, feature extraction and SVM classification are described. Furthermore, the influences of the SVM parameters to the performance of the detection algorithms are presented and discussed.

3.1 THE HYPOGLYCAEMIA DETECTION MODEL BASED ON SUPPORT VECTOR MACHINE (SVM)

The development of hypoglycaemia detection which employs SVM is constructed as in Figure 3.1. The construction consists of three main parts, namely ECG acquisition, feature extraction and SVM classification. The first part, ECG acquisition, captures the ECG signal from a subject. The ECG signal is the electrical activity generated by the heart and measured on the body surface. The second part, feature extraction, is developed to find the ECG parameter (such as heart rate and QT interval) from the ECG signal. Thirdly, the ECG parameter is then classified by SVM. The output of the SVM classification is a binary glycaemic level (hypoglycaemia or nonhypoglycaemia). Thus, the final output of the construction is a state of hypoglycaemia or nonhypoglycaemia of a subject.
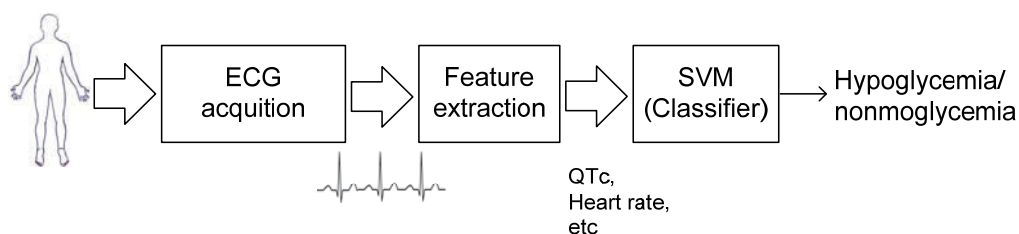
Figure 3.1: General structure of hypoglycaemia detection which employs a support vector machine and inputs of ECG

3.1.2   Electrocardiographic acquisition

The ECG signals of subjects were recorded using the data recorder from Compumedics (www.compumedics.com) which was the Siesta. The Siesta is a device which provides amplified channels for physiological signal collection. It employs a computer based technology. For the ECG acquisition the Siesta was connected to a personal computer (PC), as shown in Figure 3.2. The software of Profusion PSG was installed in the PC to operate the Siesta for the ECG acquisition. An appearance of the software can be seen in Figure 3.3. Using the software, the obtained ECG signals were exported to a file in the form of text (*.txt), as indicated in Figure 3.3. This text file was then processed in the feature extraction stage (section 3.1.3). The sampling rate of the ECG acquisition was 512 Hz. The ECG acquisition used a single lead, which was lead II. During the acquisition, blood glucose levels of the subjects were measured every five minutes using the blood glucose meter from Yellow Spring Instruments (www.ysi.com)
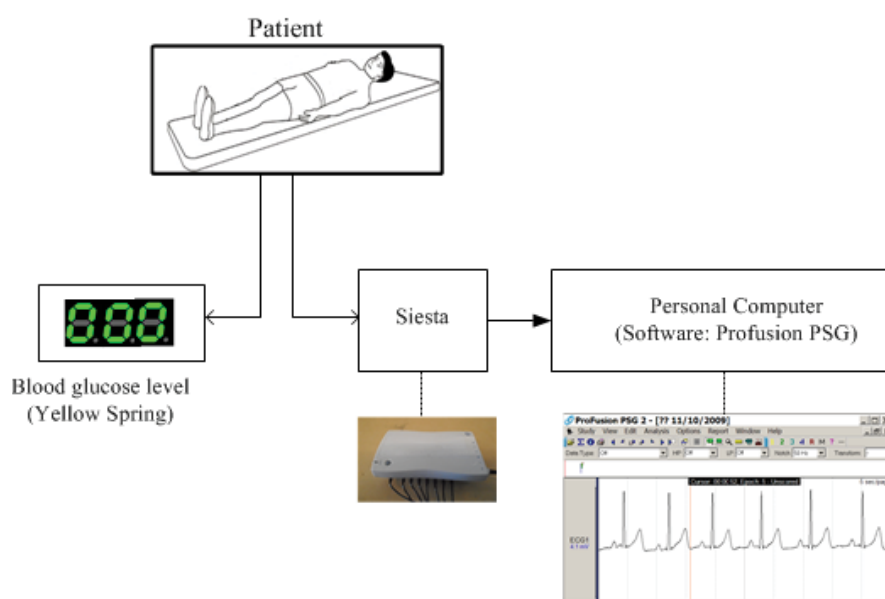
Figure 3.2: The ECG acquisition from the patients
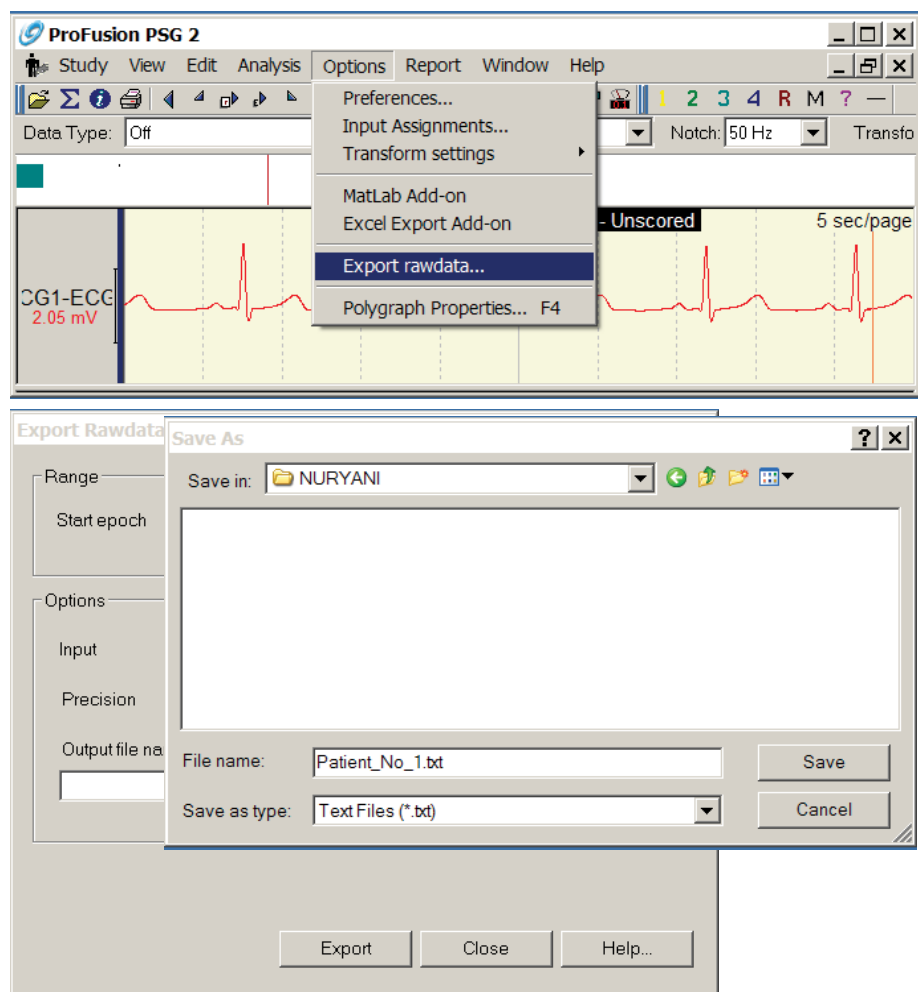
Figure 3.3: The facility for exporting ECG data in Profusion PSG 2

3.1.3   Feature extraction

The ECG signals (in the text file format) obtained from the ECG acquisition were processed in the feature extraction. The feature extraction is to extract an electrocardiogram to find the ECG parameter, which was ready to be used for the SVM classification. The extraction was developed in Matlab. Two main steps were conducted in the feature extraction, namely delineation (or marking) on the electrocardiogram to find ECG fiducial points, and finding the ECG parameters considering the fiducial points. ECG fiducial points are the points in an electrocardiogram used for references to find ECG parameters. Typical ECG fiducial points are the points of Q, R, S and so on.

Delineation of ECG fiducial points

Delineation of ECG fiducial points was necessary to find the ECG parameter. In this research work the ECG parameter indicates a time interval between two ECG fiducial points. The delineation is to find the positions (in time) of ECG fiducial points. The ECG fiducial points are described in Figure 3.4, which consists of:

- *Q*:   the start of *QRS* complex,

- *R*:   the peak of *QRS* complex,

- *S*:   the end of *QRS* complex,

- *To*:   the starting point of *T*-wave,

- *Tp*:   the peak of *T*-wave and

- *Te*:   the end of *T*-wave;

where *QRS* complex represents ventricular depolarization of the heart, and T-wave represents ventricular repolarization of the heart.
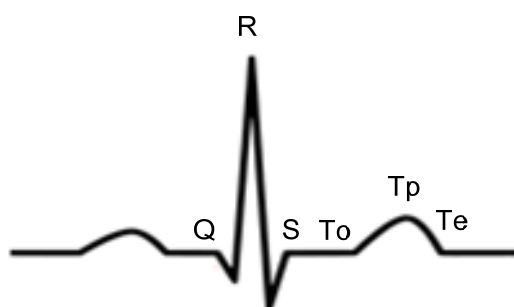
Figure 3.4: ECG fiducial points of Q, R, S, To, Tp and Te
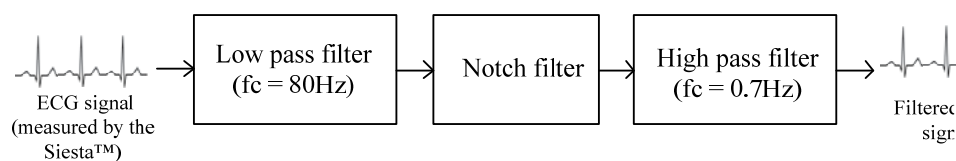
Figure 3.5: Filtering the ECG signals

Before the delineation, the ECG signals were filtered to omit noise. Because the resulting ECG signals from the Siesta had relatively low noise, a basic signal processing (Figure 3.5) was enough to tackle the noise. The ECG signals were filtered by using a low pass filter with cut-off frequency of 80 Hz, to omit high frequency noise. An ECG signal is often contaminated by high frequency noise, such as electromyography and instrumentation noise (Chang et al., 2010). Power line interference, which is noise from power line, usually contaminates an ECG signal. To remove this a 50 Hz notch filter was employed. The signals were also filtered using a high pass filter with cut-off frequency (f_c) of 0.7Hz, particularly to omit baseline wander. Baseline wander is mainly caused by the patient breathing and moving (Zhao and Chen, 2006). The filters employed a Butterworth type filter.

The *R* point of each beat of the ECG signals was obtained by finding the
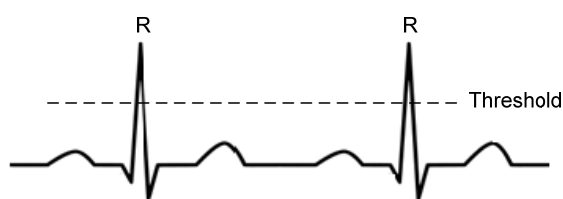
Figure 3.6: Delineation of R point.
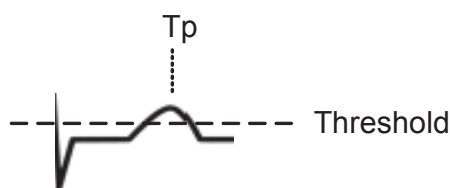
Figure 3.7: Delineation of Tp (the peak of T-wave)

maximum amplitude which is higher than a threshold value (Manriquez and Zhang, 2007), as presented in Figure 3.6. A similar method was used to obtain the T-wave peak *Tp* of each beat of the ECG signals. As presented in Figure 3.7, *Tp* was marked by obtaining the maximum amplitude which was higher than a threshold value in the segment on the right side of the *R* peak (Schneider et al., 2006) .

The *Q* point was determined using a continuous wavelet transformation (Di Virgilio et al., 1995, Di Marco and Chiari, 2011). Using the continuous wavelet transformation with the scale of 30 (WL30), the Q point was referred to the minimum of WL30 which was located in the nearest left side of the R peak (Figure 3.8). Similar to the Q point determination, S point was marked by the minimum of the wavelet signal with the scale of 21 (WL21) which was located in the nearest right side of the R peak (Figure 3.8).

The T-wave end *Te* was determined using the Philips *QT* Interval Measurement Algorithm (Sophia et al., 2009). In the algorithm, a line segment L was drawn from *Tp* forward in time to a point in the ECG signal, and the *Te* was a point that has the maximum vertical distance between the point and the line segment (Figure 3.9). The beginning of T-wave *To* was obtained by a similar method to find *Te* with the difference that the used line segment was in the left side of the *Tp*. If a U wave presented before the T wave returned to baseline, the end of the T wave was the nadir between T and U waves.
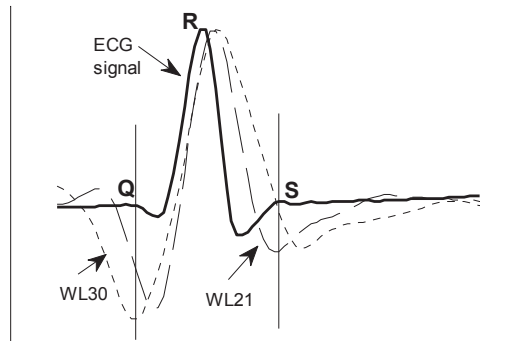
Figure 3.8: Q and S points are found using wavelet transformation using wavelet scale of 30 (WL30), for *Q* point, and wavelet scale of 21 (WL21), for *S* point. *Q* and *S* points are at the same time position with the minimum of WL30 and WL21, respectively.

Finding the ECG parameters

Based on the fiducial points obtained from the delineation, the ECG parameters were calculated. The ECG parameters were the time intervals between two fiducial points, as described in Figure 3.10. The ECG parameters used in this work were:

- *TpTe$_c$*: the interval from the peak of T-wave *Tp* to the end of T-wave *Te*,

- *ToTe$_c$*: the interval from the beginning of T-wave *T*o to the end of T-wave *Te*,

- *RTp$_c$* : the interval from *R* point to the peak of T-wave *Tp*,

- *QTe$_c$* : the interval from *Q* point to the end of T-wave *Te*,

- *QTp$_c$* : the interval from *Q* point to the peak of T-wave *Tp*,

- *STo$_c$* : the interval from *S* point to the beginning of T-wave *To* and

- *HR* : Heart rate that is 60/*RR*.

Index of *c* in the parameters indicates that the intervals are corrected by heart rate using the Bazett's formula (Moss, 1993). Using this formula, the intervals are

normalized using the square root of *RR* interval. For example, $QTc = QT/(RR)^{1/2}$.

To reduce patient-to-patient variability, normalization was performed. In a patient, the ECG parameters were normalized using the patient's ECG parameter which was in the beginning of the study, when the euglycaemia phase just started (Nguyen et al., 2008). As mentioned above, the euglycaemia phase started after one hour of the baseline phase. During the study, each subject relaxed on a bed in a clinical research room in Princess Margaret Hospital in Perth, Australia. In the more detailed calculation of the normalization, supposing that an ECG parameter at time *i* is x_i and the ECG parameter at the beginning study is x_0, normalized ECG parameter $\bar{x}_i$ equals to x_i/x_0. The resulted ECG parameters were arranged to a matrix form which has rows representing data point number and columns representing ECG parameters, such as QTe_c. Each row (or data point) was the average of 30 consecutive-beats of the ECG.

3.1.4   SVM classification

In the proposed hypoglycaemia detection, SVM is employed for the
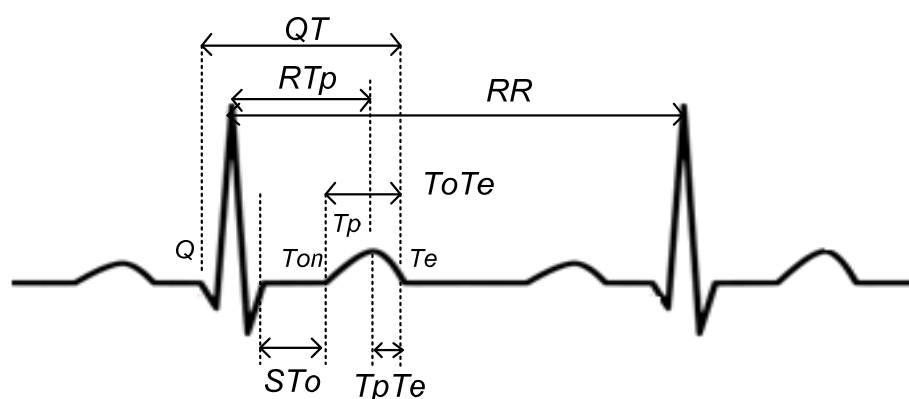
Figure 3.10: ECG parameters of *RR, QT, RTp, STo, TpTe* and *ToTe*

classification of the ECG parameters. The output of the classification is a binary state, which is hypoglycaemia or nonhypoglycaemia.

Linear support vector machine

SVM is a classifier which works through deciding an optimal hyperplane which optimally separates two class data. The optimal hyperplane is also called a decision surface which is the surface optimally separating two groups of data points. Suppose there are l linearly-separable training-data x_i (i = 1,2,3, …,k) and the associated $y_i \in \{-1,+1\}$ is a class label. y_i = +1 is for the class +1 and y_i = −1 is for the class −1. For example, the class +1 is for the data which belongs to hypoglycaemia, and −1 is for nonhypoglycaemia.

In the case of two–dimensional space, as shown in Figure 3.11, two groups of data (circles and squares) can be separated by different hyperplanes. Two possible hyperplanes are shown in Figure 3.11 (a and b). In SVM, the optimal hyperplane is right in the middle of the two class boundaries and the distance of the two boundaries is maximized. The optimal hyperplane promises good classification while facing unseen data and provides a good generalization. In Figure 3.11 the two parallel lines in the left and right of the hyperplane are supporting hyperplanes. The supporting hyperplanes are parallel to the hyperplane. The decision surface (or hyperplane) and the supporting hyperplanes are defined as follow:

The decision surface: $\qquad\qquad\qquad\qquad\qquad\qquad$ $\mathbf{w}\cdot\mathbf{x} + b = 0$ $\qquad$ 3.1

Supporting hyperplane for class +1: $\qquad\qquad\qquad$ $\mathbf{w}\cdot\mathbf{x} + b = +1$ $\qquad$ 3.2

Supporting hyperplane for class -1: $\qquad\qquad\qquad$ $\mathbf{w}\cdot\mathbf{x} + b = \text{-}1$ $\qquad$ 3.3

where w is the *perpendicular* distance from the hyperplane to the origin, and b is called bias.
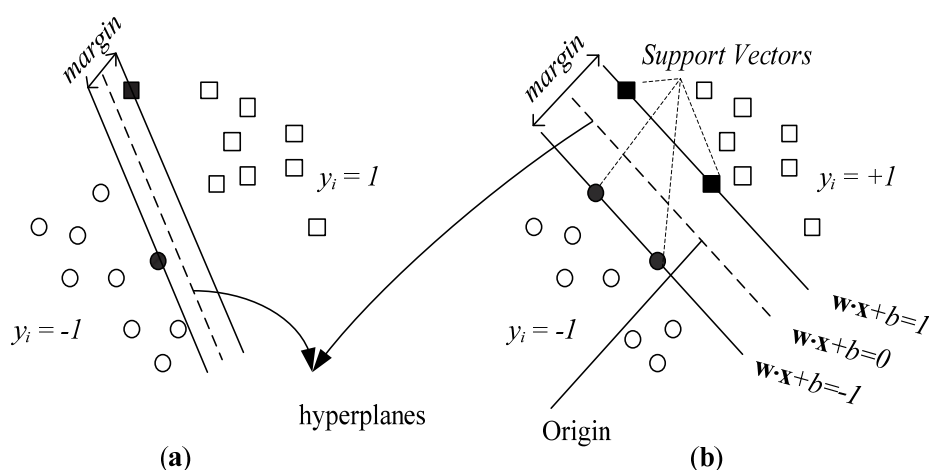
Figure 3.11: Two-out-of-many separating lines; (a) with smaller margin and (b) with larger margin

The distance between the two supporting hyperplanes is referred to as a margin (*m*). The optimization problem of SVM is to find the decision boundaries so that the distance between the supporting hyperplanes is as far as possible. Therefore, the optimization is to maximize the margin and to keep the decision surface equidistant from the two supporting hyperplanes. As in Figure 3.11, the margin is constrained by the points which are indicated by the filled circles and the filled squares. These points are called support vectors.

Because the optimization problem of SVM is to find the optimal hyperplane, the feasible solutions to the optimization problem are all possible hyperplanes, with their associated supporting hyperplanes. The constraints are the positions of the supporting hyperplanes in order not to cross their respective class boundaries. Considering Figure 3.12, the margin (*m*) between the two supporting hyperplanes can be defined as (see in appendix A)

$$m = \frac{2}{|\boldsymbol{w}|}$$

3.4

Thus, the maximum margin $\hat{m}$ is obtained by maximizing Eq. 3.4, as

$$\hat{m} = \max \frac{2}{|\boldsymbol{w}|}$$

3.5

or

$$\widehat{m} = \min \frac{|\boldsymbol{w}|}{2}$$ 3.6

Eq. 3.6 can also be stated as

$$\widehat{m} = \min \frac{|\boldsymbol{w}|^2}{2},$$ 3.7

because optimizing over $|\boldsymbol{w}|^2$ is the same as optimizing $|w|$. Eq. 3.7 can be formulated as

$$\widehat{m} = \min \frac{1}{2}\boldsymbol{w}.\boldsymbol{w}$$ 3.8

As mentioned above, the constraints of the optimization problem are the positions of the supporting hyperplanes which do not cross their respective class boundaries. Mathematically, it can be formulated as

$$\boldsymbol{w}.\boldsymbol{x_i} + b \geq +1 \text{ for all } (\boldsymbol{x_i}, y_i) \text{ such that } y_i = +1$$ 3.9

$$\boldsymbol{w}.\boldsymbol{x_i} + b \leq -1 \text{ for all } (\boldsymbol{x_i}, y_i) \text{ such that } y_i = -1$$ 3.10

Using a more compact formula, it can be stated as

$$y_i(\boldsymbol{w}.\boldsymbol{x_i} + b) \geq 1 \text{ for all } (\boldsymbol{x_i}, y_i)$$ 3.11

The optimization problem in Eq. 3.8 is solved using the Lagrangian. The
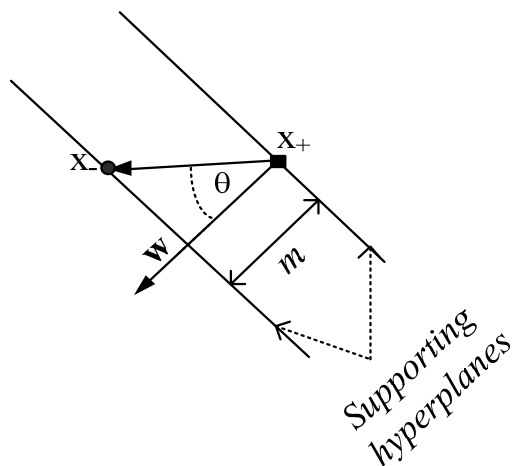
Figure 3.12: Margin *m* between two supporting hyperplanes

construction of the Lagrangian for the optimization problem is

$$L(\alpha, w, b) = \tfrac{1}{2}\boldsymbol{w} \cdot \boldsymbol{w} - \sum_{i=1}^{l} \alpha_i \left(y_i(\boldsymbol{w} \cdot \boldsymbol{x}_i - b) - 1\right)$$

3.12

where α is a Lagrangian multiplier. This gives the Lagrangian optimization problem as

$$\max_{\alpha} \min_{\boldsymbol{w},b} \; L(\alpha, w, b)$$

3.13

Subject to

$$\alpha_i \geq 0$$

3.14

which provides the Lagrangian dual optimization problem as follow:

$$L(\alpha, w, b) = \tfrac{1}{2}\boldsymbol{w} \cdot \boldsymbol{w} - \sum_{i=1}^{l} \alpha_i \, y_i \boldsymbol{w} \cdot \boldsymbol{x}_i + b \sum_{i=1}^{l} \alpha_i \, y_i + \sum_{i=1}^{l} \alpha_i$$

3.15

and the optimal decision surface is defined as (see Appendix B)

$$f(\mathbf{x}) = sgn(\mathbf{w}.\mathbf{x} - b)$$

3.16

$$f(\mathbf{x}) = sgn\left(\sum_{i=1}^{l} \alpha_i y_i \boldsymbol{x}_i \cdot \boldsymbol{x} - \sum_{i=1}^{l} \alpha_i y_i \boldsymbol{x}_i \cdot \boldsymbol{x}_{sv} - 1\right)$$

3.17

Nonlinear support vector machine

The SVM which is mentioned above is a linear SVM. The linear SVM needs to be extended to tackle non-linearly separable data, as data in the real world are, mostly, not linearly separable. The idea of the extension is by using the kernel
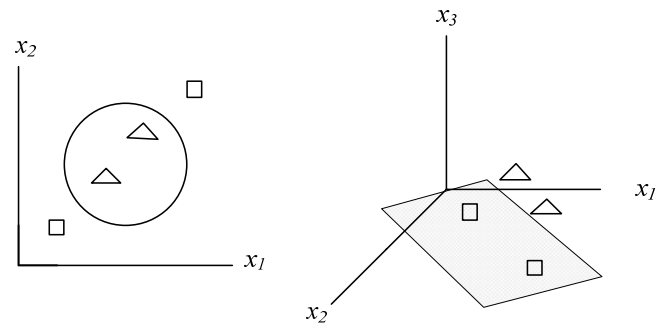
Figure 3.13: Illustration of mapping using a transform Ψ: ℝ² → ℝ³

trick. Using a kernel function, data in the input space is transformed to a higher-dimensional space, which is called a feature space. In this feature space it is possible to separate the data using a hyperplane. The transformation is illustrated in Figure 3.13. In the figure (left) the data points cannot be classified by a linear function. After the data points are transformed in three dimensional space, a linear function can be used to classify the data points. In Figure 3.13 (right) a plane can separate the data points; two triangles are above the plane and two squares are below the plane.

Using the kernel trick, the Lagrangian optimization problem is modified by replacing x_i using a mapping function $\Psi(x)$ as

$$L(\alpha, w, b) = \sum_{i=1}^{l} \alpha_i - \frac{1}{2} \sum_{i=1}^{l} \sum_{j=1}^{l} \alpha_i \alpha_j y_i y_j \Psi(\mathbf{x}_i) \cdot \Psi(\mathbf{x}_j) \qquad 3.18$$

In the compact form Eq. 3.18 can be written as

$$L(\alpha, w, b) = \sum_{i=1}^{l} \alpha_i - \frac{1}{2} \sum_{i=1}^{l} \sum_{j=1}^{l} \alpha_i \alpha_j y_i y_j k(\mathbf{x}_i \cdot \mathbf{x}_j) \qquad 3.19$$

where $k(\mathbf{x}_i \cdot \mathbf{x}_j)$ is a kernel function. Kernel functions include:

$$\text{radial basis function (RBF)}, \ k(\mathbf{x}_i, \mathbf{x}_j) = \exp\left(-\gamma \|\mathbf{x}_i - \mathbf{x}_j\|^2\right) \qquad 3.20$$

$$\text{Sigmoid}, \ k(\mathbf{x}_i, \mathbf{x}_j) = \left(-\gamma(\mathbf{x}_i - \mathbf{x}_j) + 1\right) \qquad 3.21$$

$$\text{Polynomial}, \ k(\mathbf{x}_i, \mathbf{x}_j) = (\mathbf{x}_i \mathbf{x}_j + 1)^d \qquad 3.22$$

$$\text{linear}, . \ k(\mathbf{x}_i, \mathbf{x}_j) = \mathbf{x}_i \mathbf{x}_j \qquad 3.23$$

Soft-margin nonlinear support vector machine

A soft-margin classifier of SVM is useful to tackle imperfect data containing a noisy data point, such as that which is due to improper measurement. In this soft-margin SVM, a slack variable ξ is introduced. A slack variable measures how much of an error is introduced by allowing the supporting hyperplane to be unconstrained by a data point (Figure 3.14). By introducing a nonnegative slack variable, the corresponding modified constraint is

$$y_i(\boldsymbol{w} \cdot \boldsymbol{x} - b) + \xi - 1 \geq 0 \qquad 3.24$$

and the optimization problem in 3.8 becomes

$$\hat{m} = min\left(\frac{1}{2}\boldsymbol{w}.\boldsymbol{w} + C\sum_{i=1}^{l}\xi_i\right) \qquad 3.25$$

The introduction of the slack variable as in the form of $C\sum_{i=1}^{l}\xi_i$ is to prevent the construction of trivial solutions; where all training points are considered as noise during the optimization. C is a constant, called the cost, controlling the trade-off between margin size and error. By this slack variable introduction, the Lagrangian construction of the optimization problem is (see Appendix C)

$$L(\alpha, w, b) = \sum_{i=1}^{l}\alpha_i - \frac{1}{2}\sum_{i=1}^{l}\sum_{j=1}^{l}\alpha_i\alpha_j y_i y_j k(\boldsymbol{x}_i \cdot \boldsymbol{x}_j) \qquad 3.26$$

This Lagrangian dual for soft-margin SVM is the same as the Lagrangian dual for
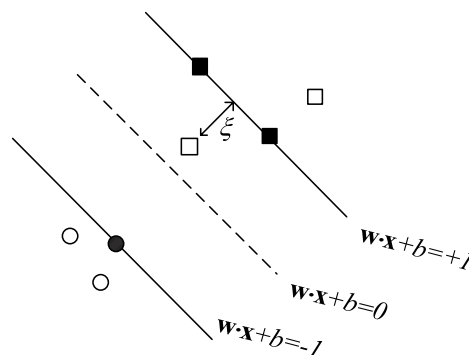
Figure 3.14: Introducing slack variable ξ in soft-margin SVM

hard-margin SVM. Therefore the objective functions of the optimization problems for both SVMs are the same. The difference is in the constraint. The constraint in the soft-margin SVM can be stated as

$$0 \leq \alpha \leq C \qquad 3.27$$

In a case of an imbalanced data point number between two classes, different error weights, w_0 and w_1, are necessary to penalize more heavily the class with the smaller population (Batuwita and Palade, 2010).

$$\hat{m} = min \frac{1}{2} \boldsymbol{w}.\boldsymbol{w} + w_0 C \sum_{i(yi=-1)=1}^{l} \xi_i + w_1 C \sum_{i(yi=+1)=1}^{l} \xi_i \qquad 3.28$$

In summary, the decision function of support vector machine can be represented as follow

$$f(\boldsymbol{x}) = sgn\left(\sum_{i=1}^{l} y_i \alpha_i \, k(\boldsymbol{x}_i, \boldsymbol{x}) - b)\right) \qquad 3.29$$

in which α is the solution of maximizing the following Lagrangian

$$\max_{\alpha} \, L(\alpha) = \left(\sum_{i=1}^{l} \alpha_i - \frac{1}{2}\sum_{i=1}^{l}\sum_{j=1}^{l} \alpha_i \alpha_j y_i y_j k(\boldsymbol{x}_i \cdot \boldsymbol{x}_j)\right) \qquad 3.30$$

Subject to constraints

$$\sum_{i=1}^{l} \alpha_i y_i = 0 \qquad 3.31$$

$$0 \leq \alpha_i \leq C \qquad 3.32$$

The optimization of Eq. 3.30 uses the method based on sequential minimal

optimization (SMO) (Plat, 1999, Keerthi et al., 2001, Fan et al., 2005). In the optimization, SMO uses analytical steps, instead of numerical quadratic programming. In each iteration SMO chooses two Lagrangian multipliers and optimize these two multipliers. Two Lagrangian multipliers at every step is the smallest number in the optimization because the Lagrangian has to obey a linear equality constraint (Eq. 3.31).

. The optimization which uses an SMO could be faster than the optimization which uses quadratic programming (QP). Using QP, the optimization for Eq. 3.30 involves a matrix with a number of elements that equals to the square of the number of training examples. This number obviously needs a large memory and can result in a very slow optimization. The description of the optimization using SMO is presented in Appendix D.

3.2   EXPERIMENTAL RESULT

Three algorithms of SVM were developed. These algorithms are SVMs with different kernel functions. Choosing a kernel function implies defining the mapping from an input space to a feature space. Essentially a kernel function used in SVM satisfies Mercer's condition. The typical kernel functions include Gaussian function, polynomial function and linear function (Li et al., 2009). There is no theoretical method to choose a suitable kernel function and its parameters for an application (Wu and Wang, 2009). Hence, the suitable kernel function needs to be chosen empirically, such as by a cross-validation (An et al., 2007).

The developed algorithms were SVMR, SVMP and SVML (Figure 3.15). SVMR, SVMP and SVML were the SVM employing RBF (Eq. 3.20), polynomial (Eq. 3.22) and linear (Eq. 3.23) kernel functions, respectively. For each of the three algorithms, five approaches of SVM for the hypoglycaemia detection with different SVM parameters were investigated. The approaches are listed in Table 3.1, namely A1, A2, A3, A4 and A5. Using A1, SVM parameters C, γ, w_0, w_1 were set to 1

and d was set to 2. Using A2, A3 and A4, the larger values of C were examined. The C values were 100, 10^4 and 10^6 for A2, A3 and A4, respectively. In A1–A4 the ratio of w_0 to w_1 was 1:1. This ratio was changed in A5. In A5 w_0 was set so that the sensitivities of the detection algorithms were about 70%. w_1, meanwhile, was set to 1.

The performances of the detection algorithms were measured in terms of sensitivity, specificity and geometric mean. Sensitivity was defined as the ratio of correct detection of hypoglycaemic events to the actual number of hypoglycaemia events. Specificity was defined as the ratio of correct detection of nonhypoglycaemic events to the actual number of nonhypoglycaemic events.
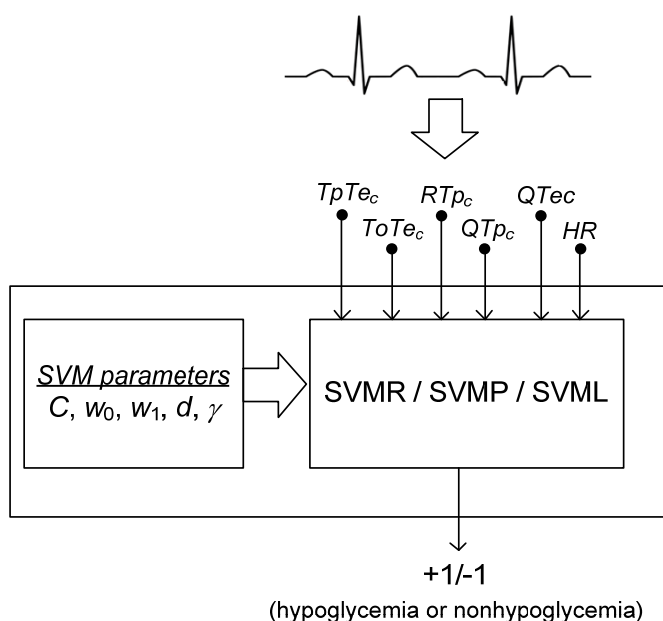
Figure 3.15: The approaches A1–A5; the hypoglycaemia detection employs SVM (SVMR, SVMP, SVML); the SVM parameters are given as presented in Table 3.1. The input is ECG parameters and the output is hypoglycaemia/nonhypoglycaemia

Mathematically, sensitivity, specificity and geometric mean can be formulated as in the following

$$Sensitivity = \frac{TP}{TP + FN}$$ 3.33

$$Specificity = \frac{TN}{TN + FP}$$ 3.34

$$Geometric\ mean = \sqrt{Sensitivity \times Specificity}$$ 3.35

where:

- *TP* (true positive) is the number of inputs which correspond to hypoglycaemia classified as hypoglycaemia.

- *FP* (false positive) is the number of inputs which correspond to nonhypoglycaemia classified as hypoglycaemia.

Table 3.1: Hypoglycaemia detection with different SVM algorithms and different SVM parameters

SVM Algorithm	A1				A2				A3			
	SVM parameters				SVM parameters				SVM parameters			
	C	γ/d	w_0	w_1	C	γ/d	w_0	w_1	C	γ/d	w_0	w_1
SVMR	1	1	1	1	100	1	1	1	10^4	1	1	1
SVMP	1	2	1	1	100	2	1	1	10^4	2	1	1
SVML	1	-	1	1	100	-	1	1	10^4	-	1	1

SVM Algorithm	A4				A5			
	SVM parameters				SVM parameters			
	C	γ/d	w_0	w_1	C	γ/d	w_0	w_1
SVMR	10^6	1	1	1	1	1	-	1
SVMP	10^6	2	1	1	1	2	-	1
SVML	10^6	-	1	1	1	-	-	1

Time (second)   Frequency (Hz)
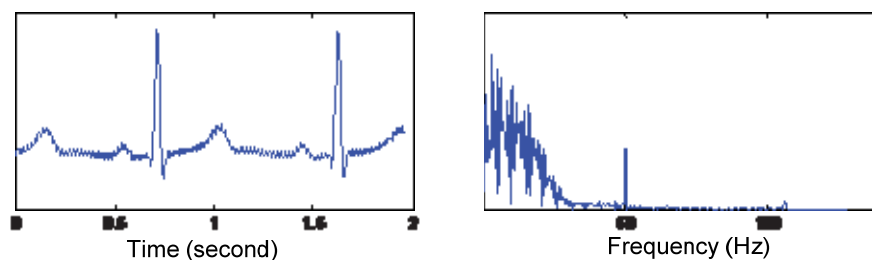
**Figure 3.16: The ECG signal recorded from the study (left) and
the associated frequency spectrum (right)**

- *TN* (true negative) is the number of inputs which correspond to nonhypoglycaemia classified as nonhypoglycaemia.
- *FN* (false negative) is the number of inputs that correspond to hypoglycaemia classified as nonhypoglycaemia.

The geometric mean (*gm*) is suitable for indicating the performance of a case with imbalanced data (Georgoulas and Stylios, 2006). The imbalanced data means that the data point number of a class is significantly more than that of another class, as is the data in this research.

Time (second)   Frequency (Hz)
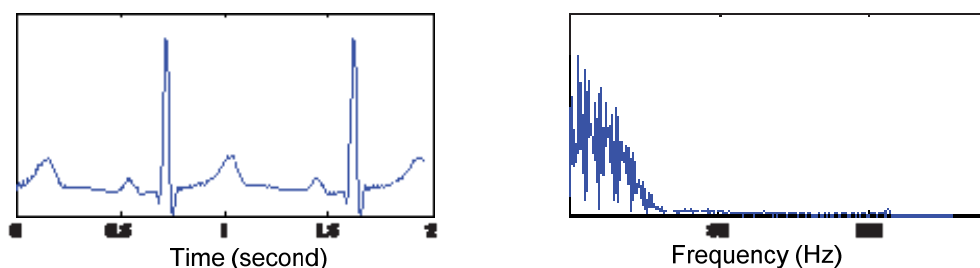
**Figure 3.17: The ECG signal after the Notch filtering (left) and
the associated frequency spectrum (right)**

The performance of the detection algorithms is measured in trems of sensitivity, specificity and geometric mean, instead of a root mean square error or RMSE (Deeb and Goodarzi, 2010). Using sensitivity the correct detection of hypoglycaemic class data can be known, and using specificity the correct detection of nonhypoglycaemic class data can be seen. On the other hand, RMSE only provides one value for the correct detection of both classes, instead of one value for each class.

The numbers of support vectors of the approach are presented. As described before, the support vector is the point which is included in the decision function of SVM (Eq. 3.29). In Figure 3.11, the support vectors are the points indicated by the filled circles and filled squares.

3.2.1   **Data set**

The data sets for the input of the developed algorithms were acquired from ECG of the subjects. For the ECG acquisition, the electrocardiograms of the subjects were recorded in an overnight hypoglycaemia study. Five patients voluntarily participated for the study. The subjects were patients with type 1 diabetes, aged 16±0.7 years. The hypoglycaemia study was performed at Princess Margaret Hospital in Perth, Australia. The study was approved by the Women's and
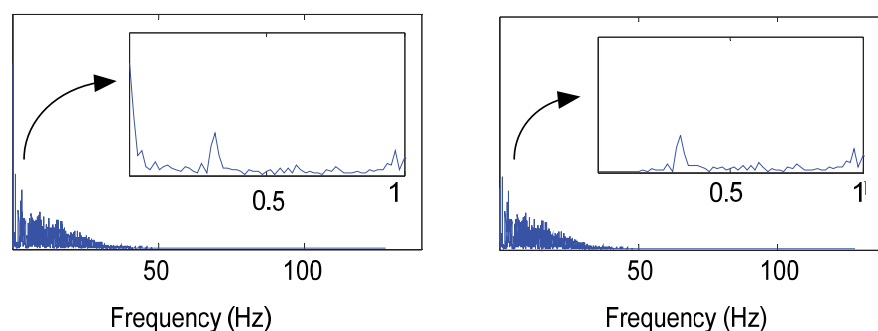
Figure 3.18: The ECG signals before the high pass filtering (left) and after the high pass filtering (right). The inserted figures are the signals in frequency of less than 1 Hz.

Children's Health Service, Department of Health, Government of Western Australia. Written informed consent was provided. Each study consisted of five phases approximately: one hour of baseline, three hours of euglycaemia, one hour of ramp, one and half hours of hypoglycaemia and four and half hours of recovery. During the ECG acquisition, blood glucose levels of the subjects were measured using Yellow Spring Instruments (www.ysi.com) in each five minutes.

The obtained electrocardiogram was then processed to find ECG parameters. The process followed the procedure of the feature extraction as described in section 3.1.3. In general the electrocardiogram was filtered and then was delineated. The result of the delineation was used to find the ECG parameters.

The obtained ECG parameters (also called data points) were randomly divided into three subsets, which were the same size. The three subsets were called training, validation and testing data sets. The training set was used in SVM training to find an SVM model. The SVM model was used to classify the ECG parameters. The performance of the SVM model was tested using the testing data set. The validation data set was used in the experiments in chapter IV and V.

The feature extraction obtained 1327 and 399 data points of nonhypoglycaemia and hypoglycaemia, respectively. The data points were randomly divided into three subsets with the each subset consisting of 442 data points of nonhypoglycaemia and 133 data points of hypoglycaemia.

3.2.2   Electrocardiogram obtained from the study

The electrocardiograms of the 5 patients who voluntarily participated in the study have been obtained. The electrocardiogram was obtained from both nonhypoglycaemic– and hypoglycaemic–phase. An example of the electrocardiogram signal with its frequency spectrum is shown in Figure 3.16. As in the figure (left), one of the noises is a ripple in the signal. The noise is a 50 Hz

wave, which can be seen in the frequency spectrum with high amplitude at 50Hz, as in Figure 3.16 (right). The result of the filtering can be seen in Figure 3.17, in which the 50 Hz noise has vanished.

Another noise is a baseline wander with low frequency (less than around 0.3 Hz) as in Figure 3.18 (left). Using the Butterworth high-pass filter of fourth order, the low frequency noise can be omitted from the ECG signals as shown in Figure 3.18 (right). It can be seen in the inserted graph in which the noise with frequency of less than about 0.3 Hz vanishes.

Example of the annotation of the ECG fiducial point is shown in Figure 3.19. As in the figure, the fiducial points *Q, R, S, To, Tp* and *Te* of the ECG have been correctly annotated. The result of the annotation was checked visually. The improper annotation, mostly because of incorrect ECG signals, was not used in this study.

The comparison between the patients' ECG parameters obtained in the hypoglycaemic phase (BGL < 3.0 mmol/l), and the nonhypoglycaemic phase is presented in Table 3.2. The ECG parameters are presented in the form of (mean ± standard deviation) with the associated significance value p, which resulted from a t test. The comparison shows that the ECG parameters in hypoglycaemia differ significantly from those in nonhypoglycaemia ($p<0.01$) except STo_c ($p<0.1$). STo_c is the interval from the S point to the beginning of the T-wave T_o of the ECG signal.

Table 3.2: The comparison of the ECG parameters obtained in the hypoglycaemic phase against the nonhypoglycaemic phase

ECG Parameter	Nonhypoglycaemia	Hypoglycaemia	p-value
HR	1.052 ± 0.061	1.197 ± 0.128	<0.0001
QTe_c	1.040 ± 0.031	1.074 ± 0.054	<0.0001
$TpTe_c$	1.031 ± 0.032	1.074 ± 0.071	<0.0001
QTp_c	1.058 ± 0.071	1.106 ± 0.096	<0.005
$ToTe_c$	1.058 ± 0.071	1.106 ± 0.096	<0.005
RTp_c	1.044 ± 0.039	1.068 ± 0.056	<0.01
STo_c	0.994 ± 0.141	0.940 ± 0.193	<0.1

Those ECG parameters which differ significantly are longer in hypoglycaemia than in nonhypoglycaemia.

The graph in Figure 3.20 shows the BGL profiles of the five patients. Euglycaemic phase (5.0–6.0 mmol/l) is around the first 50 minutes. The next 50
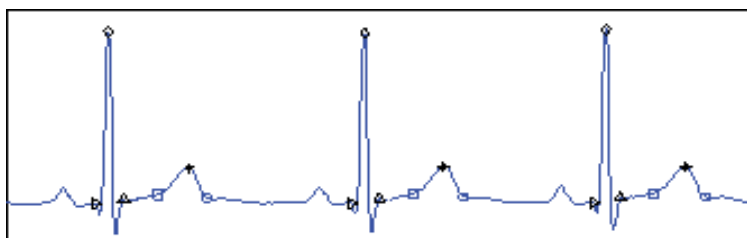
Figure 3.19: Example of the ECG fiducial points from the delineation

minutes is the ramp phase or the transition phase (3.0–5.0 mmol/l). The hypoglycaemic phase (2.5–3.0 mmol/l) is in the last 50 minutes. At around one hour a baseline phase was conducted before the euglycaemic phase and around 4.5 hours of recovery was performed after the hypoglycaemic phase.

3.2.3   Performances of hypoglycaemia detections using SVM

In the approach A1, SVM parameters C, γ, w_0 and w_1 were set to 1, and d was set to 2. The result is presented in Table 3.3. The result shows that all the specificities of all the SVM algorithms are more than 95%, but the sensitivities are low, both in the training and testing. In terms of geometric mean, SVMP performs the best with a geometric mean of 63.82%.

The approach A2 differed from the A1 in its parameter C, which was set to be 100. The other parameters were kept the same as in A1. The result of the A2 is shown in Table 3.5. The sensitivities and geometric means of all the detection algorithms in A2 were significantly higher than those resulting in A1. The specificities in A2 were slightly worse than in A1. The support vector numbers
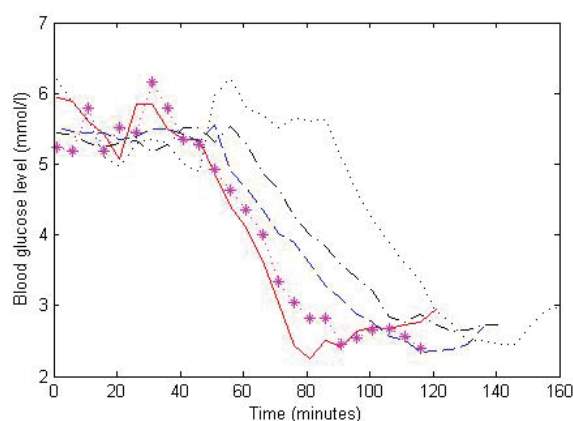
Figure 3.20: The profiles of the blood glucose levels of the diabetic patients.

found in A2 were less than those in the A1. In A2, SVMR performs the best in the testing with the geometric mean of 68.01%. The geometric means of the other algorithms were just slightly worse.

The A3 differed from the A1 and A2 in its parameter *C,* which was set to be 10^4. The other parameters were kept the same as in the A1 and A2. The performance of the approach A3 is described in (Table 3.5). It shows that the sensitivities and geometric means of the testing of all the algorithms are just slightly better than those found in the A2. The SVMR perform the best with the geometric mean of 69.12% in the testing, which is just slightly better than the geometric mean of SVMR found in the A2, which is 68.01%. The support vector numbers of the detection algorithms found in the A3 are worse than those found in the A2.

Table 3.3: The performances of the detection algorithm using A1; all the parameters are set to be 1, except the degree of the polynomial kernel function *d* which is set to be 2.

Detection Algorithm	*C*	*γ/d*	*w₀*	*w₁*	*n_s*	Training			Testing		
						Sens (%)	Spec (%)	Gm (%)	Sens (%)	Spec (%)	Gm (%)
SVMR	1	1	1	1	262	19.55	98.64	43.91	18.05	97.74	42.00
SVMP	1	2	1	1	266	39.10	96.15	61.31	42.86	95.02	63.82
SVML	1	-	1	1	268	3.76	99.32	19.32	3.01	99.32	17.28

Sens: Sensitivity
Gm:Geometric mean
d is only for SVMP

spec: specificity
γ is only for SVMR,
n_s: Support vector number

Table 3.4: The performances of the detection algorithm in A2; all the parameters are set to be 1, except the degree of the polynomial kernel function d which is set to be 2, and C = 100.

Detection Algorithm	C	γ/d	w_0	w_1	n_s	Training			Testing		
						Sens (%)	Spec (%)	Gm (%)	Sens (%)	Spec (%)	Gm (%)
SVMR	100	1	1	1	219	54.14	95.48	71.89	49.62	93.21	68.01
SVMP	100	2	1	1	229	50.38	95.70	69.43	47.37	93.89	66.69
SVML	100	-	1	1	223	50.38	95.70	69.43	48.12	93.67	67.14

Sens: Sensitivity
Gm:Geometric mean
d is only for SVMP

spec: specificity
γ is only for SVMR,
n_s: Support vector number

The result of the A4 is presented in Table 3.6. The approach A4 differed from the A1, A2 and A3 only in its parameter C, which is set to 10^6. Compared to the result of the A3, the sensitivities and geometric means found in the A4 were lower. Thus, increasing parameter C from 10^4 to 10^6 reduces the performances of the testing. It is contrary to increasing parameter C from 1 to 10^2 and from 10^2 to 10^4 which increase the testing performance. The sensitivities and the geometric

Table 3.5: The performances of the detection algorithm using Approach A3; all the parameters are set to be 1, except the degree of the polynomial kernel function d which is set to be 2, and $C = 10^4$.

Detection Algorithm	C	γ/d	w_0	w_1	n_s	Training			Testing		
						Sens (%)	Spec (%)	Gm (%)	Sens (%)	Spec (%)	Gm (%)
SVMR	10^4	1	1	1	205	54.14	95.93	72.06	51.13	93.44	69.12
SVMP	10^4	2	1	1	220	54.14	95.48	71.89	51.13	93.44	69.12
SVML	10^4	-	1	1	220	53.38	95.48	71.39	49.62	92.99	67.93

Sens: Sensitivity
Gm:Geometric mean
d is only for SVMP

spec: specificity
γ is only for SVMR,
n_s: Support vector number

means of all three algorithms are around 48% and 66%, respectively. As in the A1–A3, the increasing C in the A4 also reduces the number of support vector.

The top figure is the training performance and the bottom one is the testing performance. In the testing, the geometric means of SVML and SVMP increase significantly when C changes from 1 to 100. However, the change of C from 10^4 to 10^6 reduces the geometric mean. In the training, the increasing C always provides the better geometric mean of all the three algorithms.
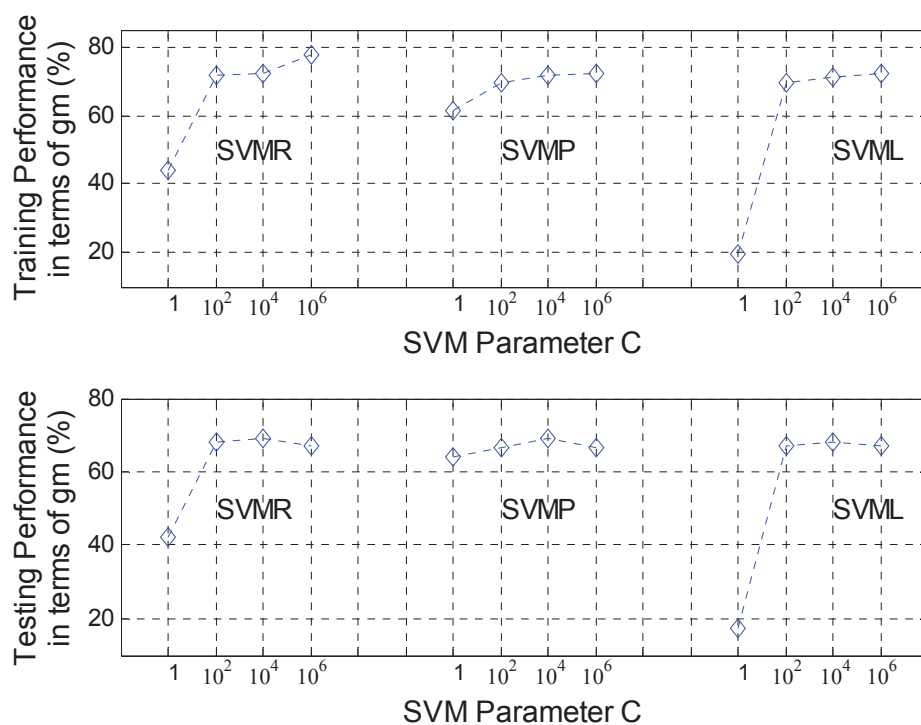
Figure 3.21: The effects of the increase in C from 1 to 10^6 to the performance in the training and the testing.

Table 3.6: The performances of the detection algorithm using the approach A4; all the parameters are set to be 1, except the degree of the polynomial kernel function *d* which is set to be 2, and C = 10^6.

Detection Algorithm	C	γ/d	w_0	w_1	n_s	Training			Testing		
						Sens (%)	Spec (%)	Gm (%)	Sens (%)	Spec (%)	Gm (%)
SVMR	10^6	1	1	1	186	62.41	96.83	77.74	47.37	94.34	66.85
SVMP	10^6	2	1	1	191	54.14	96.61	72.32	48.12	92.53	66.73
SVML	10^6	-	1	1	203	54.89	95.02	72.22	48.87	91.63	66.92

Sens: Sensitivity
Gm:Geometric mean
d is only for SVMP

spec: specificity
γ is only for SVMR,
n_s: Support vector number

In the A5 w_0 was set in such a way that the sensitivities of the detection algorithms were about 70%. The other parameters were set with the same values as in the A1. The result is presented in Table 3.7. As desired, the sensitivities found in this approach were about 70%. The specificities and geometric means of the detection algorithms were more than 70%. The support vector numbers are larger compared to the other approaches (A1, A2 and A3). SVMR performs the best in the Approach A5 with the geometric mean of the testing at 73.63%.

Table 3.7: The performances of the detection algorithm using the E5; w_0 was set in such a way that the sensitivities were about 70%. The other SVM parameters were set to be the same with the A1.

Detection algorithm	C	γ/d	w_0	w_1	n_s	Training			Testing		
						Sens (%)	Spec (%)	Gm (%)	Sens (%)	Spec (%)	Gm (%)
SVMR	1	1	0.280	1	439	75.94	79.19	77.55	70.68	76.70	73.63
SVMP	1	2	0.271	1	535	81.20	72.85	76.91	71.43	70.81	71.12
SVML	1	-	0.260	1	494	80.45	74.43	77.38	71.43	73.08	72.25

Sens: Sensitivity
Gm:Geometric mean
d is only for SVMP

spec: specificity
γ is only for SVMR,
n_s: Support vector number

3.3   DISCUSSION

The proposed hypoglycaemia detection has been presented. It employs SVM algorithm and the input of ECG parameters. Its construction (Figure 3.1) follows a general structure of a medical instrumentation system (Belegundu and Chandrupatla, 2011b). The system consists of a sensing part, signal conditioner and display/alarm. In this research, the sensing part is represented by the ECG acquisition probe. The signal conditioner is represented by the signal processing including feature extraction and SVM classification. Furthermore, the alarm is represented by the output of the SVM classifier, which is a binary value representing a nonhypoglycaemic or hypoglycaemic event.

The SVM model for the hypoglycaemia detection algorithm was found from the SVM training. The training uses the electrocardiographic clinical data. The SVM model can be used to indicate whether the ECG parameter in the input belongs to hypoglycaemia or nonhypoglycaemia. Thus, principally this system could be used for hypoglycaemia detection.

The ECG parameters are obtained from the electrocardiogram which is acquired through Lead II. In terms of the delineating the end of T–wave, using Lead II could minimize the problems with U–wave, as U–wave is less prominent in Lead II (Garson Jr, 1993). Therefore, Lead II is frequently used for QT interval measurement (Salvi et al., 2011). According to Morimoto and Fox (2011), lead II is often used for QT interval measurement as the end of T–wave is most pronounced.

The automatic delineation (section 3.1.3) for electrocardiographic fiducial points has been developed. It was used to mark the points of *Q, R, S, To, Tp* and *Te*. For the delineation of *Te,* the Phillips method was used. Its advantage is that the method suffers less from the variability caused by the arbitrariness in the ECG baseline choosing. Therefore, it could be less sensitive to an ECG baseline drift (Sophia et al., 2009).

To avoid the error of the ECG parameter finding, visually checking on the result of the delineation was performed after the automatic delineation. Only the correct delineation was used. The wrong delineations were mostly from the bad ECG signals, such as the ECG signals shown in Figure 3.22. An automatic delineation is preferable to manual delineation because manual delineation may result in variability of the inter– and intra–individual observer. Therefore, a computer measurement using an algorithm to find ECG parameters is suggested to have more stable results and to be more reproducible (Meza, 2010).

The time intervals for ECG parameters used in this research were corrected by heart rate (or by RR interval). The need for this correction is due to the dependency of the time interval on heart rate or cardiac cycle. The correction was introduced by Bazett (Dantzig, 1951). The six ECG parameters in the hypoglycaemia phase are significantly different from those in the nonhypoglycaemia phase. It implies that the six ECG parameters are important parameters which possibly contribute to hypoglycaemia detection. Therefore, the six ECG parameters are used for inputs of hypoglycaemia detection in this research. STo_c is not significantly different in hypoglycaemic and nonhypoglycaemic phase, and therefore it is not used for input of hypoglycaemia detection. The longer QTc in hypoglycaemia is confirmed in another study (Lee SP et al., 2004). The higher heart
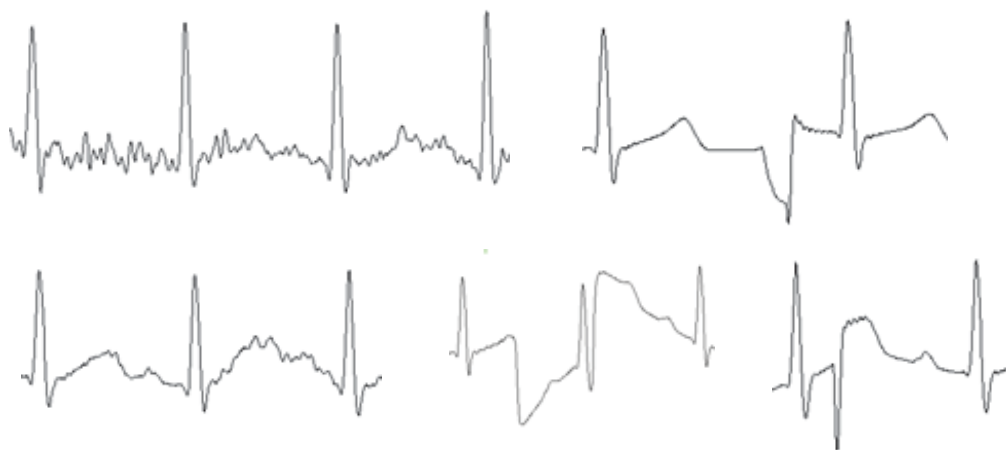
Figure 3.22: Bad ECG signals found from the study

rate in hypoglycaemia is confirmed by (Heger et al., 1996). The longer values of the other ECG parameters (RTp_c, QTp_c, $TpTe_c$, QTe_c, and $ToTe_c$) in hypoglycaemia might be considered as part of repolarization, in which repolarization prolongs hypoglycaemia (Robinson RTCE et al., 2003).

TpTe (a descending part of the T-wave) is suggested as transmural dispersion in the myocardium (Yan and Antzelevitch, 1998). The dispersion is caused by the deviation between endocardial and the M cells action potentials, during repolarization. The interval represents the differences in repolarization time of myocardial cells, as illustrated in Figure 3.23. Benhorin et al. (1990) reported that *TpTe* interval is an important parameter in identifying a patient with long *QT* syndrome. Furthermore, the ratio of *TpTe* interval to *QT* interval is a potentially significant index for an arrhythmic event (Gupta P et al., 2008).
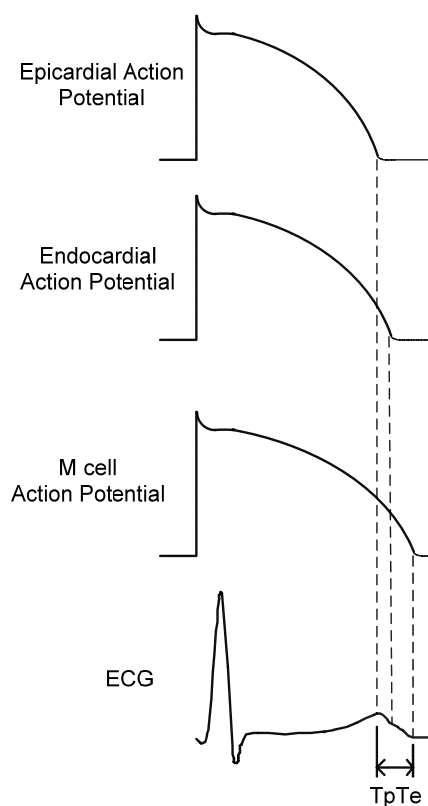
Figure 3.23 Epicardial, endocardial and the M cell action potentials and *TpTe* interval in ECG

ToTe or *T*-wave width might also have a contribution to hypoglycaemia detection. *ToTe* correlates with *T*-wave morphology which is possibly affected by hypoglycaemia (Ireland et al., 2000). *T*-wave begins due to the deviation between epicardial and the M cells action potentials. The deviation between endocardial and the M cells action potentials contribute to the descending part of the *T*-wave. The end of the *T*-wave can be found when all M cells are fully repolarized (Antzelevitch, 2001). The difference of *ToTe* and *TpTe* with the other four ECG variables is that the two variables represent repolarization only, while the other four variables involve depolarization and repolarization. For an evaluation of repolarization, exclusion of the *QRS* complex may be needed so that the evaluation is independent from depolarization (Can et al., 2002).

The relation of hypoglycaemia with an interval from R-peak to the peak of-T wave (*RTp*) is confirmed in Alexakis et al. (2006). For an estimation of repolarization, *RTp* is easier to be estimated than the other parameters. *RTp* is marked by the sharp R peak and the peak of T-wave. This easier estimation could reduce error for repolarization.

SVM has been developed with output of +1, which means that a hypoglycaemic event is happening, and −1, which means that there is no hypoglycaemia. An SVM training has been conducted so that the electrocardiographic situation associated with blood glucose level of less than 3.0 mmol/l is defined as hypoglycaemia, and those with more than 3.0 mmol/l are defined as nonhypoglycaemia.

Table 3.3–Table 3.7 present the performances of the detection algorithms in terms of sensitivity, specificity and geometric mean. The assessment, in terms of sensitivity, is to measure the correct detection of hypoglycaemic events. A detection algorithm with high sensitivity means that it can predict hypoglycaemic events well.

A higher specificity in a hypoglycaemic detector minimizes a false alarm, which is a nonhypoglycaemic event, and recognizes it as a hypoglycaemic event.

The increase in C does not always provide improvement of the performances of the SVM algorithms in the hypoglycaemia detection. The reason could be that conceptually an increasing C value allows more points to cross the supporting hyperplanes of SVM (Figure 3.14). This could reduce the generalization performance of the detection algorithm.

The increase in C value from 10^4 to 10^6 decreases the testing sensitivities in terms of geometric means. On the other hand, this increase in C raises the training performances in all terms –sensitivities, specificities and geometric means. The increase of the training performances (although the testing performance decreases) means that the generalization of the algorithm becomes worse. Results of the A1-A5 also imply that C is a trade-off of performance in training and generalization. Too low C yields a low training performance, whereas too high C value yields a low generalization.

Furthermore, increase in C in the A1–A4 reduces the number of support vectors. The geometric mean increases from A1 to A3, but it decreases from A3 to A4. Thus, it implies that an SVM model with fewer support vector numbers, does not always have better generalization.

Increasing the sensitivities in the Approach A5 compared to those in Approach A1 relates to the decreasing w_0 (in this case the other parameters are retained). The decreasing w_0 yields the increase of the ratio w_1 to w_0. In other words, the increasing of the ratio w_1 to w_0 yields the higher sensitivities.

Essentially, modification of w_0 or w_1 is similar to modification of C in the associated class. Modification of w_0 means modification of C for the data points in the nonhypoglycaemic class, and modification of w_1 means modification of C for the data points in the hypoglycaemic class. In the other words, modification of

thweight factor for a class means modification of *C* to that class, but it does not modify *C* in another class. In the A5, SVMR performs the best where sensitivity, specificity and geometric mean are 70.68%, 76.70% and 73.63%, respectively.

3.4 CONCLUSION

The ECG parameters have been extracted from the electrocardiogram of the patients with type 1 diabetes. The six ECG parameters in hypoglycaemia were significantly different from those in nonhypoglycaemia. This indicates that the ECG parameters could contribute in hypoglycaemia detection. The ECG parameters were tested for the hypoglycaemia detection with SVM algorithms. The SVM algorithms with different kernel functions and different SVM parameters were investigated. The investigation was to explore these differences in relation to the performance of hypoglycaemia detection. In addition, the number of support vectors in relation to the performance of the detection algorithm was also presented. The SVM parameter *C* and the weight factor (w_0 and w_1) could play an important role in finding the good performance of SVM models for hypoglycaemia detection. The best performance of hypoglycaemia detection found in the experiment is 73.63% in term of geometric mean. The best performance was found when hypoglycaemia detection employs SVM with the RBF kernel function, with the SVM parameters $C = 1$, $\gamma = 1$, $w_0 = 0.280$ and $w_1 = 1$. This performance was slightly low and hence a more advanced SVM is necessary to find a higher performance.

CHAPTER 4.
SWARM BASED SUPPORT VECTOR MACHINE FOR HYPOGLYCAEMIA DETECTION

The experimental results presented in Chapter 3 show the influence of SVM parameters to the performances of hypoglycaemia detections. One of the results shows that different values of SVM parameters can vary the sensitivity from 18.05% to 70.68% and the geometric mean from 42.00% to 73.63%. The influence of SVM parameters to the performance of the SVM algorithm is also presented in another study (Zhou et al., 2011).Therefore, it is necessary to optimize SVM parameters in such a way that the performance of the detection algorithm is optimal for hypoglycaemia detection.

A method to find the optimal SVM parameter is by varying the SVM parameters in the SVM training. This method was applied in a study by Elif Derya (2007). The study varies the RBF kernel width γ between 0.1 and 0.6, with interval 0.1. The study found that $\gamma = 0.4$ yields the minimum misclassification rate. Meanwhile, the optimal parameter C was determined by varying the C value; $C = 80$ was found as the optimal one. Determining the optimal SVM parameters using this method might not be suitable for this research as this research needs to find four optimal SVM parameters. Determining the four optimal-parameters should be conducted simultaneously, instead of individually, as together they are used in the SVM training. Finding one optimal-parameter in the SVM training cannot exclude

the other three parameters. Furthermore, the interval used in the study (Elif Derya, 2007) was 0.1. This interval might not guarantee that the optimization provides the optimal value, which might be in the smaller interval. Furthermore, if the interval is made smaller, for example 0.01, a larger number of experiments need to be conducted.

Another method to find the optimal SVM parameters is by using a grid search technique (Devos et al., 2009). Using the technique, an objective function is used to evaluate all the grid points in the design space. Figure 4.1 presents grid points of two parameters (x and y). Each parameter from the lower bound l to the upper bound u consists of 5 points. Using this grid search, an objective function is evaluated with the points of (x_1,y_1), (x_2,y_1), ..., (x_5,y_5). The total points are 25. In general, the number of total points is n^p where n is the number of points in each parameter and p is the number of parameters. In this research, four SVM parameters are used. Suppose each parameter comprises 20 points, an objective function is evaluated by $20^4 = 160,000$ points. This means the objective function is evaluated 160,000 times with different parameter values; it needs a great deal of time. Therefore, a grid search method might not be suitable to find the optimal SVM
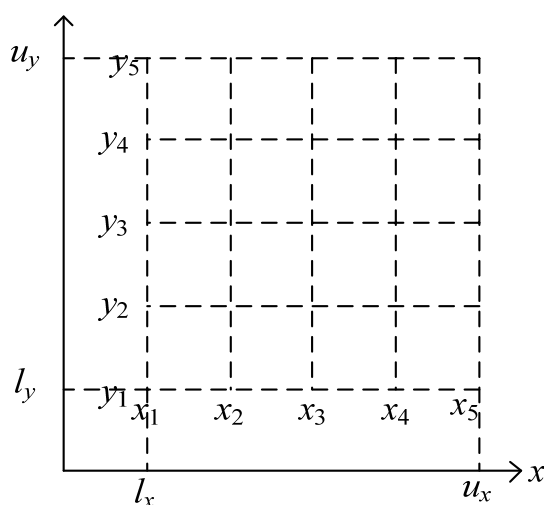
Figure 4.1: A Grid with two parameters and five points in each parameter.

parameters in this research.

In this research a particle swarm optimization (PSO) was chosen to optimize SVM parameters (or to find the optimal SVM parameters). By using PSO, a search space for SVM parameters can be made wider, rather than just 0.1–0.6 as in Elif Derya (2007) , and also can be made with an interval of far less than 0.1. The SVM parameters (C, γ, d, w_0, w_1) could be optimized simultaneously by using PSO, instead of individually. By applying PSO in the optimization of SVM parameters, this research developed a hybrid PSO and SVM, forming a swarm based support vector machine (SSVM), which is presented in this chapter.

4.1   INTRODUCTION TO PARTICLE SWARM OPTIMIZATION (PSO)

An optimization relates to the process of maximizing or minimizing an objective function with a defined contraint (Belegundu and Chandrupatla, 2011a). In an optimization, one would like to find a global minimum or maximum of an objective function, subjecting to a contraint, if any. Figure 4.2 indicates the local and global minimum of a function. Optimization of $f(X)$ can be stated as in the following:

Find $X = [x_1\ x_2\ x_3\ \ldots\ x_n]$ which minimizes $f(X)$.
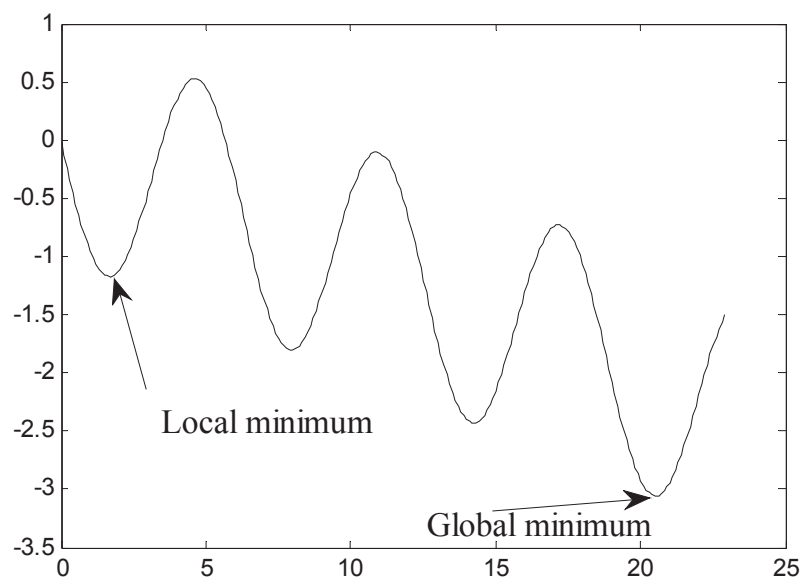
Figure 4.2: Local and global minimum of a function.

Initially, in 1847, a minimization using derivatives of a function (or the gradient method) was presented by Cauchy; this is one of the oldest methods for the minimization of a general nonlinear function (Beni and Wang, 1989). Gradient method or gradient descent is an iterative method with an initial point. The iteration of gradient descent follows the negative of the gradient in order to move toward a critical point, which is hopefully the minimum value. This method is popular because it is easy to implement and each iteration is cheap. A disadvantage of gradient descent is its tendency of getting trapped in a local minimum (Kavitha et al., 2010). In addition, the local minimum depends on the given initial point. This limitation could result in a poor training and poor generalization performance.

A further three optimization methods were later presented: an optimization based on penalty functions (Chan et al., 2011b), maximization of linear variables subject to linear inequalities (Burges, 1999), the "KKT" optimality conditions for constrained problems (Plat, 1999). Subsequently, other methods for solving

nonlinear optimization problems were developed.

In general, there are two major categories of algorithms for an optimization, namely, deterministic and stochastic algorithms. The main characteristic of the deterministic algorithm is the exact reproducibility of the steps in the optimization, which uses the same initial conditions for the same problem. Whereas, a stochastic algorithm produces samples of prospective solutions in the space, which often results in a different sequence of samples in different experiments, even with the same initial conditions. The methods which can be categorized to be deterministic one are grid search, covering method and trajectory-based method.

In general, stochastic approaches generate and use random variables. The approaches produce estimation models for the position of the global minimum, which are refined using information found from the previous iterations. One of the advantages of the approaches is that they can be employed in a problem (or an objective function) where its mathematical properties are not well known.

One type of stochastic optimization is pure random. To optimize an objective function in finding the optimal solution, a pure random search generates solutions at each iteration, and the objective function is evaluated using these solutions. This method needs a vast number of solutions to find an acceptable result; consequently, the method is inefficient. An improvement is needed to tackle the drawbacks of this method. One way would be to apply a method which uses a local search on several considered local points of solution, instead of all points. Alternatively, as an important improvement of the random search method, an algorithm inspired by a stochastic model in nature is used. It produces research fields such as evolutionary computation and swarm intelligence algorithms.

Swarm intelligence optimizations are typically made up of a population (swarm) of individuals (or agents). The idea of swarm intelligence optimization is based on a simple interaction between components (or agents) of a small society

(swarm). This optimization works on the collective behavior of decentralized, self-organized systems. The expression of swarm intelligence appeared in 1989 as a set of algorithms controlling a number of robots operating in n-dimensional space with distributed control (Wexler et al., 2007). There is no central controller and robots can only talk to others next to them. The robots are autonomous, but have to cooperate with the other robots to achieve some predefined goal. Thus, a swarm intelligence is typically made up of a population (swarm) of simple agents. Interactions between such agents lead to the emergence of "intelligent" global behavior, unknown to the individual agents. A swarm intelligence includes ant colony optimization, stochastic diffusion search and particle swarm optimization (PSO).

PSO was introduced by Kennedy and Eberhart (1995), performing optimization using an evolutionary technique based on the movement of swarms. It was inspired by the social behaviour of bird flocking and fish schooling (del Valle et al., 2008). Particles of swarm (or population) fly through an n-dimensional solution space with adjusted velocity and position. The velocity is adjusted according to the history of particle best-position and the neighborhood best-position, which are derived according to a user defined fitness function. A limitation of PSO or a stochastic algorithm is that it is computationally expensive (Sheikh-Bahaei et al., 2005, Alves et al., 2006). Because the optimization in this research is conducted for off-line optimization, this limitation could be ignored.

4.2 DEVELOPMENT OF A HYPOGLYCAEMIA DETECTOR BASED ON THE SWARM BASED SUPPORT VECTOR MACHINE

The structure of the swarm based support vector machine (SSVM) is presented in Figure 4.3. The input was ECG parameters, and the output was the glycaemic state –hypoglycaemia or nonhypoglycaemia. The parameters of SVM were optimized using PSO (the optimal parameters of SVM were found using PSO). The SVM parameters are C, w_o, w_1, γ, d. The parameter of C deals with a trade-off between maximum margin and the classification error of SVM. SVM with high C provides perfect classification in the training phase which uses a training data set, but it may be poor in generalization (or bad performance in classification using a test data set). On the other hand, SVM classification with low C might give a bad performance in the training phase. Therefore, optimal C has to be chosen in order to find the optimal classification. Likewise, the optimal values of parameters γ and d also need to be found to obtain the optimal performance.

4.2.1 Optimization of SVM parameters using PSO
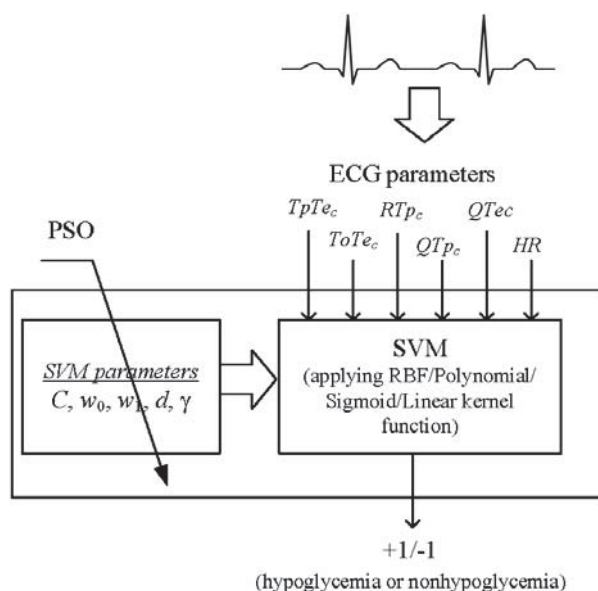
Figure 4.3: Hypoglycaemia detection using swarm based support vector machine

This research utilizes the PSO algorithm to find the optimal SVM parameters according to a defined fitness function. Four SVM parameters are optimized; they are C, γ (for RBF and sigmoid kernel functions) or d (for polynomial kernel function), w_0 and w_1 (weight factors for nonhypoglycaemic and hypoglycaemic class data, respectively).

The optimization of SVM parameters using PSO can be described as in

```
begin
    n  →1            // iteration number
    Initialize z      // z: position
    Evaluate f(z)    // f(·): fitness function (Eq. 4.4)
    Initialize v      // v: velocity
    z̃ = z              // z̃: personal best position
    ẑ = z̃              // ẑ: global best position
while (not termination condition) do
    begin
n → n +1
Update position of particle zⱼᵏ(n) and velocity vⱼᵏ(n) based on Eqs. 4.1 and
    4.2, respectively.
if v(n) > vmax , v(n) = vmax end
if v(n) <– vmax, v(n) = – vmax end
Evaluate f(x(n))     // f(x(n)) is defined in Eq. 4.4
Update z̃ if the new position is better than the previous z̃
Update ẑ if the new position is better than the previous ẑ
    end
end
```

**Figure 4.4: The pseudo of the PSO for the SVM
parameter optimization**

Figure 4.4. Suppose a swarm at n-th iteration is $z(n)$. It contains ω particles with τ dimensions. More clearly, in this work four parameters are used, and therefore, the τ

is 4. The number of particles used in the optimization of this work is 50. Each element of the swarm is presented by $z_j^k \in Z(n)$, in which $j = 1, 2,\ldots, \tau$ and $k = 1, 2,\ldots, \omega$; τ is the dimension of a particle and ω denotes the number of particles in the swarm. The particles can be expressed as in the matrix in Figure 4.5.
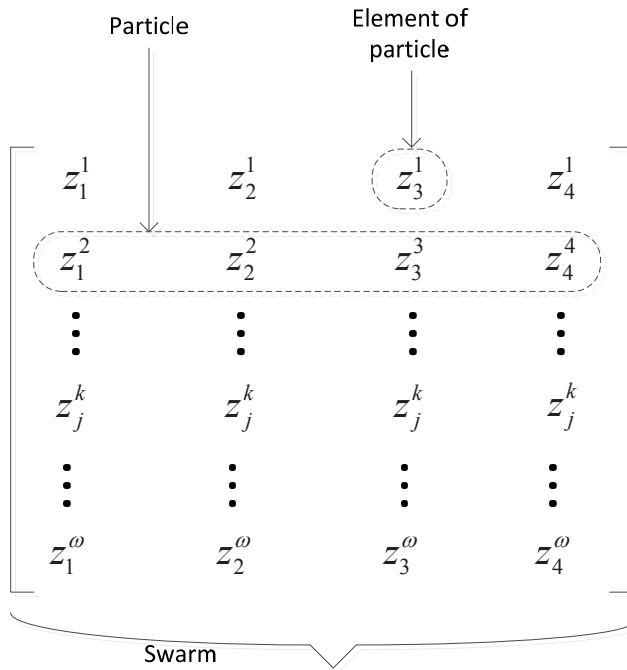
Figure 4.5: The particles of the PSO

The algorithm was initialized by generating random numbers for position and velocity. At iteration n, the position $z_j^k(n)$ is determined as follow (del Valle et al., 2008):

$$z_j^k(n) = z_j^k(n-1) + v_j^k(n) \qquad 4.1$$

in which the velocity $v_j^k(n)$ is defined as (del Valle et al., 2008)

$$v_j^k(n) = \varphi v_j^k(n-1) + c_1 r_1 \left(\tilde{z}_j^k - z_j^k(n-1) \right) + c_2 r_2 (\hat{z}_j - z_j^k(n-1)). \qquad 4.2$$

$\tilde{z}$ is the personal best position, which is the best position of the particle at iteration n. $\hat{z}$ is the global best position which is the best position among all the particles from the first iteration until iteration n. φ is an inertia weight factor, which controls the convergence of the optimization behavior. c_1 and c_2 are the acceleration

constants, which control the distance moved by a particle. r_1 and r_2 are the uniform random numbers between 0 to 1. The constants c_1 and c_2 are set to 2; and r_1 and r_2 are the random number in the range [0, 1].

The velocity v is limited in a certain region, which is between $-v_{max}$ and v_{max}. Thus, if v is more than v_{max}, v is set to v_{max} and if v is less than $-v_{max}$, v is set to $-v_{max}$. This strategy is called velocity clamping, which is used to limit the swarm particles to a search space (Siddiqui et al., 2011). For this optimization, v_{max} is set to 0.2. Furthermore, the inertia weight is set as follow:

$$\varphi = \varphi_{max} - \frac{\varphi_{max} - \varphi_{min}}{N} \times n \qquad 4.3$$

where φ_{max} and φ_{min} are upper and lower inertia weights, respectively, and are set to 1.2 and 0.1, respectively, N is the total iteration number and n is the iteration number.

4.2.2   Fitness function for the optimization

The objective of the PSO optimization was to maximize the performance of the hypoglycaemia detection. The performance was measured in terms of sensitivity ϑ and specificity $\mathcal{S}$, as defined in Eqs. 3.3 and 3.4. Sensitivity was defined as the ratio of correct detection of hypoglycaemia to the actual number of hypoglycaemia cases. Specificity was defined as the ratio of correct detection of nonhypoglycaemia to the actual number of nonhypoglycaemia cases. Thus, the PSO optimization was essentially used to maximize sensitivity ϑ and specificity $\mathcal{S}$, and then the fitness function was defined as

$$f = -(\kappa\vartheta_{tr} + (1 - \kappa)\mathcal{S}_{tr} + \kappa\vartheta_v + (1 - \kappa)\mathcal{S}_v + \hbar) \qquad 4.4$$

ϑ_{tr} and $\mathcal{S}_{tr}$ were, respectively, the sensitivity and specificity of the training. ϑ_v and $\mathcal{S}_v$, respectively, were the sensitivity and specificity of the validation The training data set was used for the SVM training to find an SVM model. The validation data set was used to test the SVM model during the optimization.

The inclusion of ϑ_v and $\mathcal{S}_v$ in the fitness function is to reduce the risk of overtraining (Astion et al., 1993). Overtraining could yield a high performance in the training stage, but it might provide a low performance in the testing. In the fitness function, κ was set to 0.58 to obtain a higher sensitivity than specificity. This strategy is to prevent the risk of the low sensitivity of the hypoglycaemia detection. Furthermore, to force the detection to have high sensitivity, parameter k is given by using the following definition

$$k = \begin{cases} 10 \ if \ \vartheta_{tr} > 0.7, \mathcal{S}_{\mathrm{tr}} > 0.4, \vartheta_v > 0.7, \mathcal{S}_v > 0.4 \\ 0 \ otherwise \end{cases} \qquad 4.5$$

By the definition of k in Eq. 4.5 the detection is forced to find sensitivity and specificity of more than 70% and 40%, respectively. Considering Eq. 4.4 and Eq. 4.5, if the detection provides sensitivity and specificity of more than 70% and 40%, respectively, the fitness function has the value of more than 10. Conversely, if the detection provides sensitivity and specificity of less than 70% and 40%, respectively, the fitness function has the value of less than 2; in this formula the maximum sensitivity and specificity is 1 (or 100%).

4.3 EXPERIMENTAL RESULTS

For comparison and analysis purposes, the following approaches were used to develop hypoglycaemia detection model:

- Approach I (A1) which was the SSVM with the inputs of all six ECG parameters (Figure 4.6). Four kernel functions were investigated (RBF, polynomial, sigmoid and linear kernel functions). There were four algorithms: SSVMR (SSVM which employed RBF kernel function), SSVMP (SSVM which employed polynomial kernel function), SSVMS (SSVM which employed sigmoid kernel function) and SSVML (SSVM which employed linear kernel function).

- Approach II (A2) which was similar to A1, but the PSO was not applied;

instead, the SVM parameters were generated randomly (Figure 4.7). The approach was called rSVM; thus, there were rSVMR, rSVMP, rSVMS and rSVML, which were the SVM algorithms employing RBF, polynomial, sigmoid and linear kernel functions, respectively, without the PSO.

- Approach III (A3), similar to A1 but the inputs were the ECG parameters which were corrected by using the Fridericia formula (Fridericia, 2003), instead of using the Bazett formula. Using the Fridericia formula means that the ECG parameters were corrected (or divided) by $RR^{1/3}$. RR was the interval between two consecutive R points of ECG. The approach is called SSVMF.

- Approach IV (A4) which was a multiple regression with PSO (called SMR), Figure 4.8. SMR was the multiple regression in which their coefficients were optimized using particle swarm optimization. The coefficients were β as in the following formula (Ling and Nguyen, 2011)

$$y_i = \beta_0 + \beta_1 x_i + \beta_2 x_i^2 + \cdots + \beta_n x_i^{n_0}. \qquad 4.6$$

where y_i was the output with binary levels, which were hypoglycaemic or
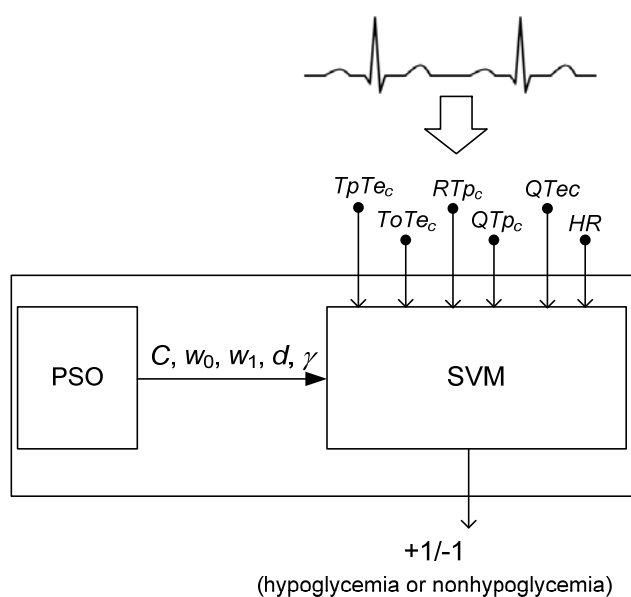
Figure 4.6: Hypoglycaemia detection using SSVM with the input of

nonhypoglycaemic levels; x_i represented the ECG parameters as the input and n_o represented the order of the multiple regression. This approach investigated linear, second order and third order multiple regression, which were called SMR1, SMR2 and SMR3, respectively;

- Approach V (A5) which was the SSVM where the inputs were varied by the combinations of the six ECG parameters (Figure 4.9). In the figure, switches were used to connect or to disconnect the ECG parameters to SSVM, to make a combination of inputs.

- Approach VI (A6) which was SSVM where the SVM weight parameters (w_0 and w_1) were not optimized (SSVMw). The inputs were the six ECG parameters.
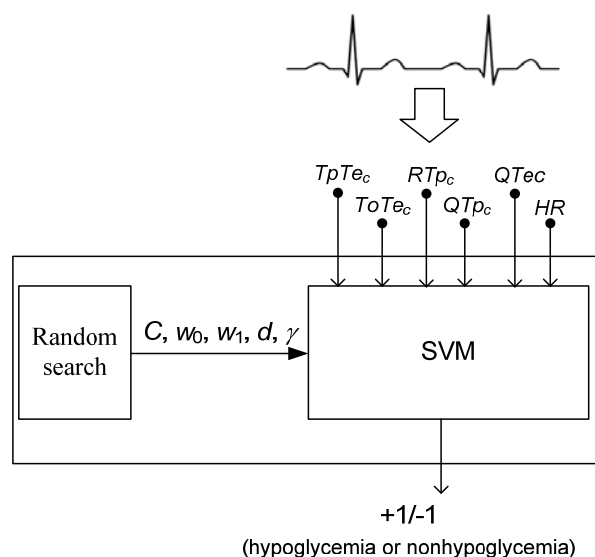
Figure 4.7: Hypoglycaemia detection using SVM with its parameters generated randomly (Approach II)
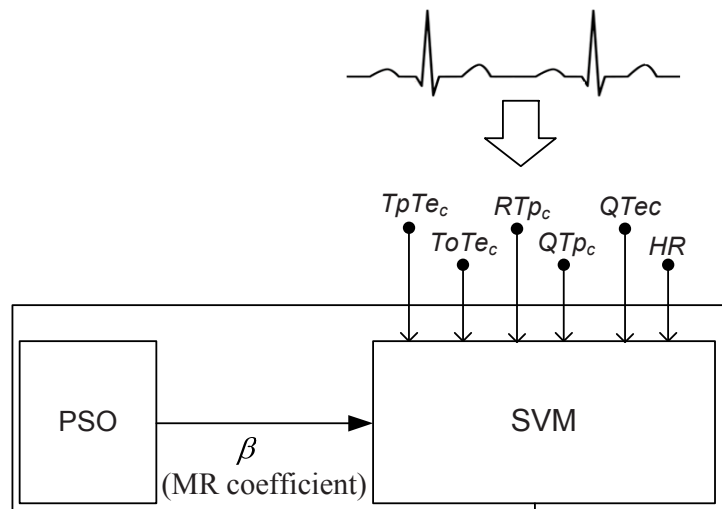
The detection of hypoglycaemia using SSVM has been conducted. SSVM was investigated with inputs of the six ECG parameters, namely $TpTe_c$, $ToTe_c$, RTp_c, QTP_c, QTe_c and heart rate (HR). PSO was used to automatically obtain the optimal SVM parameters C, w_0, w_1, γ, d considering to the fitness function (Eq. 4.4). The ranges of values of the parameters were created as the following; C: 1 to 10^5, w_0, w_1: 10^{-4} to 1, γ: 0.01 to 100, d: 1 to 50.

The hypoglycaemia detections employed the data of ECG parameters which
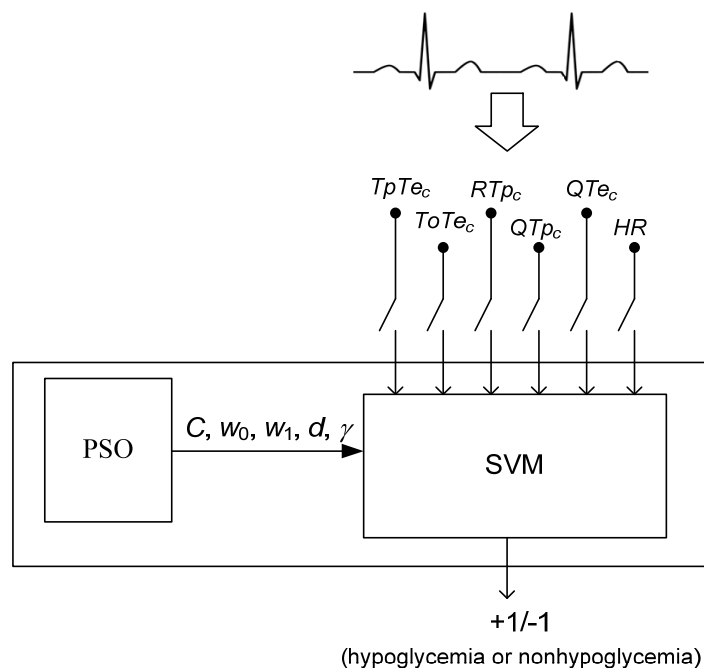
Figure 4.9: Hypoglycaemia detection using SSVM with inputs are varied by the combinations of the six ECG parameters (Approach V).

were used in Chapter III. Three data sets were used: training, validation and testing data sets. Each data set consists of 442 hypoglycaemic data points and 133 nonhypoglycaemic data points. The training data set was used during training to create a hypoglycaemia detection model. The validation data set was used to test the hypoglycaemia detection model during the optimization. The testing data set was used to test the optimal hypoglycaemia detection model obtained from the optimization.

The performances of SSVM with different four kernel functions are presented in Table 4.1. The performances are presented in terms of sensitivity, specificity and geometric mean. In Table 4.1, the sensitivities and specificities in training, validation and testing are more than 70% and 40%, respectively, except the sensitivities of SSVML. The achievement of sensitivity and specificity of more than 70% and 40%, respectively, is as desired of the optimization with definition of the fitness function (Eqs. 4.4 and 4.5).

In terms of geometric mean, the performance of SSVMR is better than the other three algorithms, in the training, validation and testing. In the test, the sensitivity, specificity and geometric mean of SSVMR are 84.21%, 67.65% and 75.48%, respectively.

Table 4.1: The performance of the hypoglycaemia detection using different techniques of SSVM and using the same input that is all six ECG parameter

Detection algorithm	Training			Validation			Testing		
	Sens.	Spec.	Gm	Sens.	Spec.	Gm	Sens.	Spec.	Gm
SSVMR	95.49	68.10	80.64	84.96	65.38	74.53	84.21	67.65	75.48
SSVMP	87.97	68.33	77.53	83.46	64.03	73.10	78.95	63.12	70.59
SSVMS	88.72	64.93	75.90	83.46	61.76	71.80	79.70	61.31	69.90
SSVML	53.38	95.25	71.31	45.86	92.31	65.07	53.38	88.69	68.81

SSVMR: Swarm-based SVM-RBF,   SSVMS: Swarm-based SVM-Sigmoid,
SSVMP: Swarm-based SVM-Polynomial,   SSVML: Swarm-based SVM-Linear.

Table 4.2: The testing performance of the hypoglycaemia detections without PSO (input: all six ECG parameter)

Detection technique	Testing		
	Sens. (%)	Spec. (%)	Gm (%)
rSVMR	53.50	90.90	69.74
rSVMP	49.35	94.20	68.19
rSVMS	24.18	75.33	42.68
rSVML	48.87	92.29	67.16

rSVMR: SVM-RBF,   rSVMP: SVM-Sigmoid,
rSVMP: SVM-Polynomial,   rSVMP: SVM-Linear,

For the comparison to the SSVM, the SVM algorithms which did not use the proposed swarm optimization were investigated. The performances of rSVMs are presented in Table 4.2. The presented performances of rSVM are the average of 100 repeated detections in which the SVM parameters are generated randomly. The results show that in general in terms of sensitivity and geometric mean, the performances of the rSVMs are worse than the swarm-based SVMs. but their specificities are higher. The sensitivities of all four rSVMs are less than 70%.

The hypoglycaemia detection which used SSVMRF has been conducted. SSVMRF used the input of ECG parameters corrected by Fridericia formula. Sensitivity of SSVMRF is higher than SSVMR, but its specificity and geometric mean are lower (Table 4.3). The geometric mean of SSVMRF is 71.04%, in which the SSVMR's geometric mean is 75.48%.

Multiple regressions with the swarm optimization (SMR1, SMR2 and SMR3) have been applied for hypoglycaemia detection, and the result is presented in Table 4.3. In term of geometric mean, the performance of SMR3 is worse than that of SMR1 and SMR2. The performances of SMR1 and SMR2 are nearly same in term of geometric mean. Furthermore, SMR1 and SMR2 perform worse than SSVMR. Thus, in general the swarm based SVM performs better than the swarm

based multiple regression. Furthermore, the SSVM which does not optimize the SVM weight factors (w_0 and w_1), called SSVMw, provide a low sensitivity (49.62%) and a high specificity (94.34%), with the geometric mean of 68.42%.

Table 4.3: Comparison of the performance of the swarm based SVM with the other methods

Detection technique	Testing		
	Sens. (%)	Spec. (%)	Gm (%)
SSVMR	84.21	67.65	75.48
SSVMRF	86.47	58.37	71.04
SSVMw	49.62	94.34	68.42
SMR1	75.53	66.09	70.65
SMR2	76.02	67.01	71.37
SMR3	56.07	65.52	60.61

SSVMRF: SSVMR with the input of the ECG parameters corrected by Fridericia formula

SSVMw: SSVMR without the optimization of w_0 and w_1

SMR1: Linear multiple regression with PSO optimization

SMR2: Second order multiple regression with PSO optimization

SMR3: Third order multiple regression with PSO optimization

Table 4.4: The performance the SSVM hypoglycaemia detection using single input.

Inputs	Testing		
	Sens.	Spec.	Gm
HR	82.71	57.01	68.67
QTe_c	75.19	57.47	65.73
$TpTe_c$	87.97	28.05	49.68
QTp_c	78.20	49.10	61.96
$ToTe_c$	73.68	52.04	61.92
RTp_c	78.20	57.92	67.30
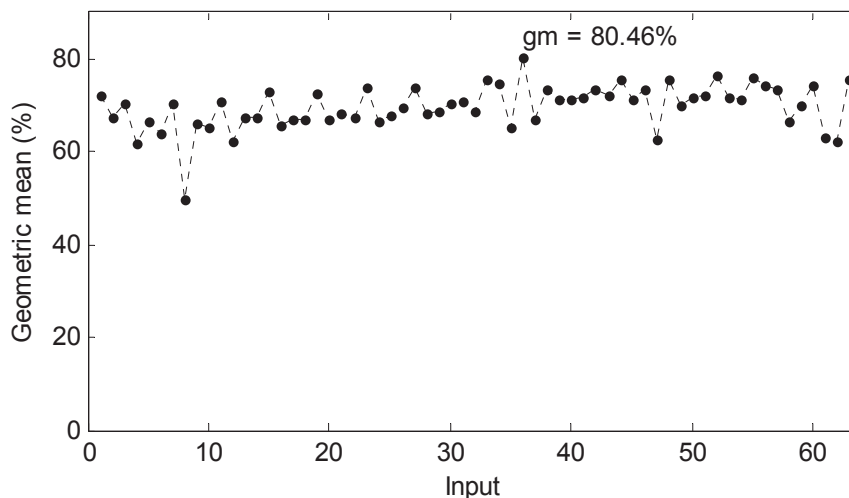
Legend of the inputs

1 :	x_1	17 :	x_3x_5	33 :	$x_2x_3x_5$	49 :	$x_1x_3x_4x_6$
2 :	x_2	18 :	x_3x_6	34 :	$x_2x_3x_6$	50 :	$x_1x_3x_5x_6$
3 :	x_3	19 :	x_4x_5	35 :	$x_2x_4x_5$	51 :	$x_1x_4x_5x_6$
4 :	x_4	20 :	x_4x_6	36 :	$x_2x_4x_6$	52 :	$x_2x_3x_4x_5$
5 :	x_5	21 :	x_5x_6	37 :	$x_2x_5x_6$	53 :	$x_2x_3x_4x_6$
6 :	x_6	22 :	$x_1x_2x_3$	38 :	$x_3x_4x_5$	54 :	$x_2x_3x_5x_6$
7 :	x_1x_2	23 :	$x_1x_2x_4$	39 :	$x_3x_4x_6$	55 :	$x_2x_4x_5x_6$
8 :	x_1x_3	24 :	$x_1x_2x_5$	40 :	$x_3x_5x_6$	56 :	$x_3x_4x_5x_6$
9 :	x_1x_4	25 :	$x_1x_2x_6$	41 :	$x_4x_5x_6$	57 :	$x_1x_2x_3x_4x_5$
10 :	x_1x_5	26 :	$x_1x_3x_4$	42 :	$x_1x_2x_3x_4$	58 :	$x_1x_2x_3x_4x_6$
11 :	x_1x_6	27 :	$x_1x_3x_5$	43 :	$x_1x_2x_3x_5$	59 :	$x_1x_2x_3x_5x_6$
12 :	x_2x_3	28 :	$x_1x_3x_6$	44 :	$x_1x_2x_3x_6$	60 :	$x_1x_2x_4x_5x_6$
13 :	x_2x_4	29 :	$x_1x_4x_5$	45 :	$x_1x_2x_4x_5$	61 :	$x_1x_3x_4x_5x_6$
14 :	x_2x_5	30 :	$x_1x_4x_6$	46 :	$x_1x_2x_4x_6$	62 :	$x_2x_3x_4x_5x_6$
15 :	x_2x_6	31 :	$x_1x_5x_6$	47 :	$x_1x_2x_5x_6$	63 :	$x_1x_2x_3x_4x_5x_6$
16 :	x_3x_4	32 :	$x_2x_3x_4$	48 :	$x_1x_3x_4x_5$	:	

(x_1:HR, x_2:QTe_c, x_3:$TpTe_c$, x_4:$ToTe_c$, x_5:RTp_c and x_6:QTp_c.)

Figure 4.10: The geometric mean of the SSVMR with different inputs. The x axis indicates the combinations of ECG parameters. The best geometric mean is 80.46% when the inputs are *HR and ToTe_c*.

SSVMR with the different inputs, which are all the possible combinations of the six ECG parameters has been investigated. There are 63 combinations ($63 = 2^6 - 1$). The SSVMR performances in terms of geometric mean with 63 combinations of ECG parameters are presented in Figure 4.10. With the input of a single ECG parameter, the performance of SSVMR is presented in Table 4.4. The table

Table 4.5: The best performance of the hypoglycaemia detection using SSVMR with the inputs of HR and *ToTe*$_c$

Training			Validation			Testing		
Sens. (%)	Spec. (%)	Gm (%)	Sens. (%)	Spec. (%)	Gm (%)	Sens. (%)	Spec. (%)	Gm (%)
88.72	83.94	86.3	80.45	77.6	79.01	80.45	79.64	80.04

indicates that each ECG parameter shows a significant contribution to the performance of the hypoglycaemia detection. In the testing, the contribution is indicated by the detection performance with sensitivity of more than 73% and geometric mean of more than 49%. Among these performances, in terms of the geometric mean, the performance of the detection using heart rate is the highest. The second and the third highest performances are the detections which use *RTp*$_c$ and *QTe*$_c$, respectively.

The investigation of SSVM with different inputs shows that the best geometric mean is obtained when the inputs are *HR* and *ToTe*$_c$. The best geometric mean is 80.46% (Figure 4.10). The performances in the training, validation and testing are presented in Table 4.5. The geometric mean of the SSVM with the inputs of the two ECG parameters above is higher than the geometric mean when all six ECG parameters are used.

The optimal parameters of *C*, γ, w_0 and w_1 of the SSVM with the inputs which provide the best performance are listed in Table 4.6. In general the optimal

Table 4.6: The optimal parameters of SSVM with the input of HR and *ToTe*$_c$.

C	γ	w_0	w_1
6.37×10^4	87.78	0.14	1.00

n_s = Support vector number
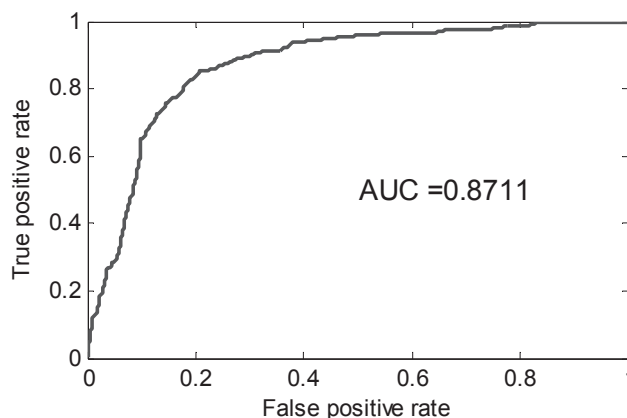
Figure 4.11: ROC of the hypoglycaemia detection using swarm based support vector machine

w_0 is less than the optimal w_1 with the ratio w_0: w_1 of 0.14:1. The optimal C is 6.37×10^4, with the associated support number of 284.

The receiver operating characteristic (ROC) curves of the SSVM with the best performance is displayed in Figure 4.11. ROC is a plot for a pair of a true positive rate (or sensitivity) vs. a false positive rate (or one minus specificity) (Zweig and Campbell, 1993). The values presented in the ROC curve are in 0 to 1, instead of percentage 0 to 100%. The graphs show that the ROC curve is closer to the left top corner rather than to the diagonal line. Area under curve (AUC) can be used to express the performance of a diagnostic test (Zweig and Campbell, 1993). AUC of 0.8711 is found by the SSVM.

4.4 DISCUSSION

The experimental results of the hypoglycaemia detections using the swarm based SVM algorithms have been presented. SSVMs with different kernel functions and different inputs have also been compared. Furthermore, the detection using SSVM has also been compared with the swarm based multiple regression and the SVM algorithms without the swarm optimization.

The performance of SSVMR (SSVM with RBF kernel function) is better

compared to the other three SSVMs, which employ polynomial, sigmoid and linear kernel functions. It is possible that the data found from the RBF mapping is more likely to be correctly classified by SVM than from the other kernel functions mappings. Furthermore, SVM-linear could be a special case of SVM-RBF (Keerthi and Lin, 2003), which means that SVM-RBF has more possibilities to obtain a better performance than SVM-linear. The better performance of the SVM based system which employs RBF is confirmed in another application (Song et al., 2011).

The proposed swarm optimization can work as desired. It is indicated by the sensitivity and specificity of SSVM algorithms. In the proposed optimization, the desired sensitivity and specificity are more than 70% and 40%, respectively (Eq. 4.5). The obtained sensitivity and specificity are more than 70% and 61%, respectively. As a comparison, the sensitivities of the SVM algorithm without the proposed optimization (rSVM) are less than 54%. The specificities of rSVM are higher against the SSVM. It might happen because rSVM tends to obtain the total sensitivity and specificity as high as possible without consideration of more than 70% in sensitivity. Therefore, the definition of σ in Eq. 4.5 (which forces the hypoglycaemia detection to have sensitivity and specificity of more than 70% and 40%) can work effectively. In other words, the proposed SSVM could be suitable to prevent a low sensitivity in hypoglycaemia detection. A high sensitivity of a disease detector means it has a high true positive. The high true positive in a hypoglycaemia detection means that the hypoglycaemic events can be detected properly.

In the fitness function (Eq. 4.4), κ was set to 0.58. This κ value was determined through several experiments. The important thing of κ value is that the coefficient for the sensitivity is set higher than the coefficient for the specificity. By this setting a low sensitivity could be avoided. This setting is necessary because the data number of the hypoglycemic class is far lower than nonhypoglycemic class. This imbalance has the risk of low sensitivity. However, if κ is too high, the

sensitivity could be very high and the specificity could be very low. Therefore, the κ value should be more than 0.50, but not too high.

The computational time required by the optimization using PSO depends on the iteration number provided and the time consumed in every iteration. Every iteration creates n SVM training to make n SVM models; n is the number particles of PSO. In this thesis, the iteration number is 200 and the particle number is 50. Hence, after 200 iterations the optimization terminates. Another termination criterion is the gradients of the global best during m iteration; if the gradients are less than a defined value, the optimization terminates. It means that if the optimal values do not change significantly during m iteration, the optimization terminates.

The SSVMR which includes all six ECG parameters in the input is not the best among the SSVMRs with different inputs. The combination of ECG parameters in the input which yields the best performances is $HR–ToTe_c$. Furthermore, considering the performances of the hypoglycaemia detections which employ single input, each of the six ECG parameters has shown a contribution for hypoglycaemia detection. This is indicated by results of the hypoglycaemia detections using single input, which resulted in the sensitivities of more than 73%.

The proposed swarm based SVM outperforms the swarm based multiple regression (SMR). The optimization methods of these two algorithms are the same, in which their parameters are optimized using the PSO. One difference of the two algorithms in finding the decision function is that SVM considers maximizing the margin between the two nearest points of the two classes in SVM, whereas SMR does not. The maximization of the margin could result in better generalization. The superiority of the SVM technique over multiple regression is also confirmed in other studies (Xue et al., 2004).

Another comparison, the performance of SSVM with input of the ECG

parameter corrected using the Bazett formula is better than that which is corrected by the Fridericia formula. Using the Fridericia formula, an ECG parameter is corrected using $RR^{1/3}$, while using the Bazzet formula an ECG parameter is corrected by $RR^{1/2}$. Two studies (Christensen et al., 2010, Koivikko et al., 2008) presented the impact of the two correction formulas to QT interval prolongation during hypoglycaemia. In the two studies, during hypoglycaemia, the QT interval corrected by the Bazett formula increased statistically significantly, but the QT interval corrected by the Fridericia formula was not associated with a statistical change.

The optimal SVM parameters have been found in the optimization stages, as is presented in Table 4.6. The optimal w_1 is higher than w_0. w_1 is the weight factor for the hypoglycaemic class. In the optimization, the weight factor is automatically tuned to prevent a low sensitivity. In other words, the automatic selection of the weight factor performs well. Regarding C values, although the C values are high (6.37×10^4) it might not be overtraining as the generalization of the algorithm is still good in that the testing performance does not dramatically drop, compared to the training and validation performance.

The fitness functions of the optimizations used for SSVM/SFSVM employ sensitivity and specificity, rather than using a root mean square error, or RSME (Deeb and Goodarzi, 2010). An RSME is a value to measure the difference between the prediction of a model (P_i) and the actual observation (O_i), or $RSME = (n^{-1} \sum_{i=1}^{n} |e_i|^2)^{1/2}$, where: $e_i = P_i - O_i$. Using RSME, the target is to minimize RSME, without a more attention in sensitivity. The two class data used in this research has a lower number in hypoglycemic class than in nonhypoglycemic class. This situation of data has the risk of low sensitivity in an SVM classification.

4.5   CONCLUSION

The detection of hypoglycaemia using a swarm-based SVM (SSVM) algorithm has been conducted. In SSVM, a particle swarm optimization (PSO) was used to optimize the SVM parameters. A fitness function was defined in the optimization to find a high performance of the hypoglycaemia detection, especially in the sensitivity. SSVM was investigated for hypoglycaemia detection using the clinical ECG parameters $TpTe_c$, $ToTe_c$, RTp_c, QTp_c, QTe_c and HR. The ECG parameters show significant contributions to hypoglycaemia detection. In hypoglycaemia detection, the proposed algorithm (SSVM) outperforms the swarm based multiple regression and the SVM without the swarm optimization. Furthermore, the performance of the detection using the swarm based SVM with the input of the ECG parameters corrected by the Bazett formula is better than that corrected by the Fridericia formula. Different kernel functions were investigated to find the suitable kernel function for the SSVM which yields a good performance in the hypoglycaemia detection. The SSVM which used RBF kernel function performs well with 80.45%, 79.64% and 80.04% in terms of sensitivity, specificity and geometric mean. This performance is achieved when the inputs are HR and $ToTe_c$, which is the interval from the beginning to the end of T–wave.

CHAPTER 5.
HYBRID FUZZY INFERENCE SYSTEM SUPPORT VECTOR MACHINE FOR HYPOGLYCAEMIA DETECTION

5.1 BACKGROUND

The SVMs algorithm was studied for hypoglycaemia detection in Chapter III. The performance was improved in Chapter IV by twofold: the optimization of SVM parameters and employing the most suitable ECG parameters for the input. The most suitable input was found by examining all the possible combinations of the ECG parameters for the input of the hypoglycaemia detection. In other words, in this stage the SVM has already employed the optimal parameters and the optimal input.

A more advanced algorithm is employed in this chapter to find a further improvement. Essentially, the algorithm refers to a hybrid of the multiple regression (MR) and fuzzy inference system (FIS) developed by Ling and Nguyen (2011). For
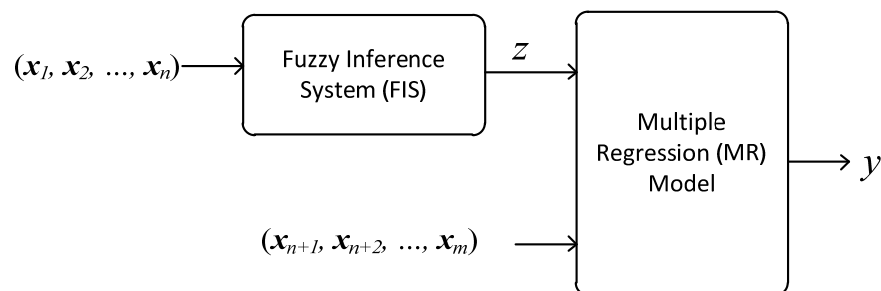
Figure 5.1: FMR developed in (Ling and Nguyen, 2011)

the simplicity the hybrid is called fuzzy multiple regression or FMR. In FMR some inputs ($x_1, x_2, \ldots, x_n$) are for FIS and the others ($x_{n+1}, x_{n+2, \ldots}, x_m$) are for MR (Figure 5.1). The study shows that FMR performs better compared to the performance obtained by its components (FIS and MR)

Instead of using FIS and MR, this research proposes a novel algorithm which employs a hybrid of FIS and SVM for hypoglycaemia detection. Thus, SVM is employed in the algorithm, instead of MR. SVM differs from MR in finding the decision function: SVM considers maximizing the margin between the two closest points of the two classes data, whereas SMR does not. The maximization of margin could provide a good generalization in classification. The superiority of SVM over MR was confirmed in several applications (Xue et al., 2004, Yao et al., 2004, Pourbasheer et al., 2010). The superiority is also indicated in the results of Chapter IV.

5.2   SWARM BASED FUZZY SUPPORT VECTOR MACHINE (SFSVM)

A swarm based fuzzy support vector machine or the SFSVM is constructed as in Figure 5.2. SFSVM is composed mainly of FIS and SVM. Some inputs ($x_1, x_2, \ldots, x_n$) are used for the input of FIS and the others ($x_{n+1}, x_{n+2}, \ldots, x_m$) are for the input of SVM. The FIS is intended to find an index from the FIS inputs. This index is then used for the input of the SVM, together with the other inputs. FIS is an effective intelligent system which employs fuzzy logic and fuzzy set theory (Ly et al., 2009). Its frameworks are the concepts of fuzzy set theory and fuzzy reasoning. The advantages of FIS include its ability to handle linguistic concepts and to function as a universal approximator, performing nonlinear relations between inputs and outputs.

The proposed algorithm employs parameters which need to be optimized. Instead of using PSO as used for SSVM in Chapter 4, the proposed algorithm employs particle swarm optimization with wavelet mutation or PSOWM as

developed by Ling et al. (2008). Thus, the algorithm proposed in this chapter is a hybrid of FIS and SVM with the optimization using PSOWM. For simplicity, the algorithm is called SFSVM. PSOWM is a modification of PSO by including a wavelet mutation to mutate a particle of swarm to reduce the risk of trapping in local minima. An experimental study shows that PSOWM performs better than the competitors in terms of convergence speed, solution quality, and solution stability (Ling et al., 2008). PSOWM might be more appropriate (rather than a standard PSO) for the optimization of SFSVM parameters as the SFSVM includes far more parameters to be optimized than SSVM includes. For example, the number of parameters existing in SFSVM with four inputs and three membership functions of FIS is 109.

Essentially, wavelet approach is a tool to model seismic signals by combining translations and dilations and of a simple, oscillatory function (mother wavelet) of a finite duration (Ling et al., 2007). The PSO's mutating space is varying dynamically along the search based on the properties of the wavelet function. The resulting mutation operation aids the hybrid PSO to perform more efficiently and provides a faster convergence than the other real-value mutation.

5.3 HYPOGLYCAEMIA DETECTION USING SFSVM

Hypoglycaemia detection using SFSVM follows the construction in Figure 5.2. Some ECG parameters (x_1, x_2, …, x_n) are used for the FIS inputs and the others (x_{n+1}, x_{n+2}, …, x_m) are for the SVM inputs. The main components of SFSVM, which are FIS and SVM, are described in the following.

5.3.1 Fuzzy Inference System
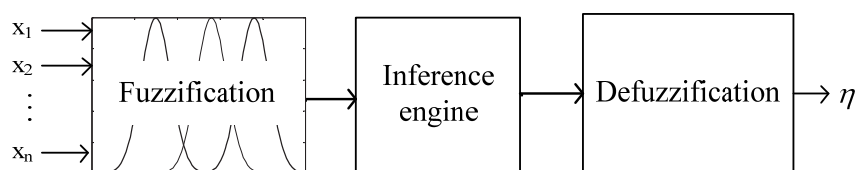
Figure 5.3 Fuzzy Inference System

As in Figure 5.2, FIS is used to find the approximating function between the ECG parameters in the FIS inputs and hypo index η. In general, three steps are conducted to find the approximating function; fuzzification, inference engine and
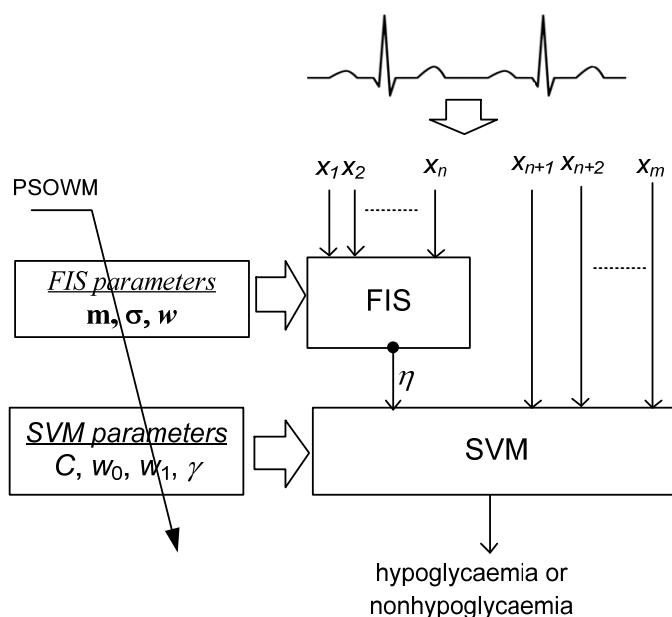
Figure 5.2: SFSVM for hypoglycaemia detection with input of ECG parameters

defuzzification (Gang, 2006), as described in Figure 5.3.

Fuzzification

The first step is fuzzification (or fuzzifier). Generally fuzzification is the mapping from a real-world space to a fuzzy space (Feng, 2006). The fuzzification is used to find the degree of the membership function (as a fuzzy set) of the ECG parameters, as illustrated in Figure 5.4. Thus, the input of the fuzzification is the ECG parameters and the output is the degree of membership function. Each point of the input has associated degree of membership, which is determined using the
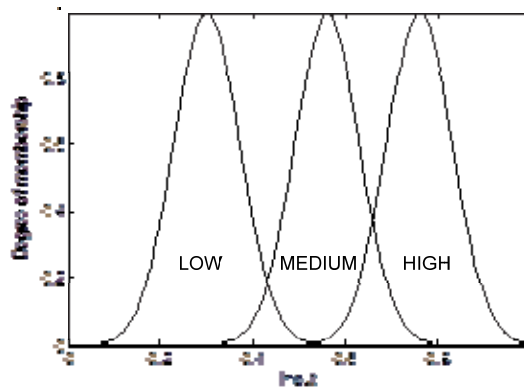
Figure 5.4: Fuzzy input and the associated membership degree

Gaussian membership function.

Using the Gaussian, the membership degree $\mu_{N_x^k}$ can be expressed as (Feng et al., 2009)

$$\mu_{N_j^k}(x_j) = e^{-\left(x - m_j^k\right)^2 / 2\sigma_j^k} \qquad 5.1$$

Where the x_j (j =1,2, …, n) are the ECG parameters (nonfuzzy input); n is the number of the FIS inputs or ECG parameters. m_j^k and σ_j^k are the mean value and

the standard deviation of the Gaussian membership function, respectively, for the associate input x_j. k denotes the number of membership function. For example, the mean and the standard deviation for the heart rate with three membership functions can be defined as $m_{HR}^k = [m_{HR}^1 \quad m_{HR}^2 \quad m_{HR}^3]$ and $\sigma_{HR}^k = [\sigma_{HR}^1 \quad \sigma_{HR}^2 \quad \sigma_{HR}^3]$.

Inference engine

The second step is the inference engine. The inference converts the fuzzy input to the fuzzy output using an IF-THEN type fuzzy rule. Generally the rule consists of two parts: antecedence (the IF part) and consequence (the THEN part). The rules are given in the following (Xiaoguang and Lilly, 2004):

Rule ρ: **IF** x_1 is N_1^k **AND** x_2 is N_2^k **AND ... AND** x_n is N_n^k **THEN** η is h_ρ
<div align="right">5.2</div>

where N_j^k ($j = 1, 2, \ldots, n$) is a fuzzy set of the associated input x_j. Rule $\rho = 1, 2, \ldots, r$ denotes the rule number; r denotes the number of rules. The number of rules is $(m_f)^n$; m_f is the number of membership functions and n is the number of inputs. For example, for a case of four FIS inputs with three membership functions the number of rules is $3^4 = 81$. h is the fuzz singleton to be optimized.

Defuzzification

The third step of FIS is defuzzification. Defuzzification is used to translate the outputs of the fuzzy rules into a real world value (Feng, 2006). The output of the defuzzification η is given by

$$\eta = \sum_{\rho=1}^{r} s_\rho h_\rho$$
<div align="right">5.3</div>

where

$$s_\rho = \frac{\mu_{N_1^\rho}(x_1) \times \mu_{N_2^\rho}(x_2) \times \ldots \times \mu_{N_n^\rho}(x_n)}{\sum_{\rho=1}^{r}\left(\mu_{N_1^\rho}(x_j) \times \mu_{N_2^\rho}(x_j) \times \ldots \times \mu_{N_n^\rho}(x_n)\right)} \qquad 5.4$$

FIS parameters

The values of mean m_j^k, standard deviation σ_j^k and the fuzzy sets of the consequent part h_ρ are determined through an optimization. Thus, the FIS parameters to be optimized are m_j^k and σ_j^k in Eq. 5.1 and w_ρ in Eq. 5.2. For example, in a case of FIS with two inputs (such as HR and *RTp*c) with three membership functions (m_f), the total parameters for the fuzzification are 12 (comprising 3 m_{HR}^k, 3 m_{RTpc}^k, 3 σ_{HR}^k and 3 σ_{RTpc}^k) and the number of the IF-THEN rules is 9. Thus, the total number of the parameters is 21.

5.3.2   Hybrid particle swarm optimization with wavelet mutation

Hybrid particle swarm optimization with wavelet mutation (PSOWM) is intended to optimize SFSVM parameters. SFSVM with the optimal parameters leads to the optimal hypoglycaemia detection. The SFSVM parameters consist of FIS parameters and SVM parameters. PSOWM performs optimization considering an evolutionary technique based on the movement of swarms and inspired by the social behavior of bird flocking and fish schooling with wavelet mutation.

```
begin
      n →1                 // iteration number
      Initialize Z(n)    // Z(n): swarm for iteration t
      Evaluate f(Z(n)) // f(·): fitness function
      while (not termination condition) do
      begin
            n → n +1
```

Update velocity $v_j^k(n)$ and position particle $z_j^k(n)$ using Eq. 5.5 and Eq. 5.6, respectively

      if v(n)>vmax , v(n)= vmax end

if v(n)<−vmax, v(n)= − vmax end

Perform wavelet mutation operation by updating

    $\bar{z}_j^p(n)$ using Eq. 5.9–5.11.

Reproduce a new Z(n)

Evaluate f(Z(n))

```
      end
end
```

Figure 5.5: Pseudo code of PSOWM

A typical algorithm of PSOWM can be expressed as in the Figure 5.5. Suppose a swarm at the *n*-th iteration is Z(n). Z(n) contains ω particles with τ dimensions. More clearly, for a case SFSVM with the FIS of two inputs and three membership functions, each data point associates 25 parameters; it consist of 21 FIS parameters and 4 SVM parameters. Therefore, the dimension of Z(n) is 25. The number of particles ω used in the optimization is 50. Each element of the swarm is presented by $z_j^k \in Z(n)$, in which $j = 1, 2,…, \tau$ and $k = 1, 2,…, \omega$. Thus, for the case mentioned above, the particles can be expressed in the matrix form in Figure 5.6.

The optimization is started by the generation of a random swarm Z(n), as an initialization. The initial swarm is then evaluated for the fitness function f(Z(n)). In

the next iteration, the swarm is updated and is then evaluated again using the fitness function. This procedure is repeated until the termination condition is found.

Essentially, the updating swarm at iteration n is conducted by the addition of velocity v_j^k to the previous position, as in the following formula

$$z_j^k(n) = x_j^k(n-1) + v_j^k(n) \qquad\qquad 5.5$$

in which velocity v_j^k is defined as

$$v_j^k(n) = q\left\{\varphi v_j^k(n-1) + c_1 r_1\left(\tilde{z}_j - x_j^k(n-1)\right) + c_2 r_2(\hat{z}_j - x_j^k(n-1))\right\} \quad 5.6$$

where $\tilde{z}$ is the personal best position of a particle, and $\hat{z}$ is the best position among all particles (global best). The personal best position is the position which provides the minimum value of the objective function (defined later). r_1 and r_2 are random functions in the range [0 1], and φ is inertia weight factor. c_1 and c_2 are acceleration constants. q is a constriction factor to ensure the system does not converge prematurely, which is defined as

z_1^1	z_1^2	z_1^3	...	z_1^k	...	z_1^ω
z_2^1	z_2^2	z_2^3	...	z_2^k	...	z_2^ω
...	...	...	...	...	...	...
z_j^1	z_j^2	z_j^3	...	z_j^k	...	z_j^ω
...	...	...	...	...	...	...
z_τ^1	z_τ^2	z_τ^3	...	z_τ^k	...	z_τ^ω

Figure 5.6: The swarm of PSOWM for the SFSVM.

$$q = \frac{2}{|2 - c - \sqrt{c^2 - 4c}|} \qquad\qquad 5.7$$

with $c = c_1 + c_2$ and $c > 4$.

The particle velocity v is limited by a maximum velocity v_{max}. The maximum velocity determines the resolution of the regions to be searched, between the present position and the target position. The value for the maximum velocity is typically 0.1 to 0.2. Furthermore, the inertia weight is set as follow:

$$\varphi = \varphi_{max} - \frac{\varphi_{max} - \varphi_{min}}{N} \times n \qquad\qquad 5.8$$

where φ_{max} and φ_{min} are upper and lower inertia weights, respectively, and are set to 1.2 and 0.1, respectively, N is the total iteration number and n is the iteration number.

By the mutation operation, every element of a particle has a chance to mutate with a probability $m \in [0\ 1]$. A random number between 0 and 1 is generated for each element of particle such that if it is less than or equal to m, a mutation is given to the element. After a mutation, an element of swarm $x_j^k(t)$ becomes $\bar{x}_j^k(t)$, with the operational formula

$$\bar{z}_j^k(n) = \begin{cases} z_j^k(n) + \delta \times \left(p_{max}^j - z_j^k(n) \right) & \text{if } \delta > 0 \\ z_j^k(n) + \delta \times \left(z_j^k(n) - p_{min}^j \right) & \text{if } \delta \leq 0 \end{cases} \qquad 5.9$$

where p_{max} and p_{min} are the upper and lower boundary of the element of a particle, respectively; δ is controlled by the Morlet wavelet function:

$$\delta = \frac{1}{\sqrt{a}} e^{-\left(\frac{c}{a}\right)^2/2} \cos\left(5 \left(\frac{c}{a}\right) \right). \qquad\qquad 5.10$$

This function is scaled by a which is used to enhance the searching performance. c is generated in the range of $-2.5a$ to $2.5a$. The parameter a is set to vary with the value of n/N as in the following:

$$a = e^{-\ln(g)x(1-\frac{n}{N})^{\beta\,wm}} + \ln(g) \qquad\qquad 5.11$$

where β_{wm} is the shape parameter of the monotonic increasing function, g is the upper limit of the parameter a. After the wavelet mutation, a new swarm is generated. The iterative process of the optimization is terminated if the defined iteration number is met.

The objective function (or fitness function) of the PSOWM is similar to the objective function defined in the optimization in Chapter III, as in the following

$$f = -(\kappa\vartheta_{tr} + (1-\kappa)\mathcal{S}_{tr} + \kappa\vartheta_v + (1-\kappa)\mathcal{S}_v + \Bbbk)) \qquad\qquad 5.12$$

where ϑ_{tr} and $\mathcal{S}_{tr}$ are the sensitivity and specificity, respectively, obtained from the hypoglycaemia detection model which is tested by using a training data set; and ϑ_v and $\mathcal{S}_v$ are the sensitivity and specificity, respectively, obtained from the hypoglycaemia detection model which is tested by using a validation data set. The inclusion of ϑ_v and $\mathcal{S}_v$ in the fitness function is to reduce the risk of overtraining (Astion et al., 1993). κ is set as 0.58 to avoid the risk of low sensitivity.

To force a high sensitivity in the detection, a parameter σ is given by using the following definition,

$$\Bbbk = \begin{cases} 10 \; if \; \vartheta_{tr} > 0.7, \mathcal{S}_{tr} > 0.4, \vartheta_v > 0.7, \mathcal{S}_v > 0.4 \\ 0 \; otherwise \end{cases} \qquad 5.13$$

The definition of $\Bbbk$ in Eq. 5.13 is to force the sensitivity and specificity to be higher than 70% and 40%, respectively.

5.4   EXPERIMENTAL RESULT

In general the experiment was started by the preparation of the data, as presented in Chapter 4. The data involves training, validation and testing data sets. Afterwards, the optimization of PSOWM (as presented in Figure 5.5) was

conducted. In the "Evaluate $f(Z(n))$" in Figure 5.5, an SVM model is created with the base of the training data set and the parameters defined by $Z(n)$, and the model is tested using the validation data set. Thus, the performances of the training and validation were obtained. Using the performances, the fitness function values can be calculated using Eq. 5.12. In the end of the optimization, the optimal model was found. The optimal model was then tested by the testing data set and the testing performance was obtained.

For comparison and analysis purposes, the following approaches were conducted:

- SFSVM employing FIS with two inputs and SVM with the other four inputs

- SFSVM employing FIS with three inputs and SVM with the other three inputs

- SFSVM employing FIS with four inputs and SVM with the other two inputs

- SFSVM employing FIS with five inputs and SVM with the other one input

- FIS with six inputs (without SVM)

- FIS with three inputs and multiple regression with the other three inputs (FMR).

In each of the arrangements, all possible combinations of the FIS inputs and the associated SVM inputs were examined. For example, the input combination of the "FIS with two inputs and SVM with the other four inputs" is HR and QTc for the FIS and $TpTe_c$, $ToTe_c$, RTp_c and QTp_c for the SVM. Furthermore, on the best of the approaches, the SVM inputs were varied, with the same FIS inputs.

The following additional approaches were conducted:

- SFSVM with the fuzzification which employs five membership

functions,

- SFSVM with the fuzzification which employs three triangular membership functions,

- SFSVM with the fuzzification which employs five triangular membership functions.

The hypoglycaemia detections using the above approaches were conducted. The first result is the performance of the SFSVM which employs all six ECG parameters with different FIS input and different SVM input. The performance in terms of geometric mean is presented in Figure 5.7. It involves the performances of the SFSVM which employs the FIS with two inputs (Figure 5.7a), three inputs (Figure 5.7b), four inputs (Figure 5.7c) and five inputs (Figure 5.7d). The associated FIS inputs are presented on each of those figures, in the right side; the rest of the ECG parameters are used for the SVM inputs. The inputs are written in the forms of $x_1, x_2, \ldots, x_6$ (x_1:HR, x_2:QTe_c, x_3:$TpTe_c$, x_4:$ToTe_c$, x_5:RTp_c, and x_6:QTp_c.). The inputs which provide the best performance of the SFSVM are indicated in Table 5.1. The best performance of the SFSVM which employs two FIS inputs is 78.34%, which is found when the FIS inputs are QTe_c and RTp_c and the SVM inputs are the rest. This performance is lower compared to the best performance obtained by the method which employs three, four and five ECG parameters for the FIS inputs. Using the three input FIS, the SFSVM find the best performance with 83.22% in terms of the geometric mean, when the FIS inputs are HR, $TpTe_c$ and $ToTe_c$. This performance is nearly the same with the best performance of which employs four and five ECG parameters in the FIS inputs. Using the four input FIS, the best performance is obtained when the FIS inputs are HR, $TpTe_c$, $ToTe_c$ and QTp_c. In the five one, the best is obtained when the FIS inputs are HR, QTe_c, $TpTe_c$, RTp_c and QTp_c. Furthermore, the approach with all six ECG parameters for the FIS inputs performs the least

(a) Two inputs in the FIS

Geometric mean (%)

78.34%

FIS input

FIS input

1 : x_1x_2 9 : x_2x_6
2 : x_1x_3 10 : x_3x_4
3 : x_1x_4 11 : x_3x_5
4 : x_1x_5 12 : x_3x_6
5 : x_1x_6 13 : x_4x_5
6 : x_2x_3 14 : x_4x_6
7 : x_2x_4 15 x_5x_6
8 : x_2x_5

(b) Three inputs in the FIS

Geometric mean (%)

83.22%

FIS input

1 : $x_1x_2x_3$ 11 : $x_2x_3x_4$
2 : $x_1x_2x_4$ 12 : $x_2x_3x_5$
3 : $x_1x_2x_5$ 13 : $x_2x_3x_6$
4 : $x_1x_2x_6$ 14 : $x_2x_4x_5$
5 : $x_1x_3x_4$ 15 : $x_2x_4x_6$
6 : $x_1x_3x_5$ 16 : $x_2x_5x_6$
7 : $x_1x_3x_6$ 17 : $x_3x_4x_5$
8 : $x_1x_4x_5$ 18 : $x_3x_4x_6$
9 : $x_1x_4x_6$ 19 : $x_3x_5x_6$
10 : $x_1x_5x_6$ 20 : $x_4x_5x_6$

1 : $x_1x_2x_3x_4$
2 : $x_1x_2x_3x_5$
3 : $x_1x_2x_3x_6$
4 : $x_1x_2x_4x_5$
5 : $x_1x_2x_3x_4$
6 : $x_1x_2x_5x_6$
7 : $x_1x_3x_4x_5$
8 : $x_1x_3x_4x_6$
9 : $x_1x_3x_5x_6$
10 : $x_1x_4x_5x_6$
11 : $x_2x_3x_4x_5$
12 : $x_2x_3x_4x_6$
13 : $x_2x_3x_5x_6$
14 : $x_2x_4x_5x_6$
15 : $x_3x_4x_5x_6$

(c) Four inputs in the FIS

Geometric mean (%)

83.10%

FIS input

(d) Five inputs in the FIS

Geometric mean (%)

83.02%

1 : $x_1x_2x_3x_4x_5$
2 : $x_1x_2x_3x_4x_6$
3 : $x_1x_2x_3x_5x_6$
4 : $x_1x_2x_4x_5x_6$
5 : $x_1x_3x_4x_5x_6$

FIS input

Figure 5.7: The geometric means of SFSVM with the different ECG parameters for the FIS input. The rest of ECG parameters for the SVM inputs. (x_1:HR, x_2:QTe$_c$, x_3:TpTe$_c$, x_4:ToTe$_c$, x_5:RTp$_c$, and x_6:QTp$_c$.)

Table 5.1: The input combinations which provide the best performance of SFSVM for each FIS input number. x_1:HR, x_2:QTe_c, x_3:$TpTe_c$, x_4:$ToTe_c$, x_5:RTp_c and x_6:QTp_c (the values in %)

FIS Input	Training			Validation			Testing		
	Sens.	Spec.	Gm	Sens.	Spec.	Gm	Sens.	Spec.	Gm
x_2x_5	96.99	80.77	88.51	83.46	74.43	78.82	81.95	74.89	78.34
$x_1x_3x_4$	96.99	81.45	88.88	91.73	77.15	84.12	87.22	79.41	83.22
$x_1x_3x_4x_6$	95.49	82.81	88.92	90.23	79.41	84.65	88.72	77.83	83.10
$x_1x_2x_3x_5x_6$	94.74	84.62	89.53	87.22	79.64	83.34	83.46	82.58	83.02
$x_1x_2x_3x_4x_5x_6$	88.72	68.10	77.73	81.20	66.52	73.49	78.20	63.12	70.26

.   A further result is obtained by the variation of the SVM input in which the FIS inputs are kept same, which are HR, $TpTe_c$ and $ToTe_c$. The result is presented in Table 5.2. The variation of the SVM inputs does not provide a better performance. Thus the best performance of SFSVM is found with 87.22%, 79.41% and 83.22% in terms of sensitivity, specificity and geometric mean. This
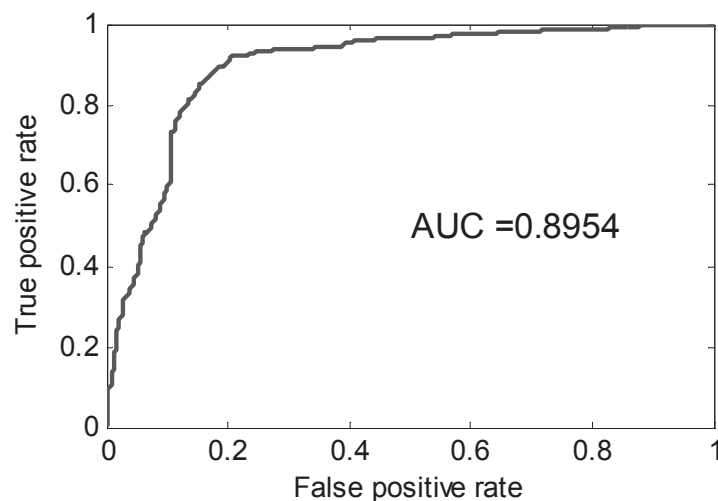
Figure 5.8: The ROC curve of SFSVM with the FIS inputs are HR, $TpTe_c$ and $ToTe_c$ and the SVM inputs are QTe_c, RTp_c and QTp_c.

Table 5.2: The performance of SFSVM in the variation of the SVM inputs; x_2:QTe_c, x_5:RTp_c and x_6:QTp_c (the values in %)

SVM inputs	Training			Validation			Testing		
	Sens.	Spec.	Gm	Sens.	Spec.	Gm	Sens.	Spec.	Gm
$x_2x_5x_6$	96.99	81.45	88.88	91.73	77.15	84.12	87.22	79.41	83.22
x_2x_5	96.24	81.9	88.78	88.72	76.7	82.49	85.71	77.15	81.32
x_2x_6	96.99	83.03	89.74	89.47	76.24	82.59	84.21	79.86	82.01
x_2x_6	96.99	82.81	89.62	90.23	79.64	84.77	79.7	77.15	78.41
x_5	96.24	76.7	85.91	93.23	71.95	81.9	87.22	70.81	78.59
x_5x_6	96.99	82.58	89.5	90.98	76.24	83.29	87.97	77.15	82.38
x_6	95.49	77.6	86.08	90.23	74.66	82.07	83.46	74.43	78.82

performance is found when the FIS inputs are *HR*, *TpTe*$_c$ and *ToTe*$_c$ and the SVM inputs are the rest, which are *QTe*$_c$, *RTp*$_c$, and *QTp*$_c$. Using these inputs, the ROC curve of the SFSVM can be presented as in Figure 5.8.

Combination of FIS and multiple regression (MR), which forms FMR, with three inputs for the FIS and three input for the MR is tested. The performances of FMR with variation in the FIS inputs are presented in Figure 5.9. The FMR with the FIS inputs of *TpTe*$_c$, *RTp*$_c$ and *QTp*$_c$ shows better performance in term of geometric
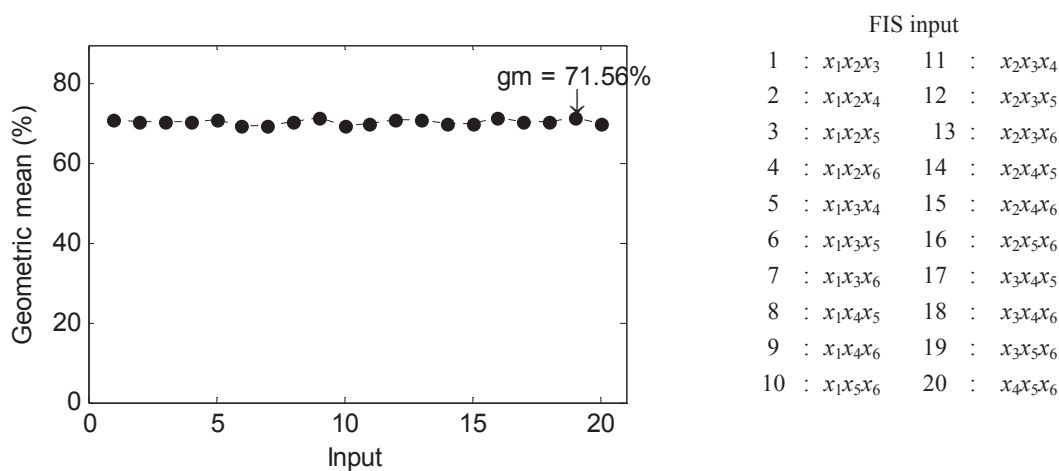
Figure 5.9: The geometric means of FMR with the different ECG parameters for the FIS input. The rest of ECG parameters are for the SVM inputs. (x_1:HR, x_2:QTe_c, x_3:$TpTe_c$, x_4:$ToTe_c$, x_5:RTp_c, and x_6:QTp_c)

Table 5.3: The performance of FMR in the variation of the SVM inputs; x_1:HR, x_2:QTe_c and x_4:$ToTe_c$ (the values in %)

SVM inputs	Training			Validation			Testing		
	Sens.	Spec.	Gm	Sens.	Spec.	Gm	Sens.	Spec.	Gm
$x_1x_2x_4$	88.72	68.33	77.86	78.95	66.06	72.22	79.70	64.25	71.56
x_1x_2	87.22	68.33	77.20	78.95	66.97	72.71	78.20	64.71	71.13
x_1x_4	88.72	66.29	76.69	84.21	61.99	72.25	81.95	61.31	70.89
x_2x_4	90.23	48.64	66.25	84.21	46.83	62.80	84.21	50.23	65.04
x_1	88.72	67.87	77.60	79.70	66.06	72.56	78.20	63.57	70.51
x_2	84.96	52.71	66.92	80.45	53.62	65.68	80.45	53.17	65.40
x_4	89.47	43.21	62.18	84.21	41.18	58.89	84.96	45.48	62.16

mean compared to which that with the other FIS inputs. Furthermore, with the $TpTe_c$, RTp_c and QTp_c for the FIS inputs, the MR inputs are varied, and the result is presented in Table 5.3. The results show the best performance is the FMR when the SVM inputs are HR, QTe_c and $ToTe_c$, This best performance is worse than the performance found by SFSVM, and thus SFSVM performs better than FMR.
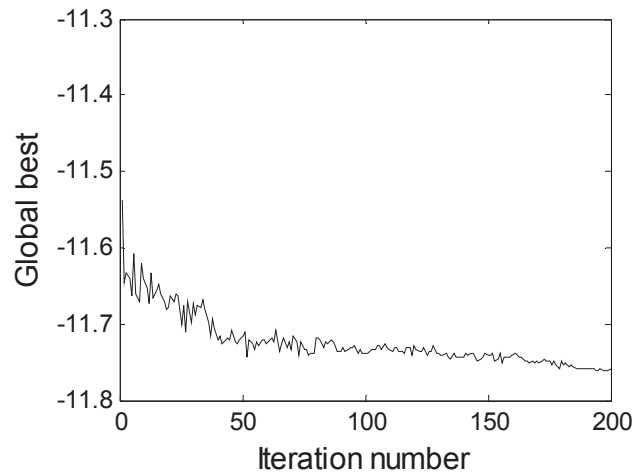
Figure 5.10: The fitness function value of the global best obtained in the optimization of the SFSVM with 200 iterations
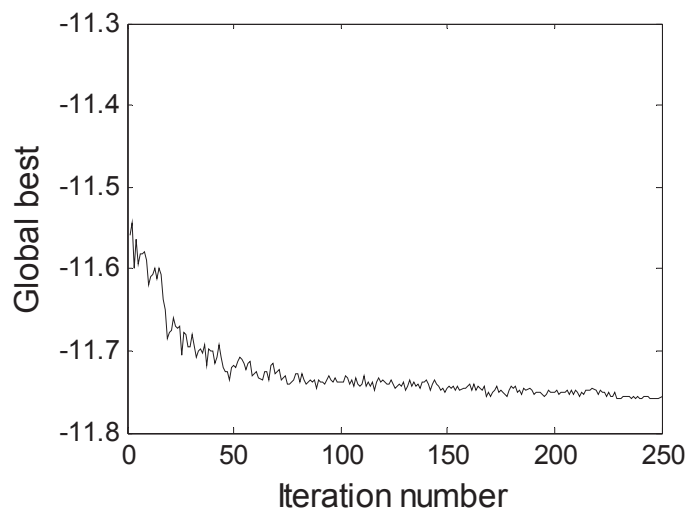
Figure 5.11: The fitness function value of the global best obtained in the optimization of the SFSVM with 250 iterations
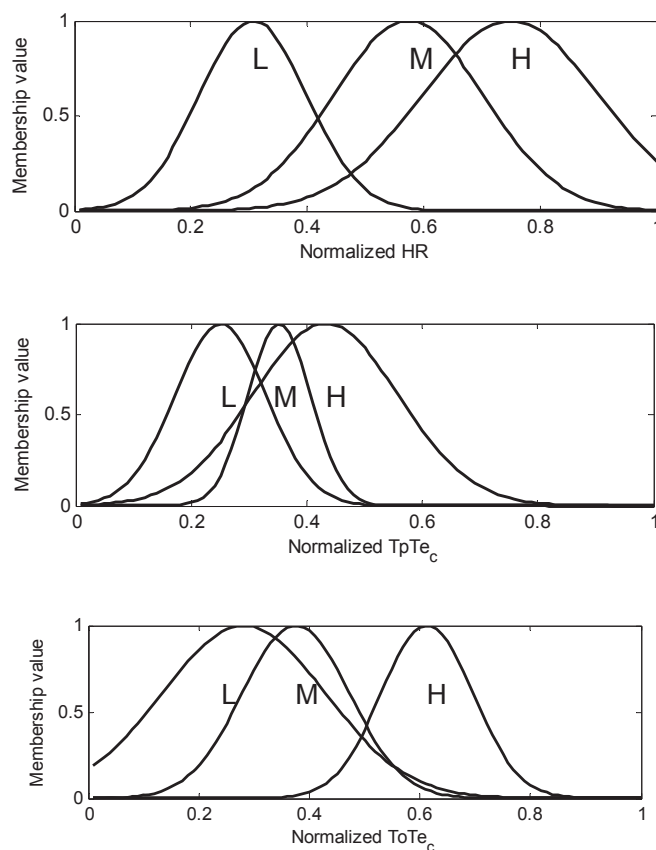
Figure 5.12: The fuzzy membership functions of heart rate, *TpTe*c and *ToTe*c

The fitness function value of the global best during the optimization of the SFSVM is described in Figure 5.10 and Figure 5.11, with the iteration numbers of 200 and 250, respectively. The figures show that the convergence rates (Gao and Xu, 2011) of the optimizations using these two different iterations are nearly same. It means that these two optimizations need nearly the same iteration number to find the same final result, which is the optimal fitness function. The optimal fitness function values obtained from the two optimizations are nearly same, which are -11.7597 and -11.7586, for the 200 and 250 iteration numbers, respectively. It shows that the optimization with 200 iterations is enough to find the optimal fitness function.

Table 5.4: The Fuzzy rule tables

$ToTe_c$: L

$TpTe_c$ / HR	L	M	H
L	0.6771	0.4678	0.9495
M	0.6077	0.3567	0.3708
H	0.1213	0.2970	0.1034

$ToTe_c$: M

$TpTe_c$ / HR	L	M	H
L	0.3096	0.4835	0.8976
M	0.6323	0.6014	0.8711
H	0.9244	0.7437	0.5857

$ToTe_c$: H

$TpTe_c$ / HR	L	M	H
L	0.7290	0.1007	0.3653
M	0.7011	0.1568	0.8690
H	0.5284	0.6631	0.3623

Furthermore, from the optimization, the optimal Gaussian membership

functions of *HR*, *TpTe*$_c$ and *ToTe*$_c$ are found as in Figure 5.12. Three membership functions are presented for each of the three inputs. The membership function consists of Low (L), Medium (M) and High (H). The optimized fuzzy terms of the IF-THEN rule are presented in Table 5.4. Considering the fuzzy terms, one of the fuzzy IF–THEN rules can be presented as follows

IF HR is "H" AND TpTe$_c$ is "H" AND TpTe$_c$ is "H" THEN *h* is 0.3623.

The optimal SVM parameters of the SFSVM obtained from the optimization are presented in Table 5.5. The weights w_0 and w_1 are 0.14 and 0.83, respectively. It means that the weight factor provided to the hypoglycaemia class w_1 is higher than that which is provided to the nonhypoglycaemia class w_0. These weight factors are determined automatically in the optimization. The number of support vectors is 221. Thus, the support vector number is 38.43%, which is 221 divided by the number of training data (575).

The SFSVMs which employ different fuzzification are tested and the result is presented in Table 5.6. The SFSVM which uses five membership functions (m_f) provides a slightly worse performance than that which employs the three. In the testing the performances are worse in terms of sensitivity, specificity and geometric mean. Using the five m_f, the geometric mean is 81.19%; the three one provides 83.22%. The other different fuzzification is in terms of the function, which is

Table 5.5: The optimal SVM parameters of the SFSVM with the input of HR, TpTe$_c$ and *ToTe*$_c$.

C	γ	w_0	w_1
5.04×10^4	31.95	0.14	0.83

n_s = Support vector number

triangular m_f. Using five triangular m_f, SFSVM performs 81.78% in terms of

geometric mean. This performance is similar to the performance of that which uses the five Gaussian m_f. Another different fuzzification tested is five triangular m_f. The performance of this approach is the lowest, which is 74.08% in terms of geometric mean.

Table 5.6: The performance of SFSVM with different fuzzification

m_f type	m_f number	Training			Validation			Testing		
		Sens (%)	Spec (%)	Gm (%)	Sens (%)	Spec (%)	Gm (%)	Sens (%)	Spec (%)	Gm (%)
Gaussian	3	96.99	81.45	88.88	91.73	77.15	84.12	87.22	79.41	83.22
	5	96.99	83.48	89.99	88.72	76.47	82.37	84.21	78.28	81.19
Triangular	3	96.99	84.16	90.35	89.47	79.86	84.53	84.21	79.41	81.78
	5	88.72	71.95	79.89	84.96	68.33	76.19	81.95	66.97	74.08

m_f: membership function

The performance comparison of SFSVM to the previous algorithms, which are SVM (Chapter 3) and SSVM (Chapter IV) is presented in Table 5.7. SFSVM perform better than the other two algorithms. In terms of geometric mean, SFSVM provides 83.22%, where SVM and SSVM provide 73.63% and 79.81%, respectively. The sensitivity of SFSVM is also higher than the others. In terms of specificity SFSVM performs slightly worse compared to SSVM, but better than SVM.

Table 5.7: Performance comparison of the SVM–based algorithms

Algorithm	Input	*Sens* (%)	*Spec* (%)	*Gm* (%)
SVM (Chapter III)	HR, QTe_c, $TpTe_c$, $ToTe_c$, RTp_c QTp_c	70.68	76.70	73.63
SSVM (Chapter IV)	HR, $ToTe_c$	80.45	79.64.	80.04
SFSVM (Chapter V)	HR, QTe, $TpTe_c$, $ToTe_c$, RTp_c QTp_c	87.22	79.41	83.22

5.5 DISCUSSION

SFSVM algorithm has been developed and investigated for hypoglycaemia detection. The algorithm consists of two main components: FIS and SVM. The input is the ECG parameter. The output is hypoglycaemia or nonhypoglycaemia. The swarm optimization with wavelet mutation is used to optimize the FIS and SVM parameters.

In the FIS, the Gaussian and triangular fuzzy membership functions have been tested. Furthermore, three and five membership functions were examined for the two functions. The result shows that with three membership functions the Gaussian distribution is the most suitable for this application, in which it provides the best performance.

In the experiment the fuzzy membership functions for FIS have been obtained. There are three membership functions which are for Low (L), Medium (M) and High (H). The mean and the standard deviation of the Gaussian membership functions are determined automatically during the optimization. Thus, the obtained membership function is the optimum, considering the data of ECG parameters and the desired fitness function.

A swarm optimization is used to optimize the FIS and SVM parameters.

PSOWM is chosen to optimize the parameters. PSOWM is the swarm optimization with wavelet mutation. The mutation is needed to avoid a trap in a local minima. PSOWN is chosen, instead of the PSO used in SSVM in Chapter III. The reason is that the number of parameters to be optimized for SFSVM is far more than which is used by SSVM; SSVM only has four parameters to be optimized, whereas SFSVM with three Gaussian *mf* and three inputs has 49 parameters. Even, SFSVM with five Gaussian *mf* and three inputs has 159 parameters. PSOWM showed a better performance than the competitor in some applications in terms of convergence speed, solution quality and solution stability (Ling et al., 2008).

The inputs of SFSVM are varied to find the appropriate input in order that the SFSVM performs well. The best performance is obtained when the SFSVM employs all six ECG parameters, three of them (*HR*, *TpTe*$_c$ and *ToTe*$_c$) for the FIS inputs and the other three (*QTe*$_c$, *RTp*$_c$ and *QTp*$_c$) are for the SVM inputs. The exclusion of some ECG parameters in the input results in a lower geometric mean. This means that all six ECG parameters might provide contribution for the hypoglycaemia detection using SFSVM.

The iteration number of the optimization is 200. In each iteration 50 parameters are used. Thus, in each iteration, 50 FIS-SVM models are created and tested. The iteration number of 200 could be enough for the optimization, as the optimization which uses 250 iterations provides nearly the same results of the optimal fitness values (-11.7597 vs. -11.7586). Obviously, the 200 iterations one is far more efficient in terms of time in the experiment than the 250 iterations one. Furthermore, the ripples in the graphs in Figure 5.10 and Figure 5.11 might be caused by the wavelet mutation approach. The ripples could be essential to avoid a trap in local minima. Two graphs in Figure 5.10 and Figure 5.11 only include the fitness values of the global best particles. Therefore, the span of the fitness values seems narrow, which is from around -11.55 to -11.76. If all the fitness values are

included in the graphs, the span could be wider; that is, the span could be from around –2.0, instead of –11.55.

The computational effort for the optimization using the PSOWM depends on the iteration given number and the time consumed in every iteration. Every iteration creates n Fuzzy-SVM training to make n Fuzzy-SVM models; n is the number particles of PSO. In this thesis, the iteration number is 200 and the particle number is 50. Hence, after 200 iterations the optimization terminates. Another termination criterion is the gradients of the global best during m iteration; if the gradients are less than a defined value, the optimization terminates. It means that if the optimal values do not change significantly during m iteration, the optimization terminates.

The inclusion of FIS in SFSVMcontributes to an improved performance. This can be seen by comparing SFSVM with SSVM, in which the SSVM does not include FIS. SFSVM provides a significantly higher sensitivity than SSVM has (87.22% vs. 79.70%). Whereas, the specificity of SFSVM is slightly lower than SSVM (79.41% vs. 81.22%). In more compact terms, which is geometric mean, SFSVM performs better than SSVM (83.22% vs. 80.46%). Including FIS in SFSVM provides a new input, which is used by SVM. This new input is provided by the FIS. Furthermore, if only FIS is used, the performance is worse in which the geometric mean is 70.26%.

5.6 CONCLUSION

A hybrid FIS and SVM with the swarm optimization (SFSVM) has been developed and tested for hypoglycaemia detection. SFSVM is a more advanced algorithm compared to the SVM and SSVM, developed in the previous chapters. In SFSVM, some ECG parameters are applied to the FIS part and the others are applied to the SVM part. The FIS with its inputs provide an index which is used for the additional input of the SVM part of the SFSVM. To find the appropriate inputs,

variations of the inputs are investigated. The variations are conducted both for the FIS and the SVM parts. The SFSVM with different fuzzification approaches are also presented. Compared to the previous algorithm, which are SVM and SSVM, SFSVM performs better. SFSVM which applies HR, $TpTe_c$ and $ToTe_c$ for the FIS part and QTe_c, RTp_c and QTp_c for the SVM part performs the best with acceptable sensitivity, specificity and geometric mean of 87.22%, 79.41% and 83.22%, respectively. The optimization of the FIS and SVM parameters using PSOWM with the defined fitness function can perform well.

CHAPTER 6.
DISCUSSION AND CONCLUSION

6.1 DISCUSSION

Hypoglycaemia is a serious problem for the management of type 1 diabetes (Pedersen-Bjergaard, 2009). This research concerns a hypoglycaemia detection strategy which is an essential system to recognize a hypoglycemic episode. Three main algorithms are developed, namely SVM, SSVM and SFSVM. These three algorithms are introduced for hypoglycaemia detection. ECG parameters (such as heart rate) are employed as inputs for the algorithms. The algorithms are tested using the ECG parameters obtained from clinical electrocardiograms of patients with type 1 diabetes.

The performances of the three algorithms have been presented. The SSVM performs better than SVM (80.04% vs. 73.63%, in terms of geometric mean). SSVM employs the SVM parameters which are optimized using a particle swarm optimization (PSO), whereas SVM does not. The better performance of SSVM could be as a result of the swarm optimization effectively optimizing the SVM parameters, and hence the SVM parameters employed in the SSVM are the optimal ones, whereas the SVM might employ the suboptimal ones. The concerned SVM parameters are C (or the cost parameter), w_0 and w_1 (the weight factors) and γ (the RBF kernel function width). In an SVM, C is in the penalty term of $C \sum_{i=1}^{l} \xi_i$ (Eq. 3.25). ξ is a slack variable which is the error committed by allowing the supporting

hyperplane to be unconstrained by a data point. Considering the term, the C value is the trade-off between the margin size and error. The larger C value could yield to the tendency of the SVM to have a small margin. The smaller C value could result in the tendency of the SVM to have a large margin, which might ignore the noisy points near the decision surface. Thus, the large C relates to the small margin, and the small C relates to the large margin. The small margin might relate to a good performance in the training, but it might be poor in the testing (the classification of the unseen data). Conversely, the larger margin might relate to the worst performance in the training, but it might be better in the testing. Moreover, in the SVM, w_0 and w_1 are used in the penalty terms of $w_0 C \sum_{i(yi=-1)=1}^{l} \xi_i + w_1 C \sum_{i(yi=+1)=1}^{l} \xi_i$ (Eq. 3.28). Therefore, w_0 and w_1 are possible to provide the different penalties to the different class data.

The SFSVM performs better than the SSVM; 87.22% vs. 80.45% in terms of sensitivity and 79.41% vs. 79.64% in terms of specificity. SFSVM differs from SSVM in which the SFSVM includes a fuzzy inference system (FIS), whereas the SSVM does not. Thus, the better performance could be as a result of the inclusion of the FIS. This FIS inclusion provides a new input η for the SVM part of the SFSVM. This input η is the output of the FIS, which has the input of ECG parameters. In other words, the FIS converts the ECG parameters into a new value η using an approximation function $\eta = g(x)$, obtained from the training of the FIS. Kosko (1994) presented a fuzzy system as a universal approximator and Zeng and Singh (1996) studied different classes of fuzzy systems for approximation functions.

When the SVM part of the SFSVM is not included, the performance decreases. It means that the hypoglycaemia which employs only the FIS performs worse than the SFSVM. The performances of the FIS vs. the SFSVM are 78.23% vs. 87.22%, in terms of sensitivity, and 63.12% vs. 79.41%, in terms of specificity.

Thus, the combination of the FIS and the SVM which forms the SFSVM provides the advantage of the better performance, compared to the FIS only or the SVM only.

It would be interesting to present the performances of hypoglycaemia detections with different algorithms used in the other studies. A linear discriminant analysis (LDA) provides the average performances of the hypoglycaemia detection of 67.79% and 50.40% in terms of sensitivity and specificity, respectively (Alexakis et al., 2003). In the experiment, the inputs of the LDA are RTp, the amplitude of T-wave, T-wave skewness and T-wave kurtosis. A study of the artificial neural network (ANN) for hypoglycaemia detection results in the average performance of 75.43% and 64.10% in terms of sensitivity and specificity, respectively (Alexakis et al., 2003). A multiple regression fuzzy inference system (FMR) is employed for hypoglycaemia detection, which uses the input of HR and QTe_c (Ling and Nguyen, 2011). The best testing performance of the FMR is 75.86% and 50.98% in terms of sensitivity and specificity, respectively. The performances of those three algorithms (LDA, ANN and FMR) are worse than the SSVM and SFSVM. The performances of the three algorithms might not be able to be compared directly to the SSVM and SFSVM because the type of the hypoglycemic ECG parameters might be different. For example, the FMR used the naturally hypoglycemic ECG parameters, whereas the SSVM/SFSVM used the hyperinsulinemic one. The hyperinsulinemic hypoglycaemia might provoke more pronounced electrocardiographic alteration than the natural one does (Robinson et al., 2004), and hence the hyperinsulinemic one might be easier to be detected by the model.

Using the same data set the FMR still performs worse than the SFSVM; 79.70% vs. 87.22%, in terms of sensitivity, and 64.25%% vs. 79.41%, in terms of specificity. The FMR comprises FIS and multiple regression (MR), whereas the

SFSVM comprises FIS and SVM. Thus, the SFSVM differs from FMR by employing SVM, instead of MR. Using the six ECG parameters for the input, the hypoglycaemia detection which employs SVM performs better than that which employs MR; 75.48% vs. 71.37%, in terms of geometric mean. The better performances of SVM over MR are also presented in Xue et al. (2004), Yao et al. (2004), Pourbasheer et al. (2010).

The objective function of the optimization of the SSVM and SFSVM includes the SVM weight factors: w_0 and w_1. Using the six ECG parameters for the input, the SSVM performs 84.21% and 67.65% in terms of sensitivity and specificity, respectively (if the weight factors are included), whereas it performs 49.62% and 94.34% in the same terms if the weight factors are not included in the optimization (the weight factors are set to 1). The optimization of the weight factors in the SSVM/SFSVM is used to prevent a low sensitivity. This research has the risk of low sensitivity as the data number of the hypoglycaemia class is far less than the nonhypoglycaemia class. To tackle this type of risk, the appropriate weight factors should be used (Batuwita and Palade, 2010, Hwang et al., 2011). In other studies, Melgani and Bazi (2008), Lin et al. (2008) and (Wei et al., 2011) studied the optimizations of SVM parameters using a swarm technique. The optimization strategies used in those studies does not include the weight factors. Thus, the strategy might be not appropriate for the data set used in this research. Including the SVM weight factors in the swarm optimization is one of the novelties provided by this research.

The objective of the optimization of the SSVM/SFSVM includes the performance of training and validation. Thus, the objective function includes an unseen data subset, instead of only the seen data subset which is the training data. Usually, the strategy of the optimization of SVM parameters does not include the performance based on the validation data subset. Huang and Dun (2008) and Lin et

al. (2008) employed the accuracy of the training performance for the fitness function. Melgani and Bazi (2008) employed the number of support vectors for the objective function based on the training data. Wei et al. (2011) considered the correct and false classification rates based on the training data. The inclusion of the validation performance in the SSVM/SFSVM has the benefit of preventing an over-fitting. In the other study, Cheng et al. (2012) avoids the over-fitting in the SVM parameter optimization by limiting the number of SVM support vectors. Conceptually, too many support vectors could result in a poor generalization. Conversely, too few support vectors could result in a poor training performance. Thus, the support vector is a trade-off between the model accuracy in the training and the model generalization. The strategy used by the SSVM/SFSVM in the avoiding of over-fitting is by inclusion of the validation performance. It means that a part of the objective of the optimization is to maximize the validation performance. The high validation performance means the over-fitting could be reduced and also a good generalization could be achieved. Although the support vector number is not included in the fitness function of the SSVM/SFSVM, indirectly the SSVM/SFSVM could achieve the appropriate support vector number as a good generalization is a part of the objective of the optimization.

To find the appropriate inputs of the SSVM/SFSVM, variations of the inputs are tested, rather than using an optimization such as in Melgani and Bazi (2008). The benefit of this strategy is that the performances of the algorithms with the different inputs can be shown. Furthermore, the tests of the variation inputs are still possible to be conducted. In Melgani and Bazi (2008) the input is optimized and therefore the most appropriate input is determined by the optimization.

In summary, the three algorithms with the base of SVM have been developed for hypoglycaemia detection. The SFSVM shows a better performance than the other two: SVM and SSVM. The best performances found by the SFSVM

are 87.22%, 79.41% and 83.22% in terms of sensitivity, specificity and geometric mean, respectively, with inputs of HR, QTe_c and $TpTe_c$ for the FIS part and $ToTe_c$, RTp_c and QTp_c for the SVM part.

Topics for further research

Concerning the inputs, the six ECG parameters related to the ventricular repolarization (VR) have been investigated for hypoglycaemia detection. These VR parameters are in the form of the interval from a point to another point in an ECG signal. There are the other forms of ventricular repolarization parameters. One of the forms is VR variability, which is a physiological phenomenon where the duration of VR varies from beat-to-beat. A future work might need to investigate VR variability for hypoglycaemia detection.

Recent studies show an increase of VR variability related to a variety of diseases, such as ventricular tachycormardia or fibrillation (Haigney et al., 2004), dilated cardiomyopathy (Berger et al., 1997) and myocardial Ischemia (Murabayashi et al., 2002). The process relating to beat-to-beat fluctuation of repolarization is likely mediated by stochastic behavior of ion channels (Zaniboni et al., 2000).

An initial study of VR variability for hypoglycaemia detection was conducted in my research group (Nuryani et al., 2011). The study showed that the variabilities of QTe_c, $TpTe_c$, $ToTe_c$ and RTp_c in hypoglycaemia were significantly different from that in nonhypoglycaemia. An algorithm for hypoglycaemia detection with the input of VR variability was also developed. Ukena et al. (2011) also reported a higher VR variability in hypoglycaemia than that which is in normoglycaemia in a patient with type 2 diabetes. Thus, a further study of hypoglycaemia detection based on VR variability might contribute to the technology of hypoglycaemia detection.

In terms of the algorithm employed for hypoglycaemia detection, the

SFSVM has showed a good performance. In the SFSVM, FIS is combined with SVM in which the FIS output is used for the SVM input, together with the other ECG parameters. A further study about the combinations of FIS and SVM might result in more advanced performance.

In addition, in terms of optimization, the other optimization techniques, such as genetic algorithm (GA) (Goletsis et al., 2004), might be able to be investigated to find the optimal SVM parameters. A hybrid of PSO and fuzzy regression (PSO-FR) might be a potential algorithm to be applied for a hypoglycemia detection. PSO-FR could handle an application having a nonlinear nature, small amount of experimental data, existing outliers and polynomial form (Chan et al., 2011a). Finally, further work could also investigate the implementation of the model to a real time device.

In terms of patient numbers, this research involves five patients only. However, the phenomenon of hypoglycaemia contributing to the alteration of an electrocardiogram is also supported by the other studies, such as the Heger et al. (1996), the Koivikko et al. (2008) and the Christensen et al. (2010), as presented in more detail in Chapter 2. Heger et al. (1996) studied with 24 type 1 diabetes mellitus (T1DM) and 7 healthy subjects. Koivikko et al. (2008) had with 16 T1DM and 8 healthy subjects. Christensen et al. (2010) involved 21 T1DM patients.

In addition, the result of this work might require further validation using different techniques of ECG measurement. This validation might assist in finding an appropriate method of the ECG feature extraction which could result in a better performance.

6.2 CONCLUSION

This thesis has presented the contributions to hypoglycaemia detection technology. The models of hypoglycaemia detection have been developed and

examined. The models are based on the phenomenon that hypoglycaemia alters the ventricular repolarization of the heart. Considering the phenomenon, several ECG parameters related to the ventricular repolarization have been investigated. Several ECG parameters were introduced for hypoglycaemia detection: the interval from Q-point to the peak of T-wave (QTp_c), T-wave interval or the interval from the beginning of T-wave to the end of T-wave ($ToTe_c$), and the interval from the peak of T-wave to the end of T-wave ($TpTe_c$). These parameters show contributions to the detection of hypoglycaemia. In addition, the hybrid algorithms with the base of SVM were introduced and tested for hypoglycaemia detection. The main algorithms are support vector machine (SVM), the hybrid of SVM and a swarm optimization technique (SSVM) and the hybrid of fuzzy inference system (FIS), SVM and PSO (SFSVM). In the SSVM, all the possible combinations of the ECG parameters are tested for the input. The SSVM performs better than SVM. In the SFSVM, FIS and SVM are combined and the FIS and SVM parameters are optimized using a swarm technique. In terms of computational time, the three algorithms differ in the off-line optimization stage. The computational time can be controlled so that the time could still be acceptable. In the experiment, the SFSVM performs better than the other two algorithms (SVM and SSVM), with the sensitivity, specificity and geometric mean of 87.22%, 79.41% and 83.22%, respectively.

Appendix A. Margin between two hyperplanes
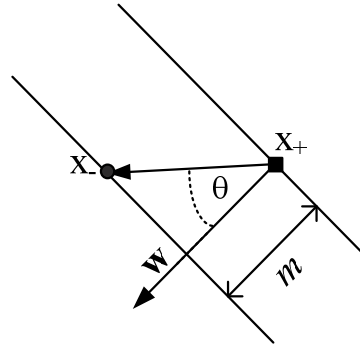
Figure A.1: Margin *m* between two supporting hyperplanes

Suppose the margin is *m*, it can be computed as

$$m = \frac{w \cdot (x_- - x_+)}{|w|} \tag{A.1}$$

which is the projection of $(x_- - x_+)$ in the direction of w. The equation above can be rewritten as

$$m = \frac{w \cdot x_- - w \cdot x_+}{|w|} \tag{A.2}$$

Considering Eqs. 3.2 and 3.2, Eq. A.2 can be written as follows:

$$m = \frac{(b+1) - (b-1)}{|w|} \tag{A.3}$$

$$= \frac{2}{|w|} \tag{A.4}$$

Appendix B. Lagrangian dual optimization

Considering Eq. 3.13, the construction of the Lagrangian for the optimization problem is

$$L(\alpha, w, b) = \frac{1}{2} \boldsymbol{w} \cdot \boldsymbol{w} - \sum_{i=1}^{l} \alpha_i \left(y_i (\boldsymbol{w} \cdot \boldsymbol{x}_i - b) - 1 \right) \tag{B.1}$$

$$(\alpha, w, b) = \frac{1}{2} \boldsymbol{w} \cdot \boldsymbol{w} - \sum_{i=1}^{l} \alpha_i \, y_i \boldsymbol{w} \cdot \boldsymbol{x}_i + b \sum_{i=1}^{l} \alpha_i \, y_i + \sum_{i=1}^{l} \alpha_i \tag{B.2}$$

This gives the Lagrangian optimization problem as

$$\max_{\alpha} \min_{w,b} \; L(\alpha, w, b) \tag{B.3}$$

Subjects to

$$\alpha_i \geq 0 \tag{B.4}$$

Since the objective function is convex and the constraint is linear, the solution for $\boldsymbol{\alpha}, \mathbf{w}$ and b has to satisfy the following KKT conditions:

Gradient condition
$$\frac{\partial L}{\partial \boldsymbol{w}} (\boldsymbol{\alpha}, \boldsymbol{w}, b) = 0 \tag{B.5}$$

$$\frac{\partial L}{\partial b} (\boldsymbol{\alpha}, \boldsymbol{w}, b) = 0 \tag{B.6}$$

Orthogonally condition
$$\alpha_i (y_i (\boldsymbol{w} \cdot \boldsymbol{x}_i - b) - 1) = 0 \tag{B.7}$$

Feasibility condition
$$y_i (\boldsymbol{w} \cdot \boldsymbol{x}_i - b) - 1 \geq 0 \tag{B.8}$$

Non-negative condition
$$\alpha_i \geq 0 \tag{B.9}$$

The Lagrangian optimization can be solved through the partial derivative as

in the following,

$$\frac{\partial L}{\partial \boldsymbol{w}}(\boldsymbol{\alpha}, \boldsymbol{w}, b) = \boldsymbol{w} - \sum_{i=1}^{l} \alpha_i y_i x_i = \boldsymbol{0} \qquad \text{B.10}$$

$$\boldsymbol{w} = \sum_{i=1}^{l} \alpha_i y_i \mathbf{x}_i \qquad \text{B.11}$$

$$\frac{\partial L}{\partial b}(\boldsymbol{\alpha}, \boldsymbol{w}, b) = \sum_{i=1}^{l} \alpha_i y_i = 0 \qquad \text{B.12}$$

The Lagrangian dual optimization problem, as

$$L(\alpha, w, b) = \sum_{i=1}^{l} \alpha_i - \frac{1}{2}\sum_{i=1}^{l}\sum_{j=1}^{l} \alpha_i \alpha_j y_i y_j x_i \cdot x_j \qquad \text{B.13}$$

.

Bias b can be determined as follow:

$$b = \boldsymbol{w}. \boldsymbol{x}_{sv} - 1 = \sum_{i=1}^{l} \alpha_i y_i x_i . \boldsymbol{x}_{sv} - \mathbf{1} \qquad \text{B.14}$$

Finally, the optimal decision surface can be defined as

$$\hat{f}(\mathbf{x}) = sgn(\boldsymbol{w}. \boldsymbol{x} - b) \qquad \text{B.15}$$

$$\hat{f}(\mathbf{x}) = sgn\left(\sum_{i=1}^{l} \alpha_i y_i x_i \cdot \boldsymbol{x} - \sum_{i=1}^{l} \alpha_i y_i x_i \cdot \boldsymbol{x}_{sv} - \mathbf{1}\right) \qquad \text{B.16}$$

Appendix C. Soft-margin nonlinear support vector machine

$$m^* = min\frac{1}{2}\boldsymbol{w}.\boldsymbol{w} + C\sum_{i=1}^{l}\xi_i \qquad \text{C.1}$$

The Lagrangian construction of the optimization problem is modified as

$$L(\alpha,\beta,\xi,w,b) = \frac{1}{2}\boldsymbol{w}\cdot\boldsymbol{w} + C\sum_{i=1}^{l}\xi_i - \sum_{i=1}^{l}\alpha_i\left(y_i(\boldsymbol{w}\cdot\boldsymbol{x}_i - b) + \xi_i - 1\right) \\ - \sum_{i=1}^{l}\beta_i\xi_i \qquad \text{C.2}$$

This gives the Lagrangian optimization problem as

$$\genfrac{}{}{0pt}{}{max}{\alpha}\genfrac{}{}{0pt}{}{min}{w,b}\ L(\boldsymbol{\alpha},\boldsymbol{\beta},\boldsymbol{\xi},\boldsymbol{w},b) \qquad \text{C.3}$$

Subject to the constraints,

$$\alpha_i \geq 0 \qquad \text{C.4}$$

$$\beta_i \geq 0 \qquad \text{C.5}$$

Since the objective function is convex and the constraint is linear, the solution for α, β, w, ξ, *b* has to satisfy the following KKT conditions:

$$\frac{\partial L}{\partial \boldsymbol{w}}L(\boldsymbol{\alpha},\boldsymbol{\beta},\boldsymbol{\xi},\boldsymbol{w},b) = 0 \qquad \text{C.6}$$

$$\frac{\partial L}{\partial \boldsymbol{\xi}}L(\boldsymbol{\alpha},\boldsymbol{\beta},\boldsymbol{\xi},\boldsymbol{w},b) = 0 \qquad \text{C.7}$$

$$\frac{\partial L}{\partial b}L(\boldsymbol{\alpha},\boldsymbol{\beta},\boldsymbol{\xi},\boldsymbol{w},b) = 0 \qquad \text{C.8}$$

$$\alpha_i(y_i(\boldsymbol{w}\cdot\boldsymbol{x}_i - b) + \xi - 1) = 0 \qquad \text{C.9}$$

$$\beta_i \xi_i = 0 \qquad \text{C.10}$$

$$y_i(\mathbf{w} \cdot \mathbf{x}_i - b) + \xi - 1 \geq 0 \qquad \text{C.11}$$

$$\alpha_i \geq 0 \qquad \text{C.12}$$

$$\beta_i \geq 0 \qquad \text{C.13}$$

$$\xi_i \geq 0 \qquad \text{C.14}$$

The partial derivatives are

$$\frac{\partial L}{\partial \mathbf{w}} L(\boldsymbol{\alpha}, \boldsymbol{\beta}, \boldsymbol{\xi}, \mathbf{w}, b) = \mathbf{w} - \sum_{i=1}^{l} \alpha_i y_i \mathbf{x}_i = \mathbf{0} \qquad \text{C.15}$$

$$\mathbf{w} = \sum_{i=1}^{l} \alpha_i y_i \mathbf{x}_i \qquad \text{C.16}$$

$$\frac{\partial L}{\partial b} L(\boldsymbol{\alpha}, \boldsymbol{\beta}, \boldsymbol{\xi}, \mathbf{w}, b) = \sum_{i=1}^{l} \alpha_i y_i = 0 \qquad \text{C.17}$$

$$\frac{\partial L}{\partial \boldsymbol{\beta}} L(\boldsymbol{\alpha}, \boldsymbol{\beta}, \boldsymbol{\xi}, \mathbf{w}, b) = C - \alpha_i - \beta_i \qquad \text{C.18}$$

$$C = \alpha_i - \beta_i \qquad \text{C.19}$$

Substituting partial derivatives above to the Lagrangian of the optimization problem gives the Lagrangian dual as

$$L(\alpha, w, b) = \sum_{i=1}^{l} \alpha_i - \frac{1}{2} \sum_{i=1}^{l} \sum_{j=1}^{l} \alpha_i \alpha_j y_i y_j \mathbf{x}_i \cdot \mathbf{x}_j \qquad \text{C.20}$$

This Lagrangian dual for soft-margin SVM is same with the Lagrangian dual for hard-margin SVM. Therefore the objective functions of the optimization problems for both SVMs are same. The difference is in the constraint. In the soft-margin SVM, the constraint can be stated as

$$0 \leq \alpha \leq C \qquad \text{C.21}$$

Appendix D. Sequential minimal optimization (SMO) for SVM

The sequential minimal optimization (SMO) is used to find the Lagrangian multiplier α in Eq. 3.30, which is the solution of the following equation

$$max \ (L(\alpha)) \tag{D.1}$$

where

$$L(\alpha) = \sum_{i=1}^{l} \alpha_i - \frac{1}{2} \sum_{i=1}^{l} \sum_{j=1}^{l} \alpha_i \alpha_j y_i y_j k(x_i \cdot x_j) \tag{D.2}$$

subjects to

$$0 \leq \alpha \leq C \tag{D.3}$$

and

$$\sum_{i=1}^{l} y_i \alpha_i = 0 \tag{D.4}$$

This maximization problem is equivalent to a minimization problem by multiplying it by -1, so that it becomes the following minimization problem

$$\max_{\alpha} \ L(\alpha) \equiv \min_{\alpha} \ (-L(\alpha)) \tag{D.5}$$

$$= \min_{\alpha} \ (\ell \ (\alpha)) \tag{D.6}$$

where

$$\ell \ (\alpha) = -L(\alpha) \tag{D.7}$$

Or

$$\ell(\alpha) = \left(\frac{1}{2} \sum_{i=1}^{l} \sum_{j=1}^{l} \alpha_i \alpha_j y_i y_j k(x_i \cdot x_j) - \sum_{i=1}^{l} \alpha_i \right) \tag{D.8}$$

Thus, to find α, minimization of $\ell \ (\alpha)$ in Eq. D.8 is used.

Eq. D.8 can be written in another form:

$$\ell(\alpha) = \tfrac{1}{2}\alpha^{\mathrm{T}} Q\alpha - q^T\alpha \qquad \text{D.9}$$

where:

- $q = [1,\dots,1]^T$ is the vector of all ones.
- $\alpha = [\alpha_1, \alpha_2, \dots, \alpha_l]^T$

- Q is an l x l symmetric matrix (l is the number of training data), with components:
-   - $Q_{ij} = y_i y_j k(x_i \cdot x_j) \qquad \text{D.10}$

Furthermore, the constraint defined in Eq. 3.31, $\sum_{i=1}^{l} \alpha_i y_i = 0$, can be written in the other form:

$$\sum_{i=1}^{l} \alpha_i y_i = \mathbf{Y}\alpha \qquad \text{D.11}$$

where Y is the vector 1 x l with components y_i.

The difficulty in the minimization of $\ell(\alpha)$ is that Q is a dense matrix which yields a problem of memory and is time consuming (Plat, 1999). SMO solves this problem by decomposition such that at each step two Lagrangian multipliers α are optimized and update the SVM at the end of each optimization.

The algorithm can be described as follow: Chen et al. (2006):

a) Defining α^1 for the initial solution (iteration $n = 1$).

b) If α^n is a stationary point of the minimization of $\ell(\alpha)$, stop. Otherwise, a two–element working set $W = \{i,j\}$ is determined.

c) Defining $V \equiv \{1,\dots,l\}\backslash W$ (the set V contains all those elements of $\{1,\dots,l\}$ which are not in W)

d) Let α_W^n and α_V^n be the sub-vectors of α^n corresponding to W and V, respectively.

e) Considering to Eq. D.9, solve for the following sub-problem with the variable α_w:

$$\min_{\alpha_B} \ell_{\alpha_B}$$

where

$$\ell_{\alpha_B} = \frac{1}{2}[\alpha_w^T \ (\alpha_V^n)^T] \begin{bmatrix} Q_{WW} & Q_{WV} \\ Q_{VW} & Q_{VV} \end{bmatrix} \begin{bmatrix} \alpha_W \\ \alpha_V^n \end{bmatrix} - [q_W^T \ q_N^T] \begin{bmatrix} \alpha_W \\ \alpha_V^n \end{bmatrix} \tag{D.12}$$

$$= \frac{1}{2}[\alpha_W^T Q_{WW} \alpha_W + \alpha_W^T Q_{WV} \alpha_V^n + (\alpha_V^n)^T Q_{VW} \alpha_V \\ + (\alpha_V^n)^T Q_{VV} \alpha_V^n] - [q_W^T \alpha_W + q_N^T \alpha_V^n] \tag{D.13}$$

$$= \frac{1}{2}[\alpha_W^T Q_{WW} \alpha_W + \alpha_W^T Q_{WV} \alpha_V^n + (\alpha_V^n)^T Q_{VW} \alpha_V - q_W^T \alpha_W] \\ + (\alpha_V^n)^T Q_{VV} \alpha_V^n - q_N^T \alpha_V^n \tag{D.14}$$

$$= \frac{1}{2}\alpha_W^T Q_{WW} \alpha_W + (-q_w + Q_{WV} \alpha_V^n)^T \alpha_W + constant \tag{D.15}$$

$$= \frac{1}{2}[\alpha_i \ \alpha_j] \begin{bmatrix} Q_{ii} & Q_{ij} \\ Q_{ji} & Q_{jj} \end{bmatrix} \begin{bmatrix} \alpha_i \\ \alpha_j \end{bmatrix} + (-q_w + Q_{WV} \alpha_V^n)^T \begin{bmatrix} \alpha_i \\ \alpha_j \end{bmatrix} + \\ constant \tag{D.16}$$

f) Set α_B^{n+1} to be the optimal solution of the sub-problem Eq. D.16 and $\alpha_B^{n+1} \equiv \alpha_W^n$. Set $n \leftarrow n + 1$ and go to Step b.

The index w is updated at every iteration, but for simplicity, w is used instead of w^n.

The stopping criteria consider that the feasible solution of α is a stationary point of Eq. D.9 (or in another form, Eq. D.10) if and only if there is a number b and two non-negative λ and μ such that (Chen et al., 2006)

$$\nabla \ell(\alpha) + by = \lambda - \mu \tag{D.17}$$

with the constraints:

$$\lambda_i \alpha_i = 0, \rho(C - \alpha)_i = 0, \lambda_i \geq 0, \rho_i \geq 0 \quad i = 1, \dots, l \tag{D.18}$$

where $\nabla \ell(\alpha) \equiv Q\alpha - q$ is the gradient of $\ell(\alpha)$. Eqs. D.17 and D.18 result in the following equation:

$$\nabla \ell(\alpha)_i + by_i \begin{cases} \leq 0, & if \ \alpha_i < C \\ \leq 0, & if \ \alpha_i > C \end{cases} \tag{D.19}$$

Because of that $y_i \in \{+1,-1\}$, considering Eq. D.19, b can be expressed as follow:

$$m(\alpha) \leq b \leq M(\alpha) \tag{D.20}$$

where

$$m(\alpha) \equiv \max_{i \in I_a(\alpha)} - y_i \nabla \ell(\alpha) \ and \\ M(\alpha) \equiv \max_{i \in I_b(\alpha)} - y_i \nabla \ell(\alpha) \tag{D.21}$$

and

$$I_a(\alpha) \equiv \{i | \alpha_i < C, y_i = 1 \ \text{or} \ \alpha_i < C, y_i = -1\},$$

$$I_b(\alpha) \equiv \{i | \alpha_i < C, y_i = -1 \ \text{or} \ \alpha_i > C, y_i = 1\}$$

D.22

- Therefore, a feasible α is a stationary point of problem in Eq. D.10 if and only if

$$m(\alpha) \leq M(\alpha).$$

D.23

and the stopping criteria can be defined as follow

$$m(\alpha) - M(\alpha) \leq \varepsilon_s$$

D.24

where ε_s is tolerance; typically $\varepsilon_s = 10^{-5}$.

-

Appendix E. Script Implementation of the Algorithms

```
% ----Swarm based support vector machine ----
global trainD labelTrain valD labelVal testD labelTest
global inpValue

inpValue = 26; % ECG parameter used

load inputdata

var_set = 4;
ParUsed = [1 2 3 4 5 6];
nresult = 0;

tr = [1 2 3];

[trainD,labelTrain,valD,labelVal,testD,labelTest] =
ParSetupTVT3SameSet(tr,InpEr,InpHr,ParUsed,partE,partH); % data set

[outpCV1,outp2CV1,trCv1,teCV1] = pso_Ssvm2('fitnessfunction',var_set);

cValue = outpCV1(1); gValue = outpCV1(2);
w0Value = outpCV1(3); w1Value = outpCV1(4);

cmd = [' -g ', num2str(gValue),' -c ', num2str(cValue),...
   ' -w0 ',num2str(w0Value) ,' -w1 ',num2str(w1Value)];

parnum = find(de2bi(inpValue,6,'left-msb'));

trainDx = trainD(:,parnum);
valDx = valD(:,parnum);
testDx = testD(:,parnum);

model = svmtrainmx(labelTrain,trainDx,cmd);

[predict_label_train, accuracy_train, dec_values_train] =...
   svmpredictionion(labelTrain, trainDx, model);
y_des_train = labelTrain;
y_act_train = predict_label_train;
[sens_tr,spec_tr,acc_tr] = accsvm(y_des_train,y_act_train);
train_result = [sens_tr,spec_tr,acc_tr];
gmTrain = sqrt(sens_tr*spec_tr);

[predict_label_val, accuracy_val, dec_values_val] =...
   svmprediction(labelVal, valDx, model);
y_des_val = labelVal;
y_act_val = predict_label_val;
[sens_val,spec_val,acc_val] = accsvm(y_des_val,y_act_val);
val_result = [sens_val,spec_val,acc_val];
```

```matlab
gmVal = sqrt(sens_val*spec_val);

[predict_label_test, accuracy_test, dec_values_test] =...
   svmprediction(labelTest, testDx, model);
y_des_test = labelTest;
y_act_test = predict_label_test;
[sens_ts,spec_ts,acc_ts] = accsvm(y_des_test,y_act_test);
test_result = [sens_ts,spec_ts,acc_ts];
gmTest = sqrt(sens_ts*spec_ts);

perf = [sens_tr spec_tr acc_tr gmTrain...
   sens_val spec_val acc_val gmVal...
   sens_ts spec_ts acc_ts gmTest];


% ----- fitness function ------
function [out]=fitnessfunction(in)

c1 = in(:,1);
g1 = in(:,2);
w0 = in(:,3);
w1 = in(:,4);

for nx=1:length(c1)

   [sens,spec,acc,sens1,spec1,acc1] = Svm( c1(nx),g1(nx),w0(nx),w1(nx));

   deltaSen = abs(sens - sens1);
   deltaSpec = abs(spec - spec1);

   if ( sens > 0.7 && sens1 > 0.7 && spec > 0.4 && spec1 > 0.4...
      && deltaSen <=0.15 && deltaSpec <= 0.15 )
   cbeta = 10;
   else
      cbeta=0;
   end

   out(nx) = 0.58 * sens + 0.42*spec + 0.58 * sens1 + 0.42*spec1 + cbeta; % for
**inp63x

end

out = out';


function [sens,spec,acc,sens1,spec1,acc1] = Svm(cValue,gValue,w0Value,w1Value)

global trainD labelTrain valD labelVal
global inpValue

cmd = [' -g ', num2str(gValue),' -c ', num2str(cValue),...
   ' -w0 ',num2str(w0Value) ,' -w1 ',num2str(w1Value)];

parnum = find(de2bi(inpValue,6,'left-msb'));

trainDx = trainD(:,parnum);
```

```
valDx = valD(:,parnum);

model = svmtrainmx(labelTrain,trainDx,cmd);

cmd = [' -g ', num2str(gValue),' -c ', num2str(cValue),...
    ' -w0 ',num2str(w0Value) ,' -w1 ',num2str(w1Value)];

model = svmtrainmx(labelTrain,trainDx,cmd);

[predict_label] = svmpredictioniont(labelTrain, trainDx, model);
[predict_label1] = svmpredictioniont(labelVal, valDx, model);

y_des = labelTrain;
y_act = predict_label;
[sens,spec,acc] = Accuracy(y_des,y_act);
[sens spec acc];

y_des = labelVal;
y_act = predict_label1;
[sens1,spec1,acc1] = Accuracy(y_des,y_act);
[sens1,spec1,acc1];


% ---- particle swarm optimization -----
function [OUT,OUT2,varargout]=pso_Ssvm2(functname,D,varargin)
% OUT: the optimal parameter

VR=[1,1e5;0.1,100;1e-4,1;1e-4,1];  % max/min optimized parameters

mv      =  0.2; % max/min velocity
me      = 200; % iteration
ps      = 50;  % population
ac1     = 2; % acceleration constant1
ac2     = 2; % acceleration constant2
iw1     = 1.2; % inertia weight
iw2     = 0.1; % inertai weight

tr = ones(1,me)*NaN;

velmaxmin = -mv*ones(ps,D);
velmaskmax = mv*ones(ps,D);
posmaskmin  = repmat(VR(1:D,1)',ps,1);
posmaskmax  = repmat(VR(1:D,2)',ps,1);
posmaskmeth = 3;

pos(1:ps,1:D) = normmat(rand([ps,D]),VR',1);

vel(1:ps,1:D) = normmat(rand([ps,D]),...
    [forcecol(-mv),forcecol(mv)]',1);

pbest = pos;

out = feval(functname,pos);

pbestval=out;
```

```
[gbestval,idx1] = max(pbestval);

bestpos     = zeros(me,D+1)*NaN;
gbest       = pbest(idx1,:);

bestpos(1,1:D) = gbest;

rstflg = 0;

iwt(1) = iw1;
nGbest = 0;

for i=1:me

   out        = feval(functname,[pos;gbest]);
   outbestval = out(end,:);
   out        = out(1:end-1,:);

   tr(i+1)       = gbestval;
   te            = i;
   bestpos(i,1:D+1) = [gbest,gbestval];

   [tempi,dum]       = find(pbestval<=out);

   pbestval(tempi,1)  = out(tempi,1);
   pbest(tempi,:)     = pos(tempi,:);

   [iterbestval,idx1] = max(pbestval);
   if gbestval <= iterbestval
      gbestval = iterbestval;
      gbest    = pbest(idx1,:);

      nGbest = nGbest+1;
      parGbest(nGbest,:) = [gbest gbestval];

   end

   rannum1 = rand([ps,D]);
   rannum2 = rand([ps,D]);

   iwt(i) = iw2 - (iw2-iw1)*i/me;

   ac11 = rannum1.*ac1;
   ac22 = rannum2.*ac2;

   vel = iwt(i).*vel + ac11.*(pbest-pos) + ac22.*(repmat(gbest,ps,1)-pos);
   vel = ( (vel <= velmaxmin).*velmaxmin ) + ( (vel > velmaxmin).*vel );
   vel = ( (vel >= velmaskmax).*velmaskmax ) + ( (vel < velmaskmax).*vel );

   pos = pos + vel;

   minposmask_throwaway = pos <= posmaskmin;
   minposmask_keep      = pos >  posmaskmin;
   maxposmask_throwaway = pos >= posmaskmax;
   maxposmask_keep      = pos <  posmaskmax;
```

```
  pos = ( minposmask_throwaway.*posmaskmin ) + ( minposmask_keep.*pos );
  pos = ( maxposmask_throwaway.*posmaskmax ) + ( maxposmask_keep.*pos );

  vel = (vel.*minposmask_keep) + (-vel.*minposmask_throwaway);
  vel = (vel.*maxposmask_keep) + (-vel.*maxposmask_throwaway);

end

OUT=[gbest';gbestval]
varargout{1}=[1:te];
varargout{2}=[tr(find(~isnan(tr)))];
OUT2 = parGbest

return
 -

 -    % ----- swarm based fuzzy support vector machine ----
global trainD labelTrain valD labelVal testD labelTest
global SvmInp FisInp

load inputdata
ParUsed = [1 2 3 4 5 6];

tr = [1 2 3];
[trainD,labelTrain,valD,labelVal,testD,labelTest] = ...
   ParSetupTVT3SameSet(tr,InpEr,InpHr,ParUsed,partE,partH);  % dataset

% --- PSO setting ----

no_para_delta = 9;
vl_delta = 0.05;
vu_delta = 0.20;

no_para_mean = 9;
vl_mean = 0.25;
vu_mean = 0.75;

vlb_delta = ones(1,no_para_delta)*(vl_delta);
vub_delta = ones(1,no_para_delta)*(vu_delta);

vlb_mean = ones(1,no_para_mean)*(vl_mean);
vub_mean = ones(1,no_para_mean)*(vu_mean);

no_para_w = 27;
vl_w = 0.1 ;
vu_w = 0.95;
vlb_w = ones(1,no_para_w)*(vl_w) ;
vub_w = ones(1,no_para_w)*(vu_w) ;

vlb_svm=[1     0.1    1e-4   1e-4]; % C, g(RBF),w0,w1
vub_svm=[1e5   100    1      1  ];

vlb = [vlb_delta vlb_mean vlb_w vlb_svm];
vub = [vub_delta vub_mean vub_w vub_svm];
```

```
[a,dim]=size(vlb)  ;
bounds = [vlb' vub'];
initvar= bounds;

no_iters=200;
pop_size=50;
pc=0.8;
pm=0.7;
mu_b=2;

c1 = 2.05;
c2 = 2.05;
k1=2;          % wavelet mutation shape parameter
vmax=0.2;      % max value of velocity of PSO
dt=0.00001;     % parameter for pso_noel ONLY
psopts=[c1,c2,vmax,k1,pm,dt];
startPop=initialize(pop_size,bounds); %

fun = 'fitnessfunctionwm';

FisInp = [1 3 4];
SvmInp = [6];

 [resultx1,endPop,bPop,traceInfo] =
psowm2(bounds,fun,[],startPop,psopts,'maxGenTerm',no_iters);

cmd = [' -g ', num2str(resultx1(47)),' -c ', num2str(resultx1(46)),...
    ' -w0 ',num2str(resultx1(48)) ,' -w1 ',num2str(resultx1(49))];

wTrain = FIS3inpForPsoMut(resultx1,trainD(:,FisInp)); % fuzzy output
trainDx =[wTrain trainD(:,SvmInp)];

wVal = FIS3inpForPsoMut(resultx1,valD(:,FisInp)); % fuzzy output
valDx =[wVal valD(:,SvmInp)];

wTest = FIS3inpForPsoMut(resultx1,testD(:,FisInp)); % fuzzy output
testDx =[wTest testD(:,SvmInp)];

model = svmtrainmx(labelTrain,trainDx,cmd);

[predict_label_train, accuracy_train, dec_values_train] =...
    svmprediction(labelTrain, trainDx, model);
y_des_train = labelTrain;
y_act_train = predict_label_train;
[sens_tr,spec_tr,acc_tr] = accsvm(y_des_train,y_act_train);
train_result = [sens_tr,spec_tr,acc_tr];
gmTrain = sqrt(sens_tr*spec_tr);

[predict_label_val, accuracy_val, dec_values_val] =...
    svmprediction(labelVal, valDx, model);
y_des_val = labelVal;
y_act_val = predict_label_val;
[sens_val,spec_val,acc_val] = accsvm(y_des_val,y_act_val);
val_result = [sens_val,spec_val,acc_val];
gmVal = sqrt(sens_val*spec_val);
```

```
[predict_label_test, accuracy_test, dec_values_test] =...
   svmprediction(labelTest, testDx, model);
y_des_test = labelTest;
y_act_test = predict_label_test;
[sens_ts,spec_ts,acc_ts] = accsvm(y_des_test,y_act_test);
test_result = [sens_ts,spec_ts,acc_ts];
gmTest = sqrt(sens_ts*spec_ts);

perf_class = [sens_tr spec_tr acc_tr gmTrain...
   sens_val spec_val acc_val gmVal...
   sens_ts spec_ts acc_ts gmTest];
 -

 -    % --- PSO with wavelet mutation ----
function [x,ePop,bPop,trackOpt] =
psowm2(bounds,evalFN,evalOps,sPop,opts,termFN,termOps)

c1=opts(1);c2=opts(2);vmax=opts(3);k1=opts(4);probm=opts(5);
c=c1+c2;
kk=2/abs(2-c-sqrt(c^2-4*c));

vbounds=vmax*[(bounds(:,1)-bounds(:,2)),(bounds(:,2)-bounds(:,1))];
evalstr=['[ePop(ip,numVar+1) ePop(ip,numVar+2)]=' evalFN '(ePop(ip,:),[evalOps]);'];

xZomeLength  = size(sPop,2);
numVar       = xZomeLength-3 ;
popSize      = size(sPop,1);
ePop      = sPop ;

for ip=1:popSize
   eval(evalstr);
end

pBest = ePop;
oval  = 0;

bFoundIn    = 1;
done        = 0;
itNum       = 1;
collectTrace = (nargout>3);

minbounds=ones(popSize,1)*bounds(:,1)';
maxbounds=ones(popSize,1)*bounds(:,2)';
minvbounds=ones(popSize,1)*vbounds(:,1)';
maxvbounds=ones(popSize,1)*vbounds(:,2)';

ve=vmax*(-1+2*rand(popSize,numVar)).*(maxbounds-minbounds);

while(1)

  [bval,bindx] = min(ePop(:,numVar+1));
     gBest = ePop(bindx,:);
  mgBest=ones(popSize,1)*gBest;

  for ipop=1:popSize
```

```
        if ( (ePop(ipop,numVar+1) < pBest(ipop,numVar+1)) | (itNum==1) )
            pBest(ipop,:)=ePop(ipop,:);
        end
    end

    if ( (bval <= oval) | (itNum==1))
        bPop(bFoundIn,:)=[itNum ePop(bindx,:)];
        bFoundIn=bFoundIn+1;
        oval=bval;
    end

    if collectTrace
        trackOpt(itNum,1)=itNum;
        trackOpt(itNum,2:xZomeLength+1)=ePop(bindx,:);
        trackOpt(itNum,xZomeLength+2)=mean(ePop(:,numVar+1));
        trackOpt(itNum,xZomeLength+3)=std(ePop(:,numVar+1));
    end

    done=feval(termFN,[itNum termOps],bPop,ePop);
    if done==1
        break;
    end
    itNum=itNum+1;


    ww=1.2-1.1*itNum/termOps;

    ve=kk*(ww*ve+c1*rand(popSize,numVar).*(pBest(:,1:numVar)-
ePop(:,1:numVar))+c2*rand(popSize,numVar).*(mgBest(:,1:numVar)-
ePop(:,1:numVar)));

    change1 = ve > maxvbounds;
    ve     = ve.*(~change1)+maxvbounds.*change1;
    change2 = ve < minvbounds;
    ve     = ve.*(~change2)+minvbounds.*change2;

    ePop(:,1:numVar)=ePop(:,1:numVar)+ve;

    change1        = ePop(:,1:numVar) > maxbounds;
    ePop(:,1:numVar)  = ePop(:,1:numVar).*(~change1)+maxbounds.*change1;
    change2        = ePop(:,1:numVar) < minbounds;
    ePop(:,1:numVar)  = ePop(:,1:numVar).*(~change2)+minbounds.*change2;

    pm=probm;
    [Pop_size Pop_elements]=size(ePop);

    for im=1:(round(pm*Pop_size))
        Select_chromo = round(rand*(Pop_size-1)+1);
        [ePop(Select_chromo,1:(numVar))] = waveletMutation2(ePop(Select_chromo,
1:(numVar) ),bounds,[itNum 0 termOps k1]);
    end


    ePop=regularVar(ePop,bounds);
```

```
   for ip=1:popSize
     eval(evalstr);
   end

end


[bval,bindx] = min(ePop(:,numVar+1));
if ( (bval < oval) )
   bPop(bFoundIn,:)=[itNum ePop(bindx,:)];
   bFoundIn=bFoundIn+1;
end
x=bPop(bFoundIn-1,2:numVar+4);

if collectTrace
   trackOpt(itNum,1)=itNum;
   trackOpt(itNum,2:xZomeLength+1)=ePop(bindx,:);
   trackOpt(itNum,xZomeLength+2)=mean(ePop(:,numVar+1));
   trackOpt(itNum,xZomeLength+3)=std(ePop(:,numVar+1));
end
 -

 -    % --- wavelet mutation -----

function [newPos] = waveletMut(newPos,bounds,Ops)

cg=Ops(1);
mg=Ops(3);
b=Ops(4);
df = bounds(:,2) - bounds(:,1);

[numVar,r]=size(bounds);

mPoint = round(rand * (numVar-1)) + 1;
r=cg/mg;
p=2.0;
q=(rand(1)*2*p-p);

a=10000;

c=-(log(a))*(1-r).^b+log(a);
a=exp(c);
change=Cwavelet(a,0,q*a);


if change>0

  newValue=newPos(mPoint)+change*(bounds(mPoint,2)-newPos(mPoint));
else
  newValue=newPos(mPoint)+change*(newPos(mPoint)-bounds(mPoint,1));

end

newPos(mPoint) = newValue;

% ---- fuzzy inference system ----
```

```
function w = FIS(z,X)

delta=z(1:3); % delta of gausian function
delta1=z(4:6);
delta2=z(7:9);

mean=z(10:12); % mean of gausian function
mean1=z(13:15);
mean2=z(16:18);

x1=X(:,1); % input
x2=X(:,2);
x3=X(:,3);

mx1=[gaussmf(x1,[delta(1) mean(1)]) gaussmf(x1,[delta(2) mean(2)])
gaussmf(x1,[delta(3) mean(3)])];
mx2=[gaussmf(x2,[delta1(1) mean1(1)]) gaussmf(x2,[delta1(2) mean1(2)])
gaussmf(x2,[delta1(3) mean1(3)])];
mx3=[gaussmf(x3,[delta2(1) mean2(1)]) gaussmf(x3,[delta2(2) mean2(2)])
gaussmf(x3,[delta2(3) mean2(3)])];

m = [mx1(:,1).*mx2(:,1)  mx1(:,2).*mx2(:,1)  mx1(:,3).*mx2(:,1) ...
    mx1(:,1).*mx2(:,2)  mx1(:,2).*mx2(:,2)  mx1(:,3).*mx2(:,2) ...
    mx1(:,1).*mx2(:,3)  mx1(:,2).*mx2(:,3)  mx1(:,3).*mx2(:,3)];

 m1 = [m(:,1).*mx3(:,1) m(:,2).*mx3(:,1) m(:,3).*mx3(:,1) m(:,4).*mx3(:,1) m(:,5).*mx3(:,1)
m(:,6).*mx3(:,1) m(:,7).*mx3(:,1) m(:,8).*mx3(:,1) m(:,9).*mx3(:,1)...
    m(:,1).*mx3(:,2) m(:,2).*mx3(:,2) m(:,3).*mx3(:,2) m(:,4).*mx3(:,2) m(:,5).*mx3(:,2)
m(:,6).*mx3(:,2) m(:,7).*mx3(:,2) m(:,8).*mx3(:,2) m(:,9).*mx3(:,2)...
    m(:,1).*mx3(:,3) m(:,2).*mx3(:,3) m(:,3).*mx3(:,3) m(:,4).*mx3(:,3) m(:,5).*mx3(:,3)
m(:,6).*mx3(:,3) m(:,7).*mx3(:,3) m(:,8).*mx3(:,3) m(:,9).*mx3(:,3)];

summ = sum(m1,2);
omf=z(19:45);
w = (m1*omf')./summ;
  -
```

References

.

ALEXAKIS, C., NYONGESA, H., SAATCHI, R., HARRIS, N., DAVIES, C., EMERY, C., IRELAND, R. & HELLER, S. 2003. Feature extraction and classification of electrocardiogram (ECG) signals related to hypoglycaemia. *Proceedings of Computers in Cardiology,* 30**,** 537-540.

ALEXAKIS, C., RODRIGUES, M., SAATCHI, R., NYONGESA, H., DAVIES, C., IRELAND, R., HARRIS, N. & HELLER, S. 2006. A knowledge-based electrocardiogram-monitoring system for detection of the onset of nocturnal hypoglycaemia in type 1 diabetic patients. *Proceedings of Computers in Cardiology,* 33**,** 5-8.

ALVES, R., ANTUNES, F. & SALVADOR, A. 2006. Tools for kinetic modeling of biochemical networks. *Nature Biotechnology,* 24**,** 667-672.

AMARAL, C. E. F. D. & WOLF, B. 2008. Current development in non-invasive glucose monitoring. *Medical Engineering & Physics,* 30**,** 541-549.

AMERICAN DIABETES ASSOCIATION WORKGROUP ON HYPOGLYCEMIA 2005. Defining and reporting hypoglycemia in diabetes: a report from the american diabetes association workgroup on hypoglycemia *Diabetes Care,* 28**,** 1245-1249.

AN, S., LIU, W. & VENKATESH, S. 2007. Fast cross-validation algorithms for least squares support vector machine and kernel ridge regression. *Pattern Recognition,* 40**,** 2154-2162.

ANTZELEVITCH, C. 2001. Tpeak-Tend interval as an index of transmural dispersion of repolarization. *European Journal of Clinical Investigation,* 31**,** 555-557.

ASTION, M. L., WENER, M. H., THOMAS, R. G., HUNDER, G. G. & BLOCH, D. A. 1993. Overtraining in neural networks that interpret clinical data. *Clinical Chemistry,* 39**,** 1998-2004.

BARAKAT, N. H., BRADLEY, A. P. & BARAKAT, M. N. H. 2010. Intelligible support vector machines for diagnosis of diabetes mellitus. *IEEE Transactions on Information Technology in Biomedicine,* 14**,** 1114-1120.

BATUWITA, R. & PALADE, V. 2010. FSVM-CIL: fuzzy support vector machines for class imbalance learning. *IEEE Transactions on Fuzzy Systems,* 18**,** 558-571.

BELEGUNDU, A. D. & CHANDRUPATLA, T. R. 2011a. *Optimization concepts and applications in engineering*, Cambridge Univ Press.

BELEGUNDU, A. D. & CHANDRUPATLA, T. R. 2011b. *Optimization Concepts and Applications in Engineering (2nd Edition)*, Cambridge University Press

BENHORIN, J., MERRI, M., ALBERTI, M., LOCATI, E., MOSS, A. J., HALL, W. J. & CUI, L. 1990. Long QT syndrome. New electrocardiographic characteristics. *Circulation,* 82**,** 521-527.

BENI, G. & WANG, J. Swarm intelligence in cellular robotic systems. *In Proceedings of* NATO Advanced Workshop on Robots and Biological Systems, June 26-30 1989. 703-712.

BERGER, R. D., KASPER, E. K., BAUGHMAN, K. L., MARBAN, E., CALKINS, H. & TOMASELLI, G. F. 1997. Beat-to-beat QT interval variability : novel evidence for repolarization lability in ischemic and nonischemic dilated cardiomyopathy. *Circulation,* 96**,** 1557-1565.

BOSER, B. E., GUYON, I. & VAPNIK, V. A Training Algorithm for Optimal Margin Classifiers. *In Proceedings of* Fifth Annual ACM Conference on Computational Learning Theory (COLT 1992), 1992. 144-152.

BRAAK, E. W. M. T. T. & STADES, A. M. E. 2009. Type 1 Diabetes. *In:* BIESSELS, G. J. & LUCHSINGER, J. A. (eds.) *Diabetes and the Brain.* New York, USA: Humana Press.

BURGES, C. J. C. 1999. Advances in kernel methods: support vector learning, The

MIT press.

CAN, I., AYTEMIR, K., K¨OSE, S. & OTO, A. 2002. Physiological mechanisms influencing cardiac repolarization and QT interval. *Cardiac Electrophysiology Review,* 6**,** 278–281.

CHAN, K. Y., DILLON, T. S. & KWONG, C. 2011a. Modeling of a liquid epoxy molding process using a particle swarm optimization-based fuzzy regression approach. *IEEE Transactions onI ndustrial Informatics,* 7**,** 148-158.

CHAN, K. Y., LING, S. H., DILLON, T. S. & NGUYEN, H. T. 2011b. Diagnosis of hypoglycemic episodes using a neural network based rule discovery system. *Expert Systems with Applications,* 38**,** 9799-9808.

CHANG, C. H., CHANG, K. M. & KO, H. J. Cancellation of high-frequency noise in ECG signals using adaptive filter without external reference. *In Proceedings of* Biomedical Engineering and Informatics (BMEI), 2010 3rd International Conference on, 2010. IEEE, 787-790.

CHEN, P. H., FAN, R. E. & LIN, C. J. 2006. A study on SMO-type decomposition methods for support vector machines. *IEEE Transactions on Neural Networks, ,* 17**,** 893-908.

CHENG, M.-Y., HOANG, N.-D., ROY, A. F. V. & WU, Y.-W. 2012. A novel time-depended evolutionary fuzzy SVM inference model for estimating construction project at completion. *Engineering Applications of Artificial Intelligence,* 25**,** 744-752.

CHRISTENSEN, T. F., TARNOW, L., RANDLØV, J., KRISTENSEN, L. E., STRUIJK, J. J., ELDRUP, E. & HEJLESEN, O. K. 2010. QT interval prolongation during spontaneous episodes of hypoglycaemia in type 1 diabetes: the impact of heart rate correction. *Diabetologia,* 53**,** 2036–2041.

CLARKE, W., CARTER, W., MOLL, M., COX, D. J., GONDER-FREDERICK, L. A. & CRYER, P. E. 1988. Metabolic and cutaneous events associated with

hypoglycemia detected by sleep sentry. *Diabetes Care,* 11**,** 630-635.

CLAUS B. JUHL, K. H., RASMUS ELSBORG, MIKAEL KJÆR POULSEN, PETER E. SELMAR, JENS JUUL HOLST, CLAUS CHRISTIANSEN, HENNING BECK-NIELSEN 2010. Automated detection of hypoglycemia-induced EEG changes recorded by subcutaneous electrodes in subjects with type 1 diabetes—The brain as a biosensor. *Diabetes Research and Clinical Practice,* 88**,** 22 - 28.

DANTZIG, G. B. Maximization of a Linear Function of Variables Subject to Linear Inequalities. *In Proceedings of* Activity Analysis of Production and Allocation, 1951. 339-347.

DARPO, B., AGIN, M., KAZIERAD, D. J., LAYTON, G., MUIRHEAD, G., GRAY, P. & JORKASKY, D. K. 2006. Man versus machine: is there an optimal method for QT measurements in thorough QT studies? *Journal of Clinical Pharmacology,* 46**,** 598-612.

DEEB, O. & GOODARZI, M. 2010. Exploring QSARs for Inhibitory Activity of Non-peptide HIV-1 Protease Inhibitors by GA-PLS and GA-SVM. *Chemical Biology and Drug Design,* 75**,** 506-514.

DEL VALLE, Y., VENAYAGAMOORTHY, G. K., MOHAGHEGHI, S., HERNANDEZ, J. C. & HARLEY, R. G. 2008. Particle swarm optimization: basic concepts, variants and applications in power systems. *IEEE Transactions on Evolutionary Computation,* 12**,** 171-195.

DEVOS, O., RUCKEBUSCH, C., DURAND, A., DUPONCHEL, L. & HUVENNE, J. P. 2009. Support vector machines (SVM) in near infrared (NIR) spectroscopy: Focus on parameters optimization and model interpretation. *Chemometrics and Intelligent Laboratory Systems,* 96**,** 27-33.

DI MARCO, L. Y. & CHIARI, L. 2011. A wavelet-based ECG delineation algorithm for 32-bit integer online processing. *Biomedical Engineering*

Online, 10**,** 1-19.

DI VIRGILIO, V., FRANCAIANCIA, C., LINO, S. & CERUTTI, S. ECG fiducial points detection through wavelet transform. *In Proceedings of* 17th Annual Conference of IEEE Engineering in Medicine and Biology Society, 1995. 1051-1052.

DONNELLY, L., MORRIS, A., FRIER, B., ELLIS, J., DONNAN, P., DURRANT, R., BAND, M., REEKIE, G. & LEESE, G. 2005. Frequency and predictors of hypoglycaemia in Type 1 and insulin-treated Type 2 diabetes: a population-based study. *Diabetic Medicine,* 22**,** 749-755.

DUIN, R. P. W. Classifiers in almost empty spaces. *In Proceedings of* 15th International Conference on Pattern Recognition, 2000. 1-7 vol.2.

ELIF DERYA, Ü. 2007. ECG beats classification using multiclass support vector machines with error correcting output codes. *Digital Signal Processing,* 17**,** 675-684.

FAN, R. E., CHEN, P. H. & LIN, C. J. 2005. Working set selection using second order information for training support vector machines. *The Journal of Machine Learning Research,* 6**,** 1889-1918.

FENG, G. 2006. A survey on analysis and design of model-based fuzzy control systems. *IEEE Transactions on Fuzzy Systems* 14**,** 676-697.

FENG, S., LI, H. & HU, D. 2009. A new training algorithm for HHFNN based on Gaussian membership function for approximation. *Neurocomputing,* 72**,** 1631-1638.

FRIDERICIA, L. S. 2003. The duration of systole in an electrocardiogram in normal humans and in patients with heart disease. *Annals of Noninvasive Electrocardiology,* 8**,** 343-351.

FRIER, B. M. & FISHER, M. 2007. *Hypoglycaemia in Clinical Diabetes*, John Wiley & Sons.

G RAO, P GLIKFELD & RH GUY 1993. Reverse iontophoresis: development of a noninvasive approach for glucose monitoring. *Pharmaceutical Research,* 12**,** 1751-1755.

GANG, F. 2006. A Survey on Analysis and Design of Model-Based Fuzzy Control Systems. *IEEE Transactions on Fuzzy Systems* 14**,** 676-697.

GAO, H. & XU, W. 2011. A new particle swarm algorithm and its globally convergent modifications. *Systems, Man, and Cybernetics, Part B: Cybernetics, IEEE Transactions on,* 41**,** 1334-1351.

GARG, S., ZISSER, H., SCHWARTZ, S., BAILEY, T., KAPLAN, R., ELLIS, S. & JOVANOVIC, L. 2006. Improvement in Glycemic Excursions With a Transcutaneous, Real-Time Continuous Glucose Sensor. *Diabetes Care,* 29**,** 44-50.

GARSON JR, A. 1993. How to measure the QT interval—What is normal? *The American Journal of Cardiology,* 72**,** B14-B16.

GEORGOULAS, G. & STYLIOS, C. D. 2006. Predicting the risk of metabolic acidosis for newborns based on fetal heart rate signal classification using support vector machines. *IEEE Transactions on Biomedical Engineering,* 53**,** 875-884.

GHEVONDIAN, N. & NGUYEN, H. Using fuzzy logic reasoning for monitoring hypoglycaemia indiabetic patients. *In Proceedings of* 19th Annual International Conference of the IEEE Engineering in Medicine and Biology Society, 1997. 1108-1111

GHEVONDIAN, N., NGUYEN, H. T. & COLAGIURI, S. A novel fuzzy neural network estimator for predicting hypoglycaemia in insulin-induced subjects. *In Proceedings of* 20th Annual International Conference of the IEEE Engineering in Medicine and Biology Society, 1997. 1371-1374.

GOLETSIS, Y., PAPALOUKAS, C., FOTIADIS, D. I., LIKAS, A. & MICHALIS,

L. K. 2004. Automated ischemic beat classification using genetic algorithms and multicriteria decision analysis. *IEEE Transactions on Biomedical Engineering,* 51**,** 1717-1725.

GRAAFF, J. C. D., HEMMES, G. J., BRUIN, T. & UBBINK, D. T. 1999. Influence of Repetitive Finger Puncturing on Skin Perfusion and Capillary Blood Analysis in Patients with Diabetes Mellitus. *Clinical Chemistry,* 45**,** 2200-2206

GUPTA P, PATEL C, PATEL H, NARAYANASWAMY S, MALHOTRA B, GREEN JT & YAN GX 2008. Tp-e ratio as an index of arrhytmogenesis. *Journal of Electrocardiology,* 41**,** 567-574.

HAIGNEY, M. C., ZAREBA, W., GENTLESK, P. J., GOLDSTEIN, R. E., ILLOVSKY, M., MCNITT, S., ANDREWS, M. L., MOSS, A. J. & THE, M. I. I. I. 2004. QT interval variability and spontaneous ventricular tachycardia or fibrillation in the multicenter automatic defibrillator implantation trial (MADIT) II patients. *Journal of American College of Cardiology,* 44**,** 1481-1487.

HANSEN, K. A. & DUCK, S. C. 1983. Teledyne Sleep Sentry: evaluation in pediatric patients for detection of nocturnal hypoglycemia. *Diabetes Care,* 6**,** 597-600.

HARRIS, N., IRELAND, R., MARQUES, J., HUDSON, S., DAVIES, C., LEE, S., ROBINSON, R. & HELLER, S. 2000. Can changes in QT interval be used to predict the onset of hypoglycemia in type 1 diabetes? *Proceedings of Computers in Cardiology***,** 375-378.

HASTINGS, G., GHEVONDIAN, N. & NGUYEN, H. A self-organising fuzzy estimator for hypoglycaemia monitoring in diabetic patients. *In Proceedings of* 20th Annual International Conference of the IEEE Engineering in Medicine and Biology Society, 1998. 1371-1374.

HEGER, G., HOWORKA, K., THOMA, H., TRIBL, G. & ZEITLHOFER, J. 1996. Monitoring set-up for selection of parameters for detection of hypoglycaemia in diabetic patients. *Medical and Biological Engineering and Computing,* 34**,** 69-75.

HEPBURN, D. A., DEARY, I. J., FRIER, B. M., PATRICK, A. W., QUINN, J. D. & FISHER, B. M. 1991. Symptoms of Acute Insulin-Induced Hypoglycemia in Humans With and Without IDDM: Factor-Analysis Approach. *Diabetes Care,* 14**,** 949-957.

HILSTED, J., BONDE-PETERSEN, F., NØRGAARD, M. B., GRENIMAN, M., CHRISTENSEN, N., PARVING, H. H. & SUZUKI, M. 1984. Haemodynamic changes in insulin-induced hypoglycaemia in normal man. *Diabetologia,* 26**,** 328-332.

HUANG, C.-L. & DUN, J.-F. 2008. A distributed PSO–SVM hybrid system with feature selection and parameter optimization. *Applied Soft Computing,* 8**,** 1381-1391.

HWANG, J. P., PARK, S. & KIM, E. 2011. A new weighted approach to imbalanced data classification problem via support vector machine with quadratic cost function. *Expert Systems with Applications,* 38**,** 8580-8585.

IRELAND, R. H., ROBINSON, R. T. C. E., HELLER, S. R., MARQUES, J. L. B. & HARRIS, N. D. 2000. Measurement of high resolution ECG QT interval during controlled euglycaemia and hypoglycaemia. *Physiological Measurement,* 21**,** 295-303.

JOHANSEN, K., ELLEGAARD, S. & WEX, S. 1986. Detection of nocturnal hypoglycemia in insulin-treated diabetics by a skin temperature - skin conductance meter. *Acta Medica Scandinavica,* 220**,** 213–217.

KAVITHA, K., RAMAKRISHNAN, K. & SINGH, M. K. 2010. Modeling and design of evolutionary neural network for heart disease detection.

International Journal of Computer Science Issues, 7**,** 1694-0814.

KEERTHI, S. S. & LIN, C.-J. 2003. Asymptotic behaviors of support vector machines with gaussian kernel. *Neural Computing,* 15**,** 1667-1689.

KEERTHI, S. S., SHEVADE, S. K., BHATTACHARYYA, C. & MURTHY, K. R. K. 2001. Improvements to Platt's SMO algorithm for SVM classifier design. *Neural Computation,* 13**,** 637-649.

KENNEDY, J. & EBERHART, R. Particle swarm optimization. *In Proceedings of* IEEE International Conference on Neural Networks Nov/Dec 1995 1995. 1942-1948.

KHANDOKER, A. H., PALANISWAMI, M. & KARMAKAR, C. K. 2009. Support vector machines for automated recognition of obstructive sleep apnea syndrome from ECG recordings. *IEEE transactions on information technology in biomedicine,* 13**,** 37-48.

KLONOFF, D. C. 2001. The need for hypoglycemia detection and prevention in type 1 diabetes. *Diabetes Technology & Therapeutics,* 3**,** 3567-570.

KLONOFF, D. C. 2005. Continuous glucose monitoring: roadmap for 21st century diabetes therapy. *Diabetes Care,* 28**,** 1231-1239.

KOIVIKKO ML, KARSIKAS M, SALMELA PI, TAPANAINEN JS, RUOKONEN A, SEPPANEN T, HUIJURI HV & JS., P. 2008. Effects of controlled hypoglycaemia on cardiac repolarisation in patients with type 1 diabetes. *Diabetologia,* 51**,** 426-435.

KOIVIKKO, M. L., KARSIKAS, M., SALMELA, P. I., TAPANAINEN, J. S., RUOKONEN, A., &, T. S., HUIKURI, H. V. & PERKIÖMÄKI, J. S. 2008. Effects of controlled hypoglycaemia on cardiac repolarisation in patients with type 1 diabetes. *Diabetologia,* 51**,** 426–435.

KOSKO, B. 1994. Fuzzy systems as universal approximators. *IEEE Transactions on Computers,* 43**,** 1329-1333.

LAHMIRI, S. & BOUKADOUM, M. Comparison of ANFIS and SVM for the classification of brain MRI Pathologies. *In Proceedings of* 54th IEEE International Midwest Symposium on Circuits and Systems, 7-10 Aug. 2011 2011. 1-4.

LAIONE, F. & MARQUES, J. L. B. 2005. Methodology for hypoglycaemia detection based on the processing, analysis and classification of the electroencephalogram. *Medical and Biological Engineering and Computing,* 43**,** 501-507.

LAITINEN, T., LYYRA-LAITINEN, T., HUOPIO, H., VAUHKONEN, I., HALONEN, T., HARTIKAINEN, J., NISKANEN, L. & LAAKSO, M. 2008. Electrocardiographic alterations during hyperinsulinemic hypoglycemia in healthy subjects. *Annals of Noninvasive Electrocardiology,* 13**,** 97-105.

LEBOULANGER, B., GUY, R. H. & DELGADO-CHARRO, M. B. 2004. Reverse iontophoresis for non-invasive transdermal monitoring. *Physiological Measurement,* 25**,** R35-R50.

LEE SP, YEOH L, HARRIS ND, DAVIES CM, ROBINSON RT, LEATHARD A, NEWMAN C, MACDONALD IA & SR, H. 2004. Influence of autonomic neuropathy on QTc interval lengthening during hypoglycemia in type 1 diabetes. *Diabetes,* 53**,** 1535-1542.

LEE, S. P., HARRIS, N. D., ROBINSON, R. T., ., C. D., IRELAND, R., MACDONALD, I. A. & HELLER, S. R. 2005. Effect of atenolol on QTc interval lengthening during hypoglycaemia in type 1 diabetes. *Diabetologia,* 48**,** 1269–1272.

LI, Q., MENG, Q., CAI, J., YOSHINO, H. & MOCHIDA, A. 2009. Applying support vector machine to predict hourly cooling load in the building. *Applied Energy,* 86**,** 2249-2256.

LIN, S.-W., YING, K.-C., CHEN, S.-C. & LEE, Z.-J. 2008. Particle swarm optimization for parameter determination and feature selection of support vector machines. *Expert Systems with Applications,* 35**,** 1817-1824.

LING, S., YEUNG, C., CHAN, K., IU, H. & LEUNG, F. H. A new hybrid particle swarm optimization with wavelet theory based mutation operation. *In Proceedings of* IEEE Congress on Evolutionary Computation, 2007. 1977-1984.

LING, S. H., IU, H. H. C., CHAN, K. Y., LAM, H. K., YEUNG, B. C. W. & LEUNG, F. H. 2008. Hybrid Particle Swarm Optimization With Wavelet Mutation and Its Industrial Applications. *IEEE Transactions on Systems, Man, and Cybernetics, Part B: Cybernetics,* 38**,** 743-763.

LING, S. S. H. & NGUYEN, H. T. 2011. Genetic-algorithm-based multiple regression with fuzzy inference system for detection of nocturnal hypoglycemic episodes. *IEEE Transactions on Information Technology in Biomedicine,* 15**,** 308-315.

LIPPONEN, J. A., KEMPPAINEN, J., KARJALAINEN, P. A., T LAITINEN, MIKOLA, H., KARKI, T. & TARVAINEN, M. P. 2011. Dynamic estimation of cardiac repolarization characteristics during hypoglycemia in healthy and diabetic subjects. *Physiological Measurement,* 32**,** 649-660.

LY, T. T., GALLEGO, P. H., DAVIS, E. A. & JONES, T. W. 2009. Impaired Awareness of Hypoglycemia in a Population-Based Sample of Children and Adolescents With Type 1 Diabetes. *Diabetes Care,* 32**,** 1802-1806.

MANRIQUEZ, A. I. & ZHANG, Q. An algorithm for QRS onset and offset detection in single lead electrocardiogram records. *In Proceedings of* 29th Annual International Conference of the IEEE Engineering in Medicine and Biology Society, 2007 Lyon, France. 541-544.

MARQUES, J. L. B., GEORGE, E., PEACEY, S. R., HARRIS, N. D.,

MACDONALD, I. A., COCHRANE, T. & HELLER, S. R. 1997. Altered ventricular repolarization during hypoglycaemia in patients with diabetes. *Diabetic Medicine,* 14**,** 648-654.

MARUO, K., TSURUGI, M., CHIN, J., OTA, T., ARIMOTO, H., YAMADA, Y., TAMURA, M., ISHII, M. & OZAKI, Y. 2003. Noninvasive blood glucose assay using a newly developed near-infrared system. *IEEE Journal of Selected Topics in Quantum Electronics* 9**,** 322-330.

MELGANI, F. & BAZI, Y. 2008. Classification of electrocardiogram signals with support vector machines and particle swarm optimization. *IEEE Transactions on Information Technology in Biomedicine,* 12**,** 667-677.

MEYER, D., LEISCH, F. & HORNIK, K. 2003. The support vector machine under test. *Neurocomputing,* 55**,** 169-186.

MEZA, J. C. 2010. Steepest descent. Wiley Interdisciplinary Reviews: Computational Statistics, 2**,** 719-722.

MILLER, M. E. & EVANS, R. W. 2006. *Systems and methods for detecting symptoms of hypoglycemia*. United States patent application 7052472.

MORIMOTO, B. H. & FOX, A. W. 2011. QT Interval Prolongation and Drug Development. *Principles and Practice of Pharmaceutical Medicine***,** 275-286.

MOSS, A. J. 1993. Measurement of the QT interval and the risk associated with QTc interval prolongation: A review. *American Journal of Cardiology,* 72**,** B23-B25.

MURABAYASHI, T., FETICS, B., KASS, D., NEVO, E., GRAMATIKOV, B. & BERGER, R. D. 2002. Beat-to-beat QT interval variability associated with acute myocardial ischemia. *Journal of Electrocardiology,* 35**,** 19-25.

MURPHY, N. P., FORD-ADAMS, M. E., ONG, K. K., HARRIS, N. D., KEANE, S. M., DAVIES, C., IRELAND, R. H., MACDONALD, I. A., KNIGHT, E.

J., EDGE, J. A., HELLER, S. R. & DUNGER, D. B. 2004. Prolonged cardiac repolarisation during spontaneous nocturnal hypoglycaemia in children and adolescents with type 1 diabetes. *Diabetologia,* 47**,** 1940-1947.

NERBONNE, J. M. & KASS, R. S. 2005. Molecular physiology of cardiac repolarization. *Physiological Reviews,* 85**,** 1205–1253.

NGUYEN, H. T., GHEVONDIAN, N. & JONES, T. W. Neural-Network Detection of Hypoglycemic Episodes in Children with Type 1 Diabetes using Physiological Parameters. *In Proceedings of* 28th Annual International Conference of the IEEE Engineering in Medicine and Biology Society, 2006. 6053-6056.

NGUYEN, H. T., GHEVONDIAN, N. & JONES, T. W. Detection of nocturnal hypoglycemic episodes (natural occurrence) in children with type 1 diabetes using an optimal bayesian neural network algorithm. *In Proceedings of* Proceeding of the 30th Annual International Conference of the IEEE Engineering in Medicine and Biology Society, 20-25 August 2008 2008. 1311 - 1314

NGUYEN, H. T., GHEVONDIAN, N. & JONES, T. W. Real-time Detection of Nocturnal Hypoglycemic Episodes using a Novel Non-invasive Hypoglycemia Monitor. *In Proceedings of* 28th Annual International Conference of the IEEE Engineering in Medicine and Biology Society, 2009. 3822-3825.

NGUYEN, H. T., GHEVONDIAN, N., NGUYEN, S. T. & JONES, T. W. Detection of hypoglycemic episodes in children with type 1 diabetes using an optimal bayesian neural network algorithm. *In Proceedings of* 29th Annual International Conference of the IEEE Engineering in Medicine and Biology Society, 2007. 3140-3143.

NGUYEN, H. T. & JONES, T. W. Detection of nocturnal hypoglycemic episodes

using EEG signals. *In Proceedings of* 32th Annual International Conference of the IEEE Engineering in Medicine and Biology Society 2010. 4930-4933.

NGUYEN, L. L., SU, S. & NGUYEN, H. T. Identification of Hypoglycemia and Hyperglycemia in Type 1 Diabetic patients using ECG parameters. *In Proceedings of* Annual International Conference of the IEEE Engineering in Medicine and Biology Society (EMBC), 2012. 2716-2719.

NOLLO, G., MARCONCINI, M., FAES, L., BOVOLO, F., RAVELLI, F. & BRUZZONE, L. 2008. An Automatic System for the Analysis and Classification of Human Atrial Fibrillation Patterns from Intracardiac Electrograms. *IEEE Transactions on Biomedical Engineering,* 55**,** 2275-2285.

NURYANI, N., LING, S. & NGUYEN, H. 2012a. Electrocardiographic Signals and Swarm-Based Support Vector Machine for Hypoglycemia Detection. *Annals of Biomedical Engineering,* 40**,** 934-945.

NURYANI, N., LING, S. & NGUYEN, H. T. Electrocardiographic T-wave Peak-to-end Interval for Hypoglycaemia Detection. *In Proceedings of* 32nd Annual International Conference of the IEEE Engineering in Medicine and Biology Society, 2010a. 618-621.

NURYANI, N., LING, S. & NGUYEN, H. T. Ventricular Repolarization Variability for Hypoglycemia Detection. *In Proceedings of* 33nd Annual International Conference of the IEEE Engineering in Medicine and Biology Society, 2011. 7961-7964.

NURYANI, N., LING, S. H. & NGUYEN, H. T. Hypoglycaemia Detection for Type 1 Diabetic Patients Based on ECG Parameters Using Fuzzy Support Vector Machine. *In Proceedings of* IEEE World Congress on Computational Intelligence, 2010b Barcelona, Spain. 2253 - 2259.

NURYANI, N., LING, S. H. & NGUYEN, H. T. Hybrid Particle Swarm - based

Fuzzy Support Vector Machine for Hypoglycemia Detection. *In Proceedings of* IEEE World Congress on Computational Intelligence, 2012b Brisbane, Australia (Accepted). 450-455.

OLIVER, N. S., TOUMAZOU, C., CASS, A. E. G. & JOHNSTON, D. G. 2008. Glucose sensors: a review of current and emerging technology. *Diabetic Medicine,* 26**,** 197–210.

OSAREH, A. & SHADGAR, B. 2008. Intrusion Detection in Computer Networks based on Machine Learning Algorithms. *International Journal of Computer Science and Network Security,* 8**,** 15-23.

OSOWSKI, S., HOAI, L. T. & MARKIEWICZ, T. 2004. Support vector machine-based expert system for reliable heartbeat recognition. *IEEE Transactions on Biomedical Engineering,* 51**,** 582-589.

PEDERSEN-BJERGAARD, U. 2009. Severe hypoglycaemia in type 1 diabetes: impact of the renin-angiotensin system and other risk factors. *Danish Medical Bulletin,* 56**,** 193-207.

PLAT, J. C. 1999. Fast Training of Support Vector Machines using Sequential Minimal Optimization. *In:* SCHÖLKOPF, B., BURGES, C. J. C. & SMOLA, A. J. (eds.) *Advances in Kernel Methods Support Vector Learning.* MIT Press.

POURBASHEER, E., RIAHI, S., GANJALI, M. R. & NOROUZI, P. 2010. QSAR study on melanocortin-4 receptors by support vector machine. *European Journal of Medicinal Chemistry,* 45**,** 1087-1093.

PRAMMING, S., THORSTEINSSON, B., STIGSBY, B. & BINDER, C. 1988. Glycaemic threshold for changes in electroencephalograms during hypoglycaemia in patients with insulin dependent diabetes. *British Medical Journal (Clinical Research Ed.),* 296**,** 665-667.

RAO, G., GUY, R. H., GLIKFELD, P., LACOURSE, W. R., LEUNG, L.,

TAMADA, J., POTTS, R. O. & AZIMI, N. 1995. Reverse iontophoresis: noninvasive glucose monitoring in vivo in humans. *Pharmaceutical Research,* 12**,** 1869-1873.

REMVIG, L. S., ELSBORG, R., SEJLING, A.-S., SØRENSEN, J. A., SØNDER, S. L., FOLKESTAD, L. & JUHL, C. B. 2012. Hypoglycemia-related electroencephalogram changes are independent of gender, age, duration of diabetes, and awareness status in type 1 diabetes. *Journal of Diabetes Science and Technology,* 6**,** 1337.

ROBINSON RTCE, HARRIS ND, IRELAND RH, LEE S, NEWMAN C & SR, H. 2003. Mechanisms of abnormal cardiac repolarization during insulin induced hypoglycemia. *Diabetes,* 52**,** 1469-1474.

ROBINSON, R. T. C. E., HARRIS, N. D., IRELAND, R. H., LEE, S., NEWMAN, C. & HELLER, S. R. 2003. Mechanisms of abnormal cardiac repolarization during insulin-induced hypoglycemia. *Diabetes,* 52**,** 1469-1474.

ROBINSON, R. T. C. E., HARRIS, N. D., IRELAND, R. H., LINDHOLM, A. & HELLER, S. R. 2002. Comparative effect of human soluble insulin and insulin aspart upon hypoglycaemia-induced alterations in cardiac repolarization. *British Journal of Clinical Pharmacology,* 55**,** 246-251.

ROBINSON, R. T. C. E., HARRIS, N. D., IRELAND, R. H., MACDONALD, I. A. & S. R. HELLER1 2004. Changes in cardiac repolarization during clinical episodes of nocturnal hypoglycaemia in adults with Type 1 diabetes. *Diabetologia,* 47**,** 312–315.

SALVI, V., KARNAD, D. R., PANICKER, G. K., NATEKAR, M., HINGORANI, P., KERKAR, V., RAMASAMY, A., DE VRIES, M., ZUMBRUNNEN, T., KOTHARI, S. & NARULA, D. 2011. Comparison of 5 methods of QT interval measurements on electrocardiograms from a thorough QT/QTc study: effect on assay sensitivity and categorical outliers. *Journal of*

Electrocardiology, 44**,** 96-104.

SCHNEIDER, R., BAUER, A., BARTHEL, P. & SCHMIDT, G. 2006. Challenge 2006: QT interval measurement. *Proceedings of Computers in Cardiology***,** 325-328.

SHEIKH-BAHAEI, S., ROPELLA, G. E. & HUNT, C. A. Agent-based simulation of in vitro hepatic drug metabolism: in silico hepatic intrinsic clearance. *In Proceedings of* Proceedings of the 2005 Agent-Directed Simulation Symposium (San Diego, CA, Apr 2-8), Simulation Series vol. 37 (2), 2005. 171-6.

SIDDIQUI, A. B., JAFFAR, M. A., HUSSAIN, A. & MIRZA, A. M. 2011. Block-Based Pixel Level Multi-Focus Image Fusion Using Particle Swarm Optimization. *International Journal of Innovative Computing, Information and Control,* 7**,** 3583 - 3596.

SIEG, A., GUY, R. H. & DELGADO-CHARRO., M. B. 2005. Noninvasive and minimally invasive methods for transdermal glucose monitoring. *Diabetes Technology & Therapeutics,* 7**,** 174-197.

SOMMERFIELD, A. J., DEARY, I. J., MCAULAY, V. & FRIER, B. M. 2003. Short-Term, Delayed, and Working Memory Are Impaired During Hypoglycemia in Individuals With Type 1 Diabetes. *Diabetes Care,* 26**,** 390-396.

SONG, S., ZHAN, Z., LONG, Z., ZHANG, J. & YAO, L. 2011. Comparative Study of SVM Methods Combined with Voxel Selection for Object Category Classification on fMRI Data. *PLoS One,* 6**,** e17191.

SOPHIA, H. Z., ERIC, D. H., JAMES, M. L., RICHARD, E. G. & DIRK, Q. F. 2009. Philips QT interval measurement algorithms for diagnostic, ambulatory, and patient monitoring ECG Applications. *Annals of Noninvasive Electrocardiology,* 14**,** S3-S8.

STRACHAN, M. W. J. 2007. Frequency, causes and risk factors for hypoglycaemia in type 1 diabetes. *In:* FRIER, B. M. & FISHER, M. (eds.) *Hypoglycaemia in Clinical Diabetes.* John Wiley & Sons Ltd.

TAKAHASHI, D., XIAO, Y., HU, F. & LEWIS, M. 2008. A survey of insulin-dependent diabetes-part I: therapies and devices. *International Journal of Telemedicine and Applications,* 2008**,** 1-15.

TATTERSALL, R. B. & GILL, G. V. 1991. Unexplained death of type 1 diabetic patients. *Diabetic Medicine,* 8**,** 49-58.

TATUM, W. O. 2007. *Handbook of EEG interpretation,* New York, NY, USA Demos Medical Publishing.

THE DCCT RESEARCH GROUP 1991. Epidemiology of severe hypoglycemia in the diabetes control and complications trial. *The American Journal of Medicine,* 90**,** 450-459.

THE DIABETES CONTROL AND COMPLICATIONS TRIAL RESEARCH GROUP 1997. Hypoglycemia in the diabetes control and complications trial. *Diabetes,* 46**,** 271.

UKENA, C., MAHFOUD, F., NEUBERGER, H.-R. & BÖHM, M. 2011. Variability of ventricular repolarization during hypoglycemia. *International Journal of Cardiology,* 149**,** 285-286.

VAPNIK, V. N. 1995. *The Nature of Statistical Learning Theory,* New York, Springer-Verlag.

WEI, J., JIAN-QI, Z. & XIANG, Z. 2011. Face recognition method based on support vector machine and particle swarm optimization. *Expert Systems with Applications,* 38**,** 4390-4393.

WEXLER, D. J., MEIGS, J. B., CAGLIERO, E., NATHAN, D. M. & GRANT, R. W. 2007. Prevalence of Hyper- and Hypoglycemia Among Inpatients With Diabetes. *Diabetes Care,* 30**,** 367-369.

WU, K. P. & WANG, S. D. 2009. Choosing the kernel parameters for support vector machines by the inter-cluster distance in the feature space. *Pattern Recognition,* 42**,** 710-717.

XIAOGUANG, C. & LILLY, J. H. 2004. Evolutionary design of a fuzzy classifier from data. *IEEE Transactions on Systems, Man, and Cybernetics, Part B: Cybernetics, ,* 34**,** 1894-1906.

XUE, C. X., ZHANG, R. S., LIU, M. C., HU, Z. D. & FAN, B. T. 2004. Study of the quantitative structure-mobility relationship of carboxylic acids in capillary electrophoresis based on support vector machines. *Journal of Chemical Information and Computer Sciences,* 44**,** 950-95.

YAN, G.-X. & ANTZELEVITCH, C. 1998. Cellular basis for the normal T wave and the electrocardiographic manifestations of the long-QT syndrome. *Circulation,* 98**,** 1928-1936.

YAO, X., PANAYE, A., DOUCET, J., ZHANG, R., CHEN, H., LIU, M., HU, Z. & FAN, B. 2004. Comparative study of QSAR/QSPR correlations using support vector machines, radial basis function neural networks, and multiple linear regression. *Journal of Chemical Information and Computer Sciences,* 44**,** 1257-1266.

ZANIBONI, M., POLLARD, A. E., YANG, L. & SPITZER, K. W. 2000. Beat-to-beat repolarization variability in ventricular myocytes and its suppression by electrical coupling. *American Journal of Physiology Heart and Circulatory Physiology,* 278**,** H677-H687.

ZENG, X. J. & SINGH, M. G. 1996. Approximation accuracy analysis of fuzzy systems as function approximators. *IEEE Transactions on Fuzzy Systems, ,* 4**,** 44-63.

ZHAO, Z. D. & CHEN, Y. Q. A new method for removal of baseline wander and power line interference in ECG signals. *In Proceedings of* Machine

Learning and Cybernetics, 2006 International Conference on, 2006. IEEE, 4342-4347.

ZHOU, J., SHI, J. & LI, G. 2011. Fine tuning support vector machines for short-term wind speed forecasting. *Energy Conversion and Management,* 52**,** 1990-1998.

ZWEIG, M. H. & CAMPBELL, G. 1993. Receiver-operating characteristic (ROC) plots: a fundamental evaluation tool in clinical medicine. *Clinical Chemistry,* 39**,** 561-77.